Modeling of isolated kidney perfusion systems in transplantation ischemic tolerance

PhD thesis

Vivien Telek

Supervisor: Ildikó Takács, MD, Med.Habil.

Leader of program: Gábor Jancsó, MD, Med.Habil.

Leader of doctoral school: Lajos Bogár, MD, Med.Habil.

University of Pécs, Medical School
Department of Surgical Research and Techniques

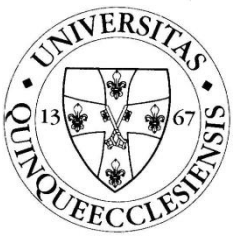

Pécs, 2021

Contents

1. Abbreviations

AGE-RAGE	advanced glycated endproducts
AMPK	5’ adenosine monophosphate-activated protein kinase
ANG II	angiotensin II
ANOVA	one-way analysis of variance
ASK1	apoptosis signal-regulating kinase 1
ATP	adenosine triphosphate
BiP/GRP78	immunoglobulin heavy chain-binding protein/glucose-related protein 78
B-ZIP	basic-leucine zipper
cNOS	constitutive nitric oxide synthase
DGF	delayed graft function
DMSO	dimethyl sulfoxide
EGTA	ethylene glycol tetraacetic acid
ER	endoplasmic reticulum
ERAD	endoplasmic reticulum-associated degradation
ERS	endoplasmic reticulum stress
ET	endothelin
GAPDH	glyceraldehyde 3-phosphate dehydrogenase
Hmox1	hepatic hemoxygenase-1
HTK	Histidine-tryptophan-ketoglutarate/Custodiol solution
i.p.	intraperitoneal

IFN-	interferon
IL-	interleukin-
IR	ischemia/reperfusion
IRI	ischemia-reperfusion injury
JNK	c-Jun N-terminal kinase
K_{ATP}	ATP-sensitive potassium channel
KH	Krebs-Henseleit Solution
KIM-1	urinary kidney injury molecule 1
MDA	malondialdehyde
MI	myocardial infarct
mPTP	mitochondrial permeability transitions pore
mRNA	messenger RNA
MTX	methotrexate
Na_3VO_4	sodium orthovanadate
NaCl	sodium chloride
NADH	nicotinamide adenine dinucleotide
NaF	sodium fluoride
NF-κB	nuclear factor kappa-light-chain-enhancer of activated B cells
NGAL	neutrophil gelatinase associated lipocalin
NMDA receptor	N-methyl-D-aspartate receptor
NO	nitrogen oxide
Nrf2	nuclear factor erythroid 2-related factor 2
PBS	phosphate-buffered saline

PDD	phorbol-12, 13-didecanoate
Pio	Pioglitazone
Pparg1	hepatic peroxisome-proliferator gamma 1
PPARγ	peroxisome proliferator-activated receptor-γ
PSGL-1	P-selectin glycoprotein ligand-1
PVDF	polyvinylidene fluoride
RBC	red blood cells
ROS	reactive oxygen species
TNF-α	tumor necrosis factor-alpha
TRAF2	TNF receptor associated factor 2
Tris	tris(hydroxymethyl)aminomethane
TRx	hepatic thioredoxin
TUNEL	terminal deoxynucleotidyl transferase dUTP nick end labeling
TZD	thiazolidinediones
UV	ultraviolet
UW	University of Wisconsin Solution/Viaspan
XBP-1	X-box binding protein 1
$ZnCl_2$	zinc chloride

2. Introduction

Kidney transplantation is considered the best treatment for patients with end stage renal disease. Ischemia-reperfusion injury (IRI) is an evitable event after deceased donor transplantation and influences short term and long-term graft outcome. After kidney transplantation, the main consequences are DGF (delayed graft function), acute and chronic graft rejection and chronic graft dysfunction. [1] The better understanding of IRI mechanisms will help to find further improvements in donated organ survival. Almost 30 % of DGF following kidney transplantation is owed to IRI. Caspases, the classical effector enzymes of apoptosis, are able to induce inflammation following IRI, which is one of the most important non-specific and non-immunologic factor affecting not only DGF but also late allograft dysfunction. [2] Transplantation of an ischemic organ can lead to distant organs' dysfunction. Several mediators are released into systemic circulation during IRI and these can be disadvantageous at distant tissues and organs (native kidneys, liver, lungs and heart). The released mediators can improve permeability of capillaries and more cytokines will secreted, like TNF-alpha, IL-1 and IL-6, which cause severe cell response and it can easily end in cell necrosis or apoptosis. [3]

IRI induces acute renal failure which is crucial for transplanted kidney survival. To minimize it, there are several studies that aim how to keep the donor organ hemodinamically stable, to prevent the extent of tubular epithelial cell injury of the kidney and to improve its recovery if injury occurs. Several types of drugs are used on this field to reduce the harmful effects of IRI, but none of them got a place at the clinical practice. Some of them aims to react on mitochondria to prevent the mPTP (=mitochondrial permeability transition pore) channel opening, [4] others treat on K_{ATP} (=ATP sensitive potassium channel) to reduce the intracellular Ca^{2+} level which can protect cells from destruction. [5] There is more need to find a possible treatment for the issue and increase the graft survival and function to assure recipients a longer dialyze-free life.

Transplanted kidneys are damaged organs and drugs can be used either alone or in combination to modify the effects of ischemia and reperfusion besides perfusion solutions and perfusion methods. Further investigations are required to eliminate the effects of IRI during kidney transplantation. [6]

2.1. Pathophysiology of ischemia-reperfusion injury (IRI)

Ischemia-reperfusion is a pathological condition characterized by an initial restriction of blood flow to an organ and it is followed by the subsequent restoration of perfusion and reoxygenation. Reperfusion is a double-edged sword, besides the re-establishing of blood supply, oxygen and ATP; it results in severe innate and adaptive immune responses and cell death programs. [7] Every organ has different ischemic tolerance, which is a period of time when the damage is still reversible. This means minutes for neurons and 6-8 hours to skeletal muscles. When the ischemic period is longer than the ischemic tolerance then we talk about critical ischemia. In that case the injury is irreversible, and revascularization will not enable for the organ to survive. Preconditioning is a non-injurious stress applied to a cell, tissue or organ that activates a protective program that results protective changes and the cell, tissue or organ will be protected against a normally injurious dose of stressors. In case of rats, the preconditioning means 10-15 seconds of ischemia and after reperfusion for several periods. Furthermore, as well we understand the mechanisms of IRI and the possible targets where we can decrease the injury as more tools will we have to minimize IRI and increase the ischemic tolerance. [8]

2.1.1. Changes due to ischemia

Blood flow can be blocked by a clot, an embolus, or constriction of an artery. One of the main causes of ischemia is atherosclerosis. Due to ischemia the blood supply of the tissue will be restricted, and several cellular mechanisms become activated. During citric acid cycle NADH accumulates because of the lack of oxygen. [9] Terminal oxidation and the generation of high energy phosphates will be cancelled. Anaerobic metabolism prevails which produces a decrease in cell pH. To buffer this accumulation of hydrogen ions, the Na^+/H^+ antiporter excretes excess hydrogen ions, which produces a large influx of sodium ions. Due to the damaged membrane functions, the Na^+/K^+ exchanger will be damaged, caused Na^+ and water influx. The intracellular Na^+ concentration will be increased, and it slows down the Na^+/Ca^{2+} exchanger. After a certain time, the way of the ion transport will be changed and a high amount of Ca^{2+} will accumulate intracellular. Some of the Ca^{2+} is transported to the mitochondria and it causes the opening of mPTP channels during the first seconds of reperfusion. Ca^{2+} activates phospholipases, calmodulin regulated proteases and endonucleases. [10] For example, these cellular changes are accompanied by activation of intracellular proteases – calpains – which damage myofibrils and produce hypercontracture and contracture band necrosis. [11]

2.1.2. Changes through reperfusion

Although prompt reperfusion restores the supply of oxygen and substrates required for aerobic ATP generation and in 40 seconds the normal pH will maintained by washing out accumulated H^+, reperfusion appears to have detrimental consequences. Reperfusion injury has complex feature, because reactive oxygen species are generated, Ca^{2+} is overloaded, mPTP channels are opened and we can mention the endothelial dysfunction and appearance of prothrombogenic phenotype as well as pronounced inflammatory responses. [12]

During reperfusion, the production of reactive oxygen species (ROS) is increased. Decomposition product from ATP is hypoxanthine which is further transformed. This process is catalyzed by the xanthine oxidase which is under normal conditions xanthine dehydrogenase but due to ischemia the Ca^{2+} dependent pathway is active, and the transformation takes place. [13] ROS (O^{2-}, H_2O_2, $HOCl^-$) cause lipid peroxidation, membrane and DNA lesion and induce local and systemic inflammatory responses through the inducing of cytokine expression and leukocyte activation. Antioxidant molecules eliminate the ROS under normal condition but during IRI this balance capsizes, and a huge amount of ROS cause the above mentioned injuries. When mPTP channels are open, the strictly regulated mitochondrial outer membrane permeability becomes damaged, therefore, mitochondria are swelling, and proton gradient cease and the oxidative phosphorylation are blocked. Furthermore, the mitochondrial components' (for example cytochrome c) free migration is initiated which is a key station to cell death. [14]

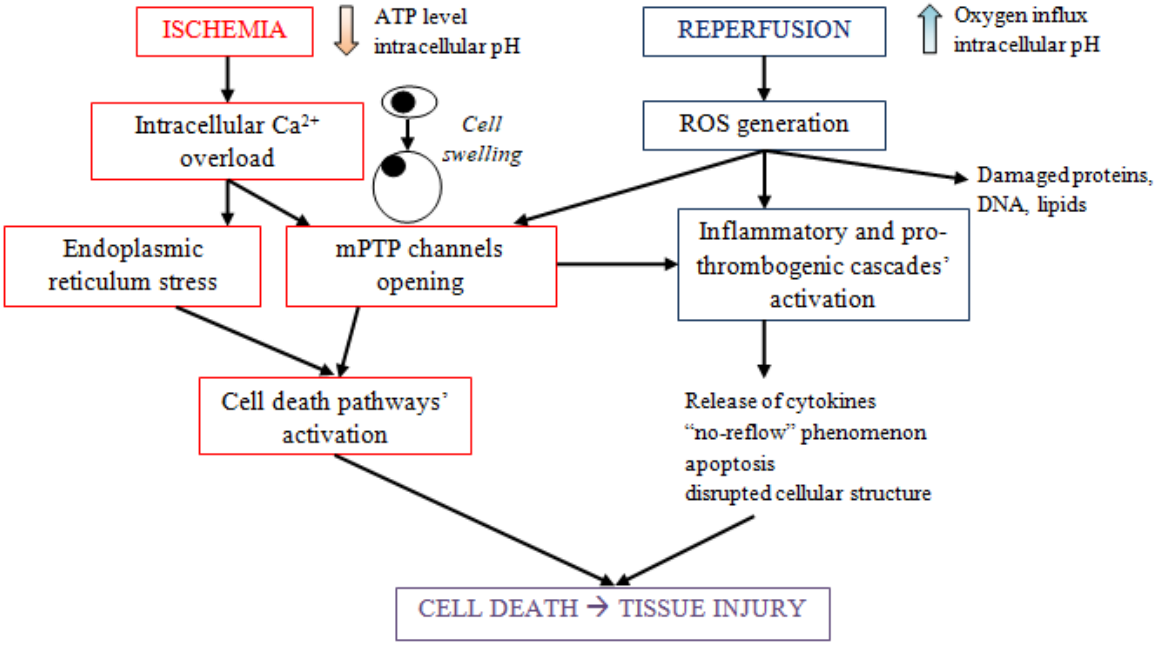

Figure 1: Ischemia-reperfusion's major pathological events (*Modified from Kalogeries et.al.[16]*)

IRI also influences the endothelial cells, and some bioactive molecules production is decreased (prostacyclin, nitrogen oxide (NO)) and others are increased (endothelin (ET), thromboxane A2), furthermore, the cell surface molecules (P-selectin) are expressed. [16] Endothelial dysfunction occurs due to ischemia which cause disorder in membrane potential and the results are the swelling endothelial cells, decreased cell membrane permeability as well as cytoskeletal changes. Translation of some genes (adhesion molecules, cytokines) accelerates or suppresses (cNOS, thrombomodulin). [17]

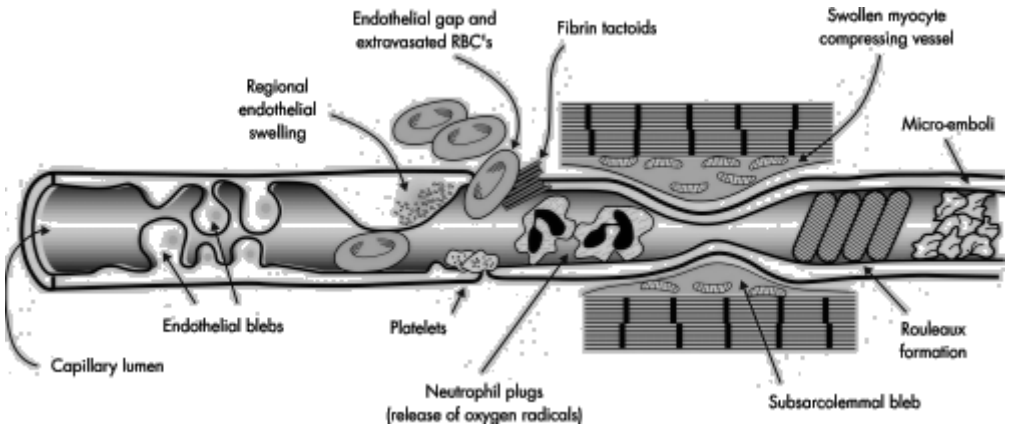

Figure 2: Microvascular injury during IRI [18]

At the phase of reperfusion, these mechanisms worsen, and the capillary lumen is clogged by platelets, micro emboli, RBC's. Invaginations cause severe damage in blood flow,

which is the swollen effect of myocyte to the vessel. Their combined effect is the no-reflow phenomenon, and the reperfusion shows spotted pattern and hypoperfusion of the injured organ. [18]

The activation of inflammatory cytokines is related to redox-sensitive transcription factors (for example NF-κB) and a local inflammation occurs in ischemic tissue. This mechanism is related to ROS which cause the above mentioned activation. Several types of mediators will be secreted. In the first period (acute phase), production of TNF-α and IL-1β happen after 1-2 hours of local injury. Subacute phase is characterized by increased release of IL-6, IL-8, IL-12, IL-18 and IFN-γ. [19]

P-selectin, a key adhesion molecule is involved in the earliest events in the adherence of circulating leukocytes in rolling to tissues under inflammatory conditions. [20, 21] It is expressed by Weibel-Palade bodies of endothelial cells and it translocates to the plasma membrane of alpha granules of platelets and endothelial cells due to various stimuli. [22, 23] This molecule has a crucial role not only in earliest cellular responses but also in chronic inflammation. P-selectin glycoprotein ligand-1 (PSGL-1) is one of the most characterized P-selectin's receptors. It can be a way of modulating IRI by blocking antibodies to P-selectin. [24, 25] However, E-selectin is expressed de novo on endothelial cells after the transcriptional induction of E-selectin mRNA by TNF-α and IL-1β (which are pro-inflammatory agents). [26]

2.2. Endoplasmic reticulum stress in general

Organelle autoregulation is a main characteristic of eukaryotic cells. The endoplasmic reticulum (ER), Golgi apparatus, mitochondria, lysosomes, peroxisomes, and nucleus also have this feature. This is the basis of proper cell function and it is strictly regulated to keep cellular homeostasis on a stable level. [27] ER is a cell structure which is responsible for secretory and membrane protein synthesis and folding. BiP/GRP78 and calnexin are two of the main ER chaperons that help in these processes. [28-30] Solely correctly folded proteins are transported to the Golgi apparatus; forasmuch unfolded or not correctly folded proteins are degraded by ER-associated degradation (ERAD). [31, 32] Several physiologic stresses (increased secretory load), pathological stresses (presence of mutated proteins, which cannot fold in the ER) can lead to an inequality between the demand of protein folding and the ER's capacity for protein folding, causing ER stress (ERS). The unfolded protein response (UPR) is the collective term of signal transduction pathways that are

involved in ERS sensing and responding. The UPR regulator factors consist of a set of transmembrane ER-resident proteins (IRE1 – inositol-requiring protein 1; PERK – PKR-like endoplasmic reticulum kinase; ATF-6 – activating transcription factor 6). When ERS is appeared, these proteins bear domains protruding into the ER lumen, couple to cytosolic effector domains. ERS is caused by factors that impair protein glycosylation or disulphide bond formation or the overexpression of or mutations in proteins entering the secretory pathway. These sensing mechanisms can protect the cell or promote cell death if stress becomes irreversible. The mechanism of UPR and the link between human diseases get more attention, because some pathologic conditions elicit ERS.[33]

The most phylogenetically conserved UPR signaling pathway is IRE1. IRE1α is presented in every cell of mammals, whereas IRE1β is expressed by intestinal epithelial cells. When ERS occurs, IRE1 oligomerizes in the ER membrane and this leads to the activation of kinases and endoribonucleases in its cytosolic domain. The method is mediated through the splicing of *Xbp-1* mRNA and the spliced *Xbp-1* encodes a transcription factor of the basic-leucine zipper (B-ZIP) family whose genetic targets code for proteins and their function is to enhance ER protein-folding capacity and degradation of misfolded ER proteins, thus protecting the cell by reducing the ERS stimulus. [34-36]

As discussed earlier, ERS can be lethal for the cells because IRE1 can promote cell death in response to the stress. The c-Jun N-terminal kinase (JNK) is activated by IRE1 signaling and it binds to the TNF receptor associated factor 2 (TRAF2) adaptor molecule and activates the apoptosis signal-regulating kinase 1(ASK1) which causes the activation and phosphorylation of JNK (which trigger cell death in response to TNF-α receptor activation or UV radiation). [37-39]

IRE1 signaling can also promote cell death after ERS by activating caspases. TRAF2, the adaptor molecule, interacts with murine procaspase-12 and ERS disrupts this interaction, possibly by causing the IRE1 kinase domain to bind TRAF2 which leads to the conversion of procaspase-12 into the active enzyme. The role of caspases-12 in cell death promotion after ERS is controversial, although Nakagawa et al. published a study, where murine *Caspase-12*$^{-/-}$ cells are largely resistant to cell death induced by ERS, [40] and another group observed no significant resistance to ER stress when they generated *Caspase-12*$^{-/-}$ cells independently. [41]

2.3. Pioglitazone (Pio)

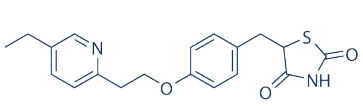

Figure 3: Chemical structure of Pioglitazone [95]

The peroxisome proliferator-activated receptor-γ (PPARγ) belongs to the family of nuclear receptors which control the expression of a huge number of genes and act like sensors of hormones, vitamins, endogenous metabolites, and xenobiotic compounds. The group of thiazolidinediones (TZDs) is the most widely studied PPARγ ligands. [42] Activation of PPARγ results in insulin sensitization by opposing the effect of TNFα in adipocytes and enhances glucose metabolism. PPARγ can be subdivided in four isoforms, which are γ1, γ2, γ3 and γ4. The difference between them is where from they are expressed. PPARγ1 is expressed in heart, muscle, colon, kidney, pancreas and spleen, while γ2 is expressed mainly in adipose tissue and this isoform is 30 amino acids longer. PPARγ3 is expressed in macrophages, white adipose tissue and large intestine and the source of γ4 is the endothelial cells. Troglitazone was the first drug than it was followed by rosiglitazone and pioglitazone. [43] The PPARγ agonist Pioglitazone (Pio) is used as an antidiabetic drug in the treatment of type 2 diabetes as efficient insulin sensitizer. Recent studies show that Pio protects kidneys, myocardium, and brain against IRI. [44-47] The potential role of Pio and other PPARγ agonists as nephroprotective agents is demonstrated in non-diabetic models of renal injury (such as IRI and induced renal toxicity by drug or chemical) [48-50] Renoprotective properties of Pio exhibits via facilitation of endothelium-dependent vasodilatation through amending abnormalities in NO production [51], developing the antioxidant profile [52] and control of the expression of inflammatory mediators [53, 54] and apoptotic factors. [55]

Besides the insulin sensitizing effect of Pio, it can reduce inflammation and consequences of oxidative stress in IRI model. [56] Experiments under hypoxic conditions on NRK-52 cells proved Pio increased the rate of cell survival and decreased the injury caused by hypoxia/reperfusion. According to TUNEL assay they ascertain that Pio could reduce the rate of apoptotised cells in treated groups compared to untreated, hypoxia/reperfusion control group. [57] Furthermore, Pio has endothelial protective function which can be used beside methotrexate (MTX) therapy. [58]

1. Table: Some of the main effects of Pioglitazone in experiments with rats (Abbreviations: AMPK – 5' adenosine monophosphate-activated protein kinase; NMDA receptor – N-methyl-D-aspartate receptor; IR – ischemia/reperfusion; IRI – ischemia/reperfusion injury; ANG II – Angiotensin II; MTX – methotrexate; NF-κB – nuclear factor kappa-light-chain-enhancer of activated B cells; IL- - interleukin; Pio – Pioglitazone; KIM-1 – urinary kidney injury molecule 1; NGAL – neutrophil gelatinase associated lipocalin; PDD – phorbol-12,13-didecanoate; MI – myocardial infarct; AGE-RAGE – advanced glycated endproducts; MDA – malondialdehyde; Nrf2 – nuclear factor erythroid 2-related factor 2; Pparg1 – hepatic peroxisome-proliferator gamma 1; Hmox1 – hepatic hemoxygenase-1; TRx – hepatic thioredoxin)

Effect	**Mechanism**	**References**
Protective effect against MTX-induced endothelial impairment	Ameliorating oxidative stress and rectifying cytokines and Fas abnormalities caused by MTX	[58]
Protective effect in renal IRI	Activation of an AMPK-regulated autophagy signaling pathway	[59]
	NMDA receptor antagonism	[60]
	Reduce renal IR injury by its anti-inflammatory and antioxidant effects	[61]
Modifies the vascular sodium-ANG II relationship	Blunted the systemic response to ANG II and abolished the increased responsiveness to ANG II indicated high-sodium diet	[62]
Preventing oxidative/inflammatory cochlear damage	Decrease NF-κB and IL-1β expression in the cochlea and had an antagonistic effect on the oxidative stress induced by noise insult	[63]
Protective effect in gentamicin-induced nephrotoxicity	Medium dose of Pio was protective (oxidative stress, biochemical parameters, total histological kidney score, KIM-1 and NGAL level	[64]
Antinociceptive and antiedematogenic effect	Inhibited paw edema induced by PDD	[65]
Reduce inflammation	Inhibited NF-κB in polymicrobial sepsis	[66]
Protect from acute MI	Downregulate AGE-RAGE axis and inhibit apoptosis	[67]

Protect liver in kidney IRI	Reduced renal IR-induced oxidative stress in liver, reduced MDA content, NADPH oxidase mRNA expression, induced further increase in Nrf2 expression, increased the Pparg1, Hmox1, TRx gene expression	[68]

There is a difference in effectiveness of Pio between women and men. In women, Pio is more effective, and has the same effect in men when we administer it at a lower dose. To talk about this sex difference, we can mention the pharmacological mechanisms which are based on differences in body fat distribution [69-71] and in sex hormones (for example: androgens, estrogens) [72-74] and pharmacokinetic mechanism have been considered. Pio is partially metabolized to M-II, M-III and M-IV to exert its pharmacological activity. [75-77] Metabolic studies of Pio using liquid chromatography/tandem mass spectrometry and 1H-nuclear magnetic resonance led to characterization of the above mentioned metabolites: the parent compound, (+/-)-5-(p-hydroxybenzyl)-2-4-thiazolidinedione (M-I), (+/-)-5-[p-[2-(5-ethyl-2-pyridil)-2-hydroxyethoxy]benzyl]-2,4-thiazolidinedione (M-II), (+/-)- 5-[p-[2-(5-acetyl-2-pyridyl)ethoxy]benzyl]2,4-thiazolidinedione (M-III), (+/-)-5-[p-[2-[5-(1-hydroxyethyl)-2- pyridyl]ethoxy]benzyl]-2,4-thiazolidinedione (M-IV), (+/-)-5-[p-[2-(5-carboxymethyl-2-pyridyl)ethoxy]- benzyl]-2,4-thiazolidinedione (M-V), and (+/-)-5-[p-[2-(5-carboxy-2- pyridyl)ethoxy]benzyl]-2,4-thiazolidinedione (M-VI). Pio is metabolized by cleavage of aliphatic C-O bond to lead to M-I, hydroxylation of aliphatic methylene groups to form M-II and M-IV, oxidation of M-IV to give M-III, oxidation of the ethyl group to form M-V, and oxidative loss of terminal carbon to lead to M-IV. Part of metabolites exists as conjugated form. [75]

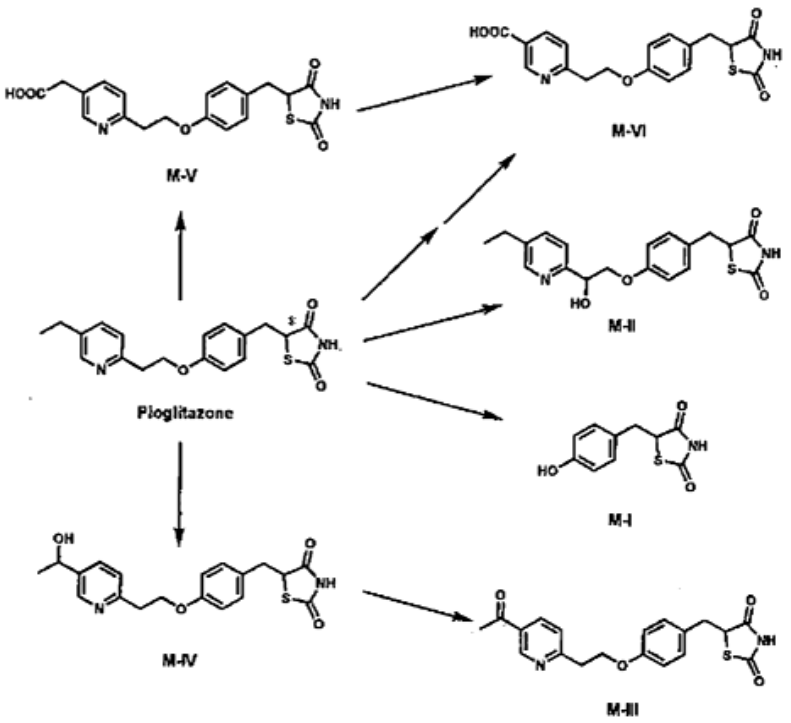

Figure 4: Pio's metabolic pathways (*: ^{14}C-labeled position) [75]

According to *Tanis et al*. the activities of the active metabolites were equivalent to or more efficient than the activity of Pio. This experiment used 3T3-L1 cells. [78] We can say that the in vivo use of Pio means not only the effect of Pio itself but also the effect of the active metabolites.

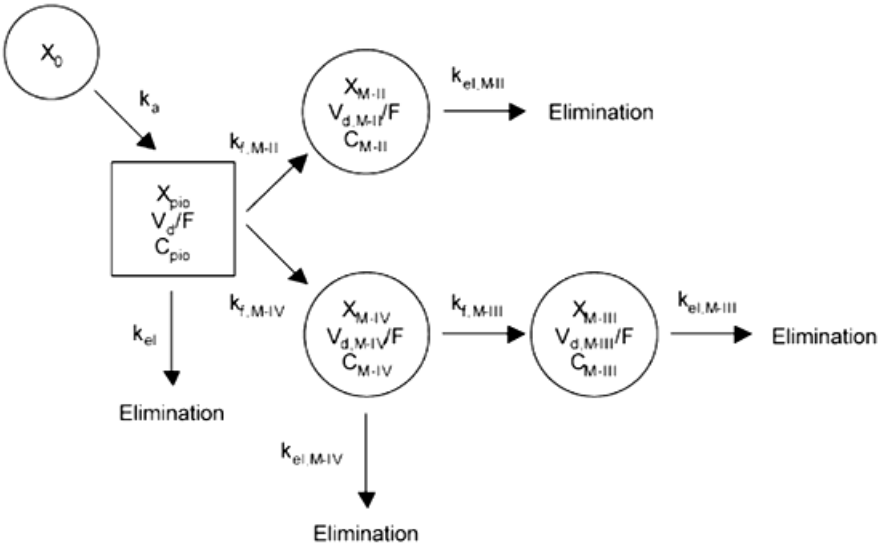

Figure 5: A kinetic one-compartment model for Pio including absorption and metabolism pathways [79]

The parameters represent the amount of Pio in the absorption compartment (X_0), the amounts of Pio, M-II, M-III and M-IV (X_{Pio}, X_{M-II}, X_{M-III}, X_{M-IV}), k_a is the absorption rate constants, $k_{f,M-II}$, $k_{f,M-III}$, $k_{f,M-IV}$ are the formation rate constant of each metabolite, k_{el}, $k_{el,M-II}$, $k_{el,M-III}$, $k_{el,M-IV}$ are the elimination rate constants and V_d/F, $V_{d,M-II}/F$, $V_{d,M-III}/F$, $V_{d,M-IV}/F$ are the volume of distribution of each compound. **[79]**

In a study, after single oral administration of Pio, C_{max} (the peak plasma level) of Pio and AUCs (the area under the plasma concentration-time curve) of Pio, M-III and M-IV were significantly high in the female rats. AUC of M-IV on female rats was three-times higher than in male rats, and AUCs of Pio and M-III were 1.5-times higher in females than in males. The majority of Pio is metabolized in the liver and excreted in urine and faeces in rats. [75] In that paper they suggest that the plasma level of Pio had significantly increased in the female rats, in male rats the apparent elimination rate of Pio was significantly higher. In that experiment they administered orally Pio in 0.5 mg/kg/day, and a higher dose was used (10 mg/kg/day), and there was no accumulation of Pio or its active metabolites was found in either male or female rats. Since Pio acts mainly on white adipose tissue, they measured the concentrations of Pio and the active metabolites in white adipose tissue, but they did not find any significant difference in $K_{p,app}$ (the apparent white adipose tissue-to-plasma concentration ratio) values in male or female rats. [79]

3. Aims

According to our idea, there are three methods, which can model the transplantation's process. In the first part, we test Pio in one concentration - which is mostly recommended by literature - and we administer it in various stages of ischemia-reperfusion in IRI model. In the second part, we focus on Pio in several doses and the possible toxic effect, and the selection of the most effective dose are our goals. In the third part, we make from the above mentioned two methods a mixture, and the purpose is to test the drug in different concentrations in a perfusion-reperfusion model, which is the closest to the clinical application.

1. We aim to investigate the effect of PPAR-γ agonist Pioglitazone in ischemia-reperfusion injury. The parameters are superoxide-dismutase activity, TNF-α, IL-1β, IL-6 and catalase activity. We would like to prove that Pio can reduce IRI by decreasing the level of inflammatory cytokines and it help to maintain the balance between ROS and antioxidants. First, we would like to examine the histological changes by hematoxylin-eosin staining. In our first experimental method, it is a crucial question if there is any difference in the timing of treatment. The aim is to show that Pio has positive effect on injured kidneys.
2. We suppose that Pio has different effect on kidneys and liver. The aim is to ascertain this deviation regarding *in situ* whole body perfusion. Another aim to this method is to investigate the extent of endoplasmic reticulum stress in case of liver and kidneys. Our expectation is that Pio decrease the ER stress. To measure this, we would like to perform Western-blot analysis.
3. We would like to compare the *in situ* perfusion to the *in situ* perfusion-reperfusion model. To demonstrate this difference, we use the same kits and experimental conditions, and we would like to measure the catalase activity, SOD activity and the level of inflammatory cytokines, furthermore, the histological parameters to evaluate the visible changes in kidneys. Our aim is to answer the question, either *in situ* perfusion or *in situ* perfusion-reperfusion result the better outcome in the case of kidneys.

4. Materials and methods

4.1. Ischemia-reperfusion injury model

4.1.1. Animal model

Thirty male Wistar rats of the same age, weighting between 250-300 g, were used for this study. The rats were housed in standardized cages, under standard conditions (temperature was 25±2 ℃, in air filtered room), with 12/12-hour light and dark cycle and were fed with standard rat chow and water *ad libitum*. The study protocol was approved by the National Scientific Ethical Committee on Animal Experimentation. (Number: BA02/2000-38/2019.)

4.1.2. Experimental protocol

The animals were divided into three groups (10 rats in each group). The first group was the control group, operation and ischemic condition was induced but they got the solvent of the drug (PBS+10 % DMSO) intraperitoneal (i.p.) one hour prior to the ischemic period. The second group was treated with Pioglitazone (20 mg/kg) one hour prior to the ischemic period, ordered from Sigma-Aldrich, St. Louis, Missouri, USA. In these two groups, after 60 minutes of ischemia, reperfusion was started for 90 minutes. The third group was first anesthetized, then ischemia was induced and prior to the start point of reperfusion, we administered 20 mg/kg Pioglitazone i.p. and after it the reperfusion was induced. To standardize the study, all procedures were performed at similar time points in all groups. The drug was freshly solved into PBS + 10 % DMSO solution before the administration.

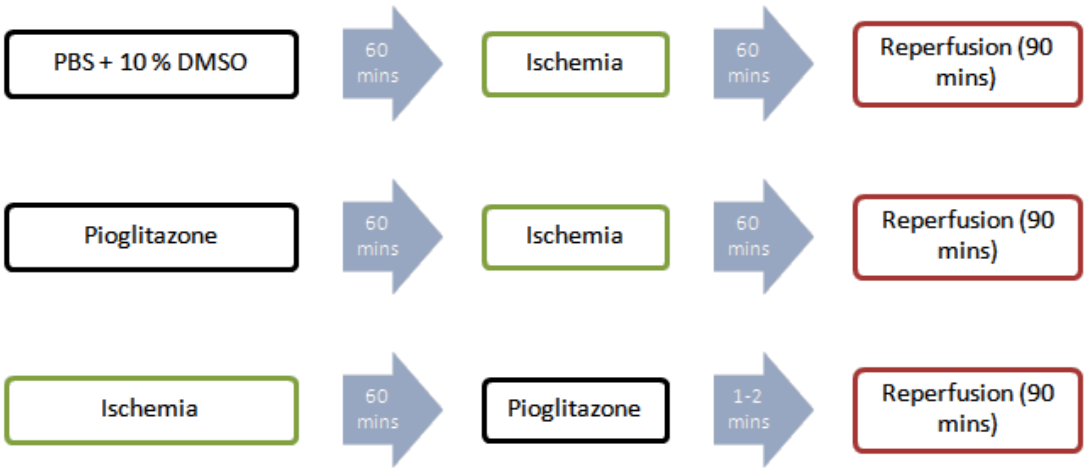

Figure 6: Investigation groups: 1: control, 2: IR preconditioning with Pio, 3: IR postconditioning with Pio (IR – ischemia-reperfusion; Pio – Pioglitazone)

4.1.3. Surgical procedure

The rats were preoperatively anesthetized with an intraperitoneal (i.p.) application of a mixture consisting of ketamine (2.7 ml/kg) and diazepam (2.7 ml/kg). The ratio was 1:1. The skin of the abdomen was depilated using an animal depilatory agent. During the operation, the animals were placed on a heated pad and ECG monitoring was also used. After median laparotomy, we administered heparin into mesenterial vein, then the left renal pedicle was clamped by the microaneurysm clamp. The clamp was removed 60 minutes after clamping and the rat was monitored alive for 90 minutes during reperfusion period. After 90 minutes, the animals were sacrificed, and kidney and blood samples were collected. The blood samples were centrifuged, and plasma was collected and stored at -80 °C. Kidney samples were stored immediately at -80 °C within individual containers. This method is widely used. [80, 81]

4.2. *In situ* whole body perfusion model

4.2.1. Animal model

Sixty male Wistar rats of the same age, weighting between 250-300 g, were used for this study. The rats were housed in standardized cages, under standard conditions (temperature

was 25±2 °C, in air filtered room), with 12/12-hour light and dark cycle and were fed with standard rat chow and water *ad libitum*. The study protocol was approved by the National Scientific Ethical Committee on Animal Experimentation. (Number: BA02/2000-38/2019.)

4.2.2. Experimental protocol

Animals were divided into six groups, ten rats in each group. The first group was the control (sham operated). The second group was the KH control (KH – Krebs-Henseleit buffer), the third group was the KH + Pio 10 mg/kg, the fourth group was the KH + Pio 20 mg/kg, the fifth group was the KH + Pio 30 mg/kg and the sixth group was the KH + Pio 40 mg/kg. To standardize the study, all procedures were performed at similar time points in all groups. The drug was freshly solved into PBS + 10 % DMSO solution before the administration. The perfusion solution's temperature was maintained on 20 °C during the whole study. (*Table 2*)

Table 2: The groups with the treatments

Groups (n=10 in each groups)	Treatments
1. group	control (sham operated)
2. group	perfused with KH
3. group	perfused with KH + 10 mg/kg Pio
4. group	perfused with KH + 20 mg/kg Pio
5. group	perfused with KH + 30 mg/kg Pio
6. group	perfused with KH + 40 mg/kg Pio

4.2.3. Surgical procedure

The rats have been preoperatively anesthetized with an intraperitoneal (i.p.) application of a mixture consisting of ketamine (2.7 ml/kg) and diazepam (2.7 ml/kg). The ratio was 1:1. The skin of the abdomen was depilated using an animal depilatory agent. During the operation, the animals were placed on a heated pad and ECG monitoring was also used. After middle laparotomy, the infrarenal abdominal aorta and inferior vena cava were dissected and heparin (400 IU/kg) was administered into mesenterial vein. After a few minutes, the inferior vena cava was catheterized (22 gauge) and the in situ whole body perfusion was initiated. In each experimental group, 200 ml perfusion solution was used. The perfusion equipment was set to 150 ml/h, and for one animal the perfusion lasted 80 minutes in all experimental groups. At the same time with catheterizing the vein, on the

aorta we made a small incision, and it was the outflow of the perfusate which was removed from the abdominal cavity by suction. (*Fig. 7*) The sham group was handled as a treated group without perfusion, in which the blood circulation was intact. During the experiment, the animals were sacrificed by bleeding out. At the end of the perfusion protocol, kidneys and liver were taken out and were placed immediately at -80 °C within individual containers.

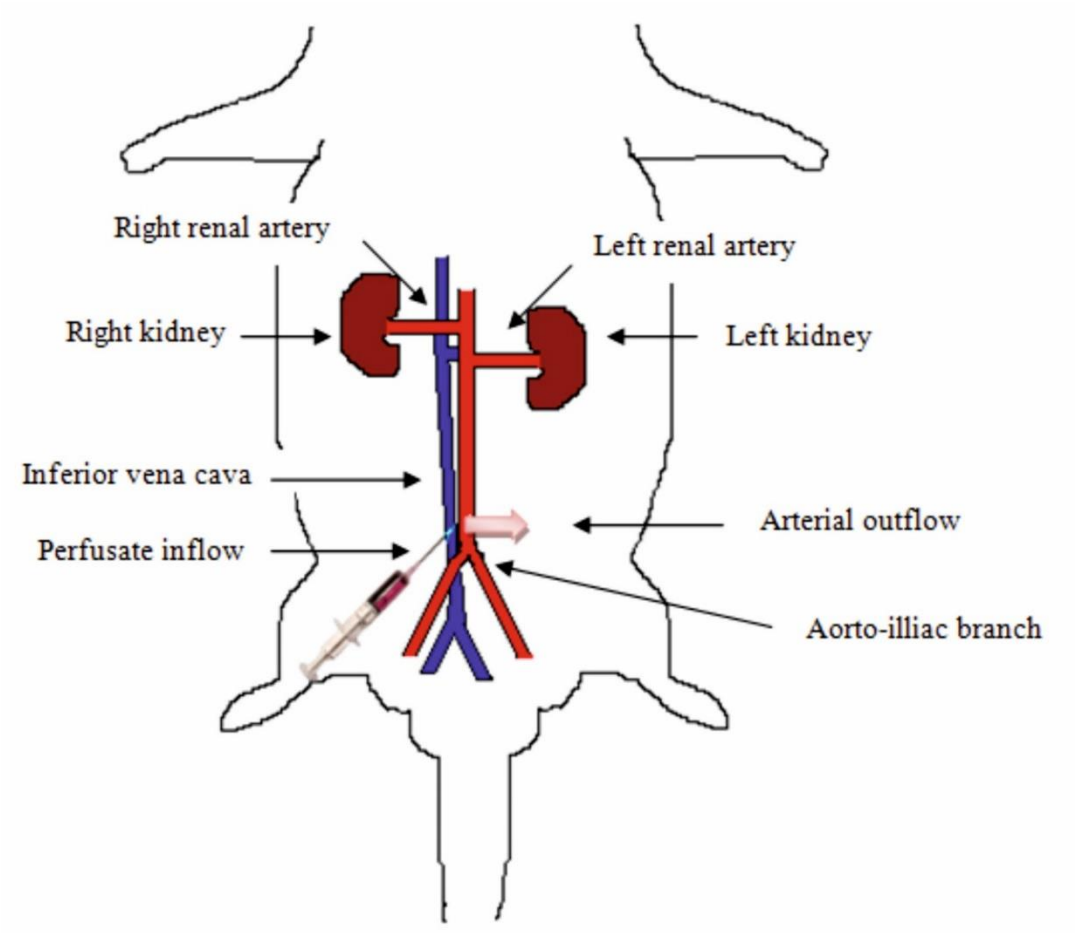

Figure 7: Schematic representation of an animal regarding *in situ* perfusion model

4.3. *In situ* perfusion-reperfusion model

4.3.1. Animal model

Sixty male Wistar rats of the same age, weighting between 250-300 g, were used for this study. The rats were housed in standardized cages, under standard conditions (temperature was 25±2 ℃, in air filtered room), with 12/12-hour light and dark cycle and were fed with standard rat chow and water *ad libitum*. The study protocol was approved by the National Scientific Ethical Committee on Animal Experimentation. (Number: BA02/2000-38/2019.)

4.3.2. Experimental protocol

Animals were divided into ten groups, six rats in each group. To standardize the study, all procedures were performed at similar time points in all groups. The drug was freshly solved into PBS + 10% DMSO solution before the administration. The perfusion solution's temperature was maintained on 20 ℃ during the whole study. (*Table 3*.)

Table 3: The experimental groups, six rats in each group

Control groups	Treated groups
KH control	KH perfused
KH + 10 mg/kg Pio_control	KH + 10 mg/kg Pio perfused
KH + 20 mg/kg Pio_control	KH + 20 mg/kg Pio perfused
KH + 30 mg/kg Pio_control	KH + 30 mg/kg Pio perfused
KH + 40 mg/kg Pio_control	KH + 40 mg/kg Pio perfused

4.3.3. Surgical procedure

The rats have preoperatively anesthetized with an intraperitoneal (i.p.) application of a mixture consisting of ketamine (2.7 ml/kg) and diazepam (2.7 ml/kg). The ratio was 1:1. The skin of the abdomen was depilated using an animal depilatory agent. During the operation, the animals were placed on a heated pad and ECG monitoring was also used. After middle laparotomy, the abdominal and suprarenal aorta section and vena cava were dissected, and heparin was administered into mesenterial vein. Then the suprarenal aorta was clamped by a microsurgical vascular clamp and the abdominal aorta was catheterized (22 gauge). The perfusion machine was connected to the catheter and the flow was maintained in each group on 110 ml/h. The perfusate volume was 55 ml. After 30 minutes

the perfusion was finished, and the catheter was removed and the whole was clamped. (*Fig. 8*) The reperfusion phase lasted 60 minutes. Thereafter the animals were sacrificed by bleeding out. The blood was centrifuged, and plasma and kidney samples were placed immediately at -80 °C within individual containers.

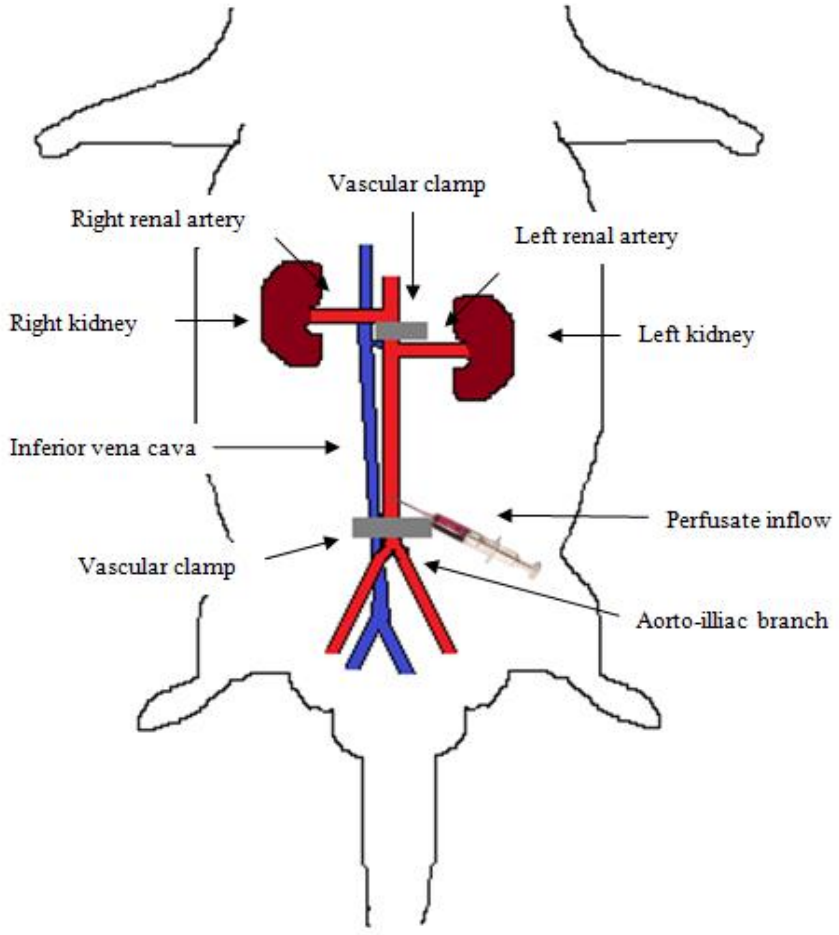

Figure 8: Schematic representation of an animal in *in situ* perfusion-reperfusion model

4.4. Analytical methods

4.4.1. Biochemical analysis

We measured the level and activity of IL-1β, IL-6, TNF-α, SOD and catalase from the kidney samples to verify the results. SOD and catalase activity was measured (inflammatory cytokines were not analyzed, due to lack of reperfusion) from kidney and liver samples regarding *in situ* perfusion model. IL-1β, IL-6 and TNF-α are the main indicators of inflammatory response and their level in blood and tissue samples were

studied by the Rat IL-1 beta ELISA Kit, Rat IL-6 Elisa Kit, Rat TNF alpha ELISA Kit (Abcam, Cambridge, UK) following the manufacturer's protocol. To measure the level of oxidative stress, we used the Superoxide Dismutase Activity Assay Kit and Catalase Activity Assay Kit (Abcam, Cambridge, UK) following the manufacturer's protocol.

4.4.2. Histopathological analysis

Hematoxylin eosin staining protocol

Tissues were fixed in 10% neutral buffered formalin, embedded in paraffin, cut in 3 micrometers thick sections with a rotational microtome (Microm HM 325, Thermo Scientific Ltd.) and mounted on coated glass microscope slides. After deparaffinization and rehydration, samples were stained with hematoxylin, bluing was performed with tap water, and tissues were stained with eosin, dehydrated in alcohol, cleared in xylene and mounted with permanent mounting medium.

4.4.3. Western blot protocol

Kidney and liver tissue samples were frozen in liquid nitrogen, then manually pulverized in mortar and dissolved in ice-cold lysis buffer (containing 50 mM Tris, pH 7.4, 150 mM NaCl, 1 mM EGTA, 1 mM Na_3VO_4, 100 mM NaF, 5 μM $ZnCl_2$, 10% glycerol, and 1% Triton X-100 plus 10 μg/ml of the protease inhibitor aprotinin). Lysates were subjected to centrifugation at 40 000 x g at 4 °C for 30 minutes, and then the protein concentration of the supernatants was determined using Protein Assay Dye Reagent Concentration (Bio-Rad Laboratories, Inc., Hercules, California, USA) and light absorption measurement at 595 nm. Samples containing 30 μg of denatured total protein have been prepared and loaded onto 10% polyacrylamide gels. Proteins separated based on size have been electro-blotted for half an hour onto PVDF membranes using the Trans-Blot Turbo semi-dry system (Bio-Rad Laboratories, Inc., Hercules, California, USA), then blocked in 3% BSA dissolved in Tris-buffered saline containing 0.2% Tween 20. Probing of the membranes with the primary antibodies (caspase12 and XBP1 [Sigma-Aldrich, St. Louis, Missouri, USA]) diluted 1:1000 in the blocking solution followed at 4 °C overnight. Binding of the antibodies to the membrane was detected by a secondary anti-rabbit IgG conjugated to horseradish peroxidase (Santa Cruz Biotechnology, Inc., Dallas, Texas, USA) diluted 1:10,000. The enhanced chemiluminescent signal was visualized using a G:box gel documentation system (Syngene, India). All membranes were then stripped from the antibodies and detected again as above for possible loading differences using a primary

antibody against GAPDH (Cell Signaling Technology, Danvers, Massachusetts, USA) at a dilution rate of 1:3000. ImageJ software was used to analyze the blots, and for the statistical evaluation, one-way analysis of variance (ANOVA) with Bonferroni correction was used.

4.4.4. Statistical analysis

For statistical evaluation, one-way analysis of variance (ANOVA) was used, followed by adequate post hoc tests (Dunnett's, Sidak) for multiple comparisons. All Western blots were performed independently in triplicates. Regarding statistical evaluation, one-way ANOVA was used, followed by post-hoc analysis of Bonferroni. All data are represented as the mean ± SD. The difference was considered statistically significant when the p-value was less than 0.05 and classified by asterisks as follows: $p<0.05$ (*); $p<0.001$ (**); $p<0.0001$ (***). The statistical analysis was calculated through GraphPad Prism software for Windows (version 5.03).

5. Results and discussion

5.1. Ischemia-reperfusion injury model

5.1.1. Results

First, to answer the question, that Pio in which setting could reduce more the oxidative stress, we performed SOD (*A*) and catalase activity (*B*) assays. All kidney samples were used, and the mean values can be seen on *Fig. 9.* All the control groups depict significant difference compared to the ischemic groups. However, we cannot detect any crucial deviation between the two treated groups. *Fig.9. A.* (control: 21.3295 ± 1.9240 vs. control ischemic: 53.36 ± 2.8284 $p<0.0001$; control ischemic 53.36 ± 2.8284 vs. pre-Pio 1h ischemic: 42.6309 ± 1.1779 and pre-Pio reperfusion ischemic: 41.531 ± 1.6525 $p<0.005$; pre-Pio 1h control: 23 ± 2.9698 vs. pre-Pio 1h ischemic: 42.6309 ± 1.1779 $p<0.001$; pre-Pio reperfusion control: 23.3029 ± 2.4082 vs. pre-Pio reperfusion ischemic: 41.531 ± 1.6525 $p<0.001$) *Fig.9. B.* (control: 1.445 ± 0.0777 vs. control ischemic: 2.25 ± 0.0707 $p<0.0001$; control ischemic: 2.25 ± 0.0707 vs. pre-Pio 1h ischemic: 1.875 ± 0.0353 and pre-Pio reperfusion ischemic: 1.9061 ± 0.05103 $p<0.005$; pre-Pio 1h control: 1.625 ± 0.0353 vs. pre-Pio 1h ischemic: 1.875 ± 0.0353 $p<0.005$; pre-Pio reperfusion control: 1.595 ± 0.0788 vs. pre-Pio reperfusion ischemic: 1.9061 ± 0.0510 $p<0.005$)

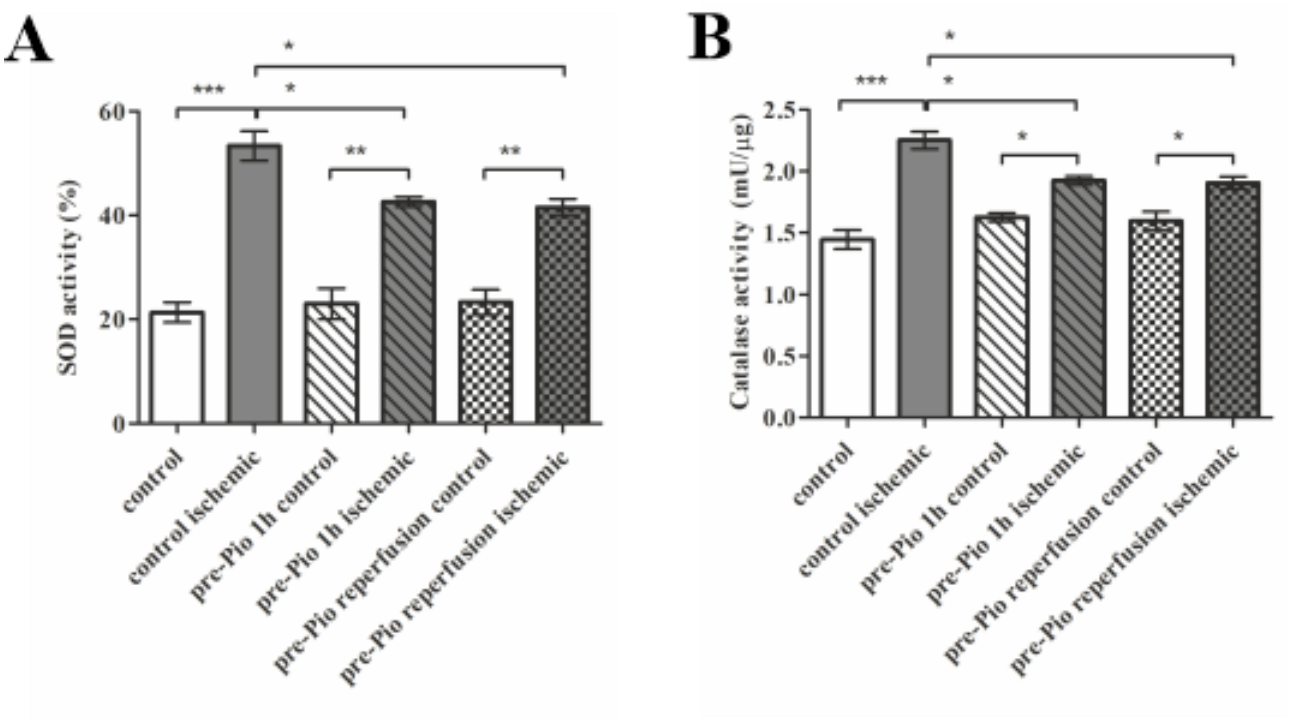

Figure 9: SOD (%) and Catalase (mU/µg tissue) activity from kidney samples (n=10). ELISA quantification of superoxide dismutase (SOD) and catalase activity. A statistically significant difference can be detected between the control ischemic and the treated experimental groups. Data is represented as mean ± SD. ($p<0.005$ - *; $p<0.001$ - **; $p<0.0001$ - ***)

The expression of IL1-beta, IL6 and TNF-alpha was detected by ELISA. All samples were analyzed, and the mean and the standard deviation values are represented in *Fig.10*. Control samples depict statistically significant difference compared to treated groups, and the most effective time point of the treatment is in case of IL1-beta (*A*) the Pio treatment before the initiation of reperfusion period (pre-Pio reperfusion ischemia). However, the Pio treatment before the induction of ischemic period effectively reduced the IL6 (*B*) and TNF-alpha (*C*) expressions compared to the control ischemic group. However, there were not any significant difference between the two treated groups, pre-Pio 1h ischemic and pre-Pio reperfusion ischemic. *Fig.10. A.* (control: 191.5 ± 12.0208 vs. control ischemic: 654.5 ± 20.5061 $p<0.0001$; control ischemic: 654.5 ± 20.5061 vs. pre-Pio 1h ischemic: 571.5 ± 12.0208 $p<0.005$; pre-Pio 1h control: 214.5 ± 21.9203 vs. pre-Pio 1h ischemic: 571.5 ± 12.0208 $p<0.0001$; pre-Pio reperfusion control: 227 ± 21.2132 vs. pre-Pio reperfusion ischemic: 501.5 ± 12.0208 $p<0.0001$) *Fig.10. B.* (control: 92.5 ± 10.6066 vs. control ischemic: 453.68 ± 16.0089 $p<0.0001$; control ischemic: 453.68 ± 16.0089 vs. pre-Pio 1h ischemic: 381 ± 12.7279 $p<0.005$; pre-Pio 1h control: 110 ± 14.1421 vs. pre-Pio 1h ischemic: 381 ± 12.7279 $p<0.0001$; pre-Pio reperfusion control: 122.5 ±17.6777 vs. pre-

Pio reperfusion ischemic: 406 ± 8.4852 $p<0.0001$) *Fig.10. C*. (control: 17.5 ± 3.5355 vs. control ischemic: 153.5 ± 16.2634 $p<0.0001$; control ischemic: 153.5 ± 16.2634 vs. pre-Pio 1h ischemic: 66.5 ± 4.9497 and pre-Pio reperfusion ischemic: 92 ± 9.8994 $p<0.001$ and $p<0.005$; pre-Pio 1h control: 25.5 ± 7.7781 vs. pre-Pio 1h ischemic: 66.5 ± 4.9497 $p<0.005$; pre-Pio reperfusion control: 21.5 ± 14.8492 vs. pre-Pio reperfusion ischemic: 92 ± 9.8994 $p<0.001$)

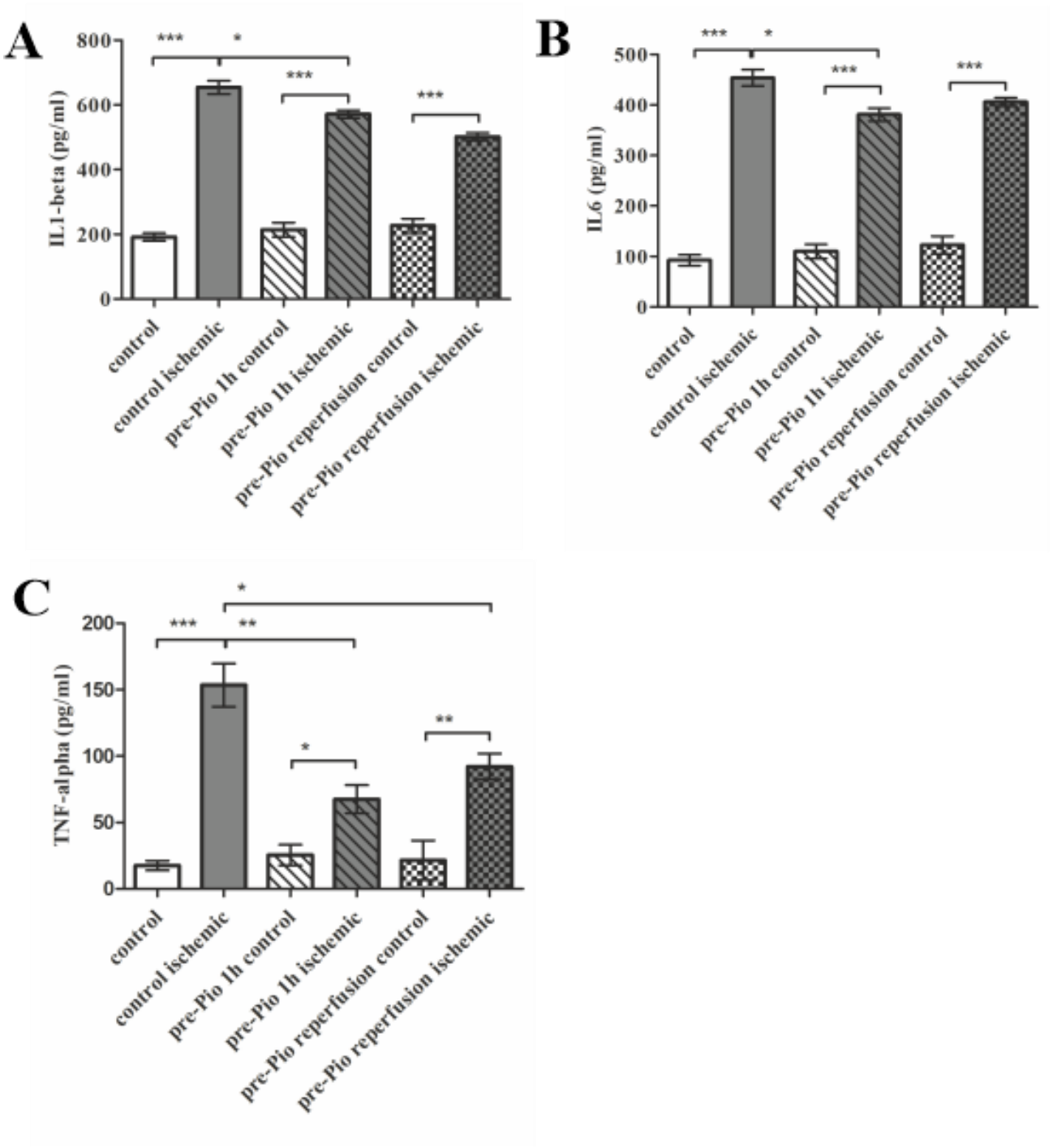

Figure 10: Inflammatory cytokines; IL1-beta, IL6 and TNF-alpha expressions (n=10). The quantification of cytokines was performed with ELISA. Statistically significant difference can be observed between control ischemic and pre-Pio 1h ischemic group in all three diagrams. Data is represented in mean ± SD. ($p<0.005$ - *; $p<0.001$ - **; $p<0.0001$ - ***)

The histopathological analysis did not depict any apoptotic or oncotic sign in control groups in *Fig.11*. The basic tissue structure was kept. However, in control ischemic group, the swelled tubules and Bowman's capsules and eosinophilia represent the damage in kidney tissue. The difference between the treated groups is in the swelled endothelial

tubules. In pre-Pio 1h ischemic group, arrowhead shows the swelling, but not the same extent as in the previous group, the pre-Pio 1h ischemic. The pre-Pio reperfusion ischemic correlates to the control's tissue structure. The histopathological findings correlate to the ELISA and Western blot results.

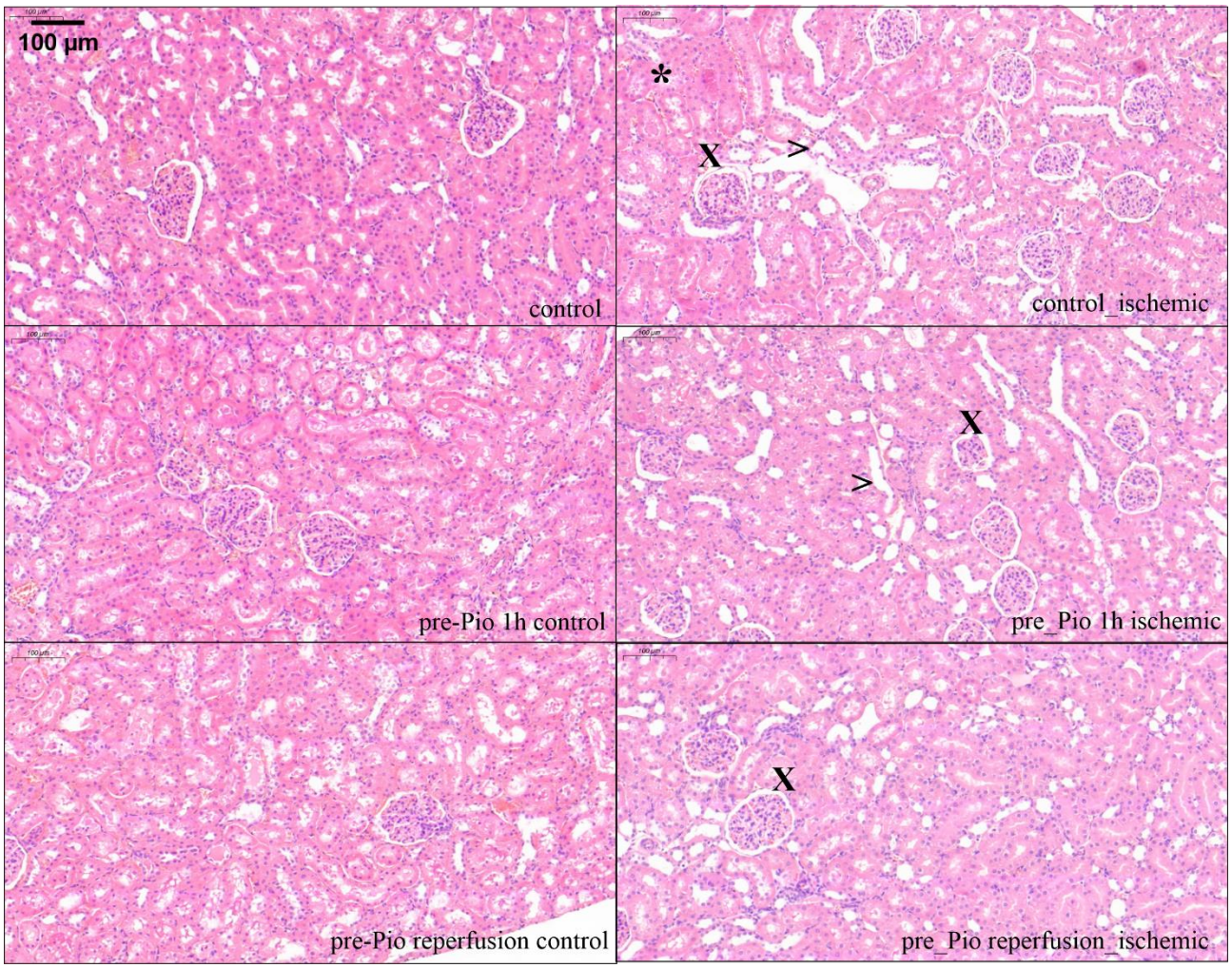

Figure 11: Hematoxylin-eosin staining of kidney samples. Magnification: 11.3x. In the control groups the tissue structure was kept. In untreated control-ischemic group, several damages can be detected. The pre-Pio 1h ischemic and pre-Pio reperfusion-ischemic groups depict swelling of Bowman's capsule. However, the pre-Pio reperfusion ischemic group correlates to the control group's section, and the basic tissue structure is mainly kept. Asterisk (*) depict eosinophilia, arrowhead (>) represents the swelling of endothelial tubules and X's show the swelling of Bowman's capsule.

Caspase 12 expression was measured performing Western blot. The bands of the experimental groups can be seen in *Fig. 12*. Control samples' bands are weaker and the untreated, but ischemic (control ischemic) group's pixel density is significantly higher compared to control and pre-Pio 1h ischemic group. However, the Pio administration before reperfusion initiation (pre-Pio reperfusion ischemic group) could reduce the

Caspase 12 expression, not in a statistically significant extent. (control: 0.9739 ± 0.0761 vs. control ischemic: 1.945 ± 0.2192 p<0.001; control ischemic: 1.945 ± 0.2192 vs. pre-Pio 1h ischemic: 1.2849 ± 0.1201 p<0.005)

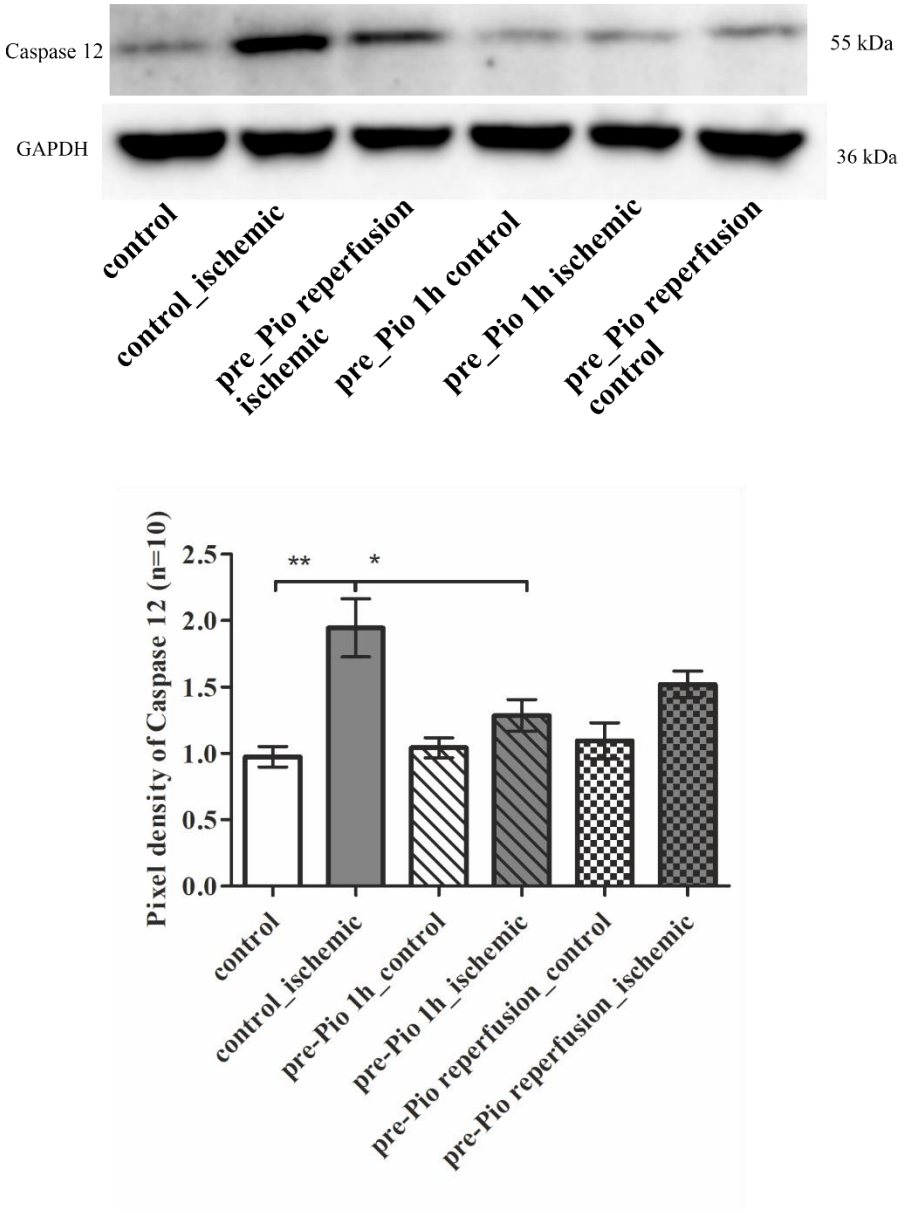

Figure 12: Pixel density of Caspase 12 Western blots. Blots and relative quantities are depicted, and GAPDH serves as a normalization control.

Figure 13 represents the pixel density and Western blot bands of XBP1s (56 kDa molecular weight) protein expression. Treated groups decreased the XBP1s expression compared to control ischemic group. Control ischemic and the treated groups differed significantly to their controls. (control: 0.9883 ± 0.1249 vs. control ischemic: 3.195 ± 0.0777 p<0.0001; control ischemic: 3.195 ± 0.0777 vs. pre-Pio 1h ischemic: 2.17 ± 0.2687

and pre-Pio reperfusion ischemic: 2.25 ± 0.2121 p<0.005; pre-Pio 1h control: 1.12 ± 0.1838 vs. pre-Pio 1h ischemic: 2.17 ± 0.2687 p<0.005; pre-Pio reperfusion control: 0.9262 ± 0.2459 vs. pre-Pio reperfusion ischemic: 2.25 ± 0.2121 p<0.001)

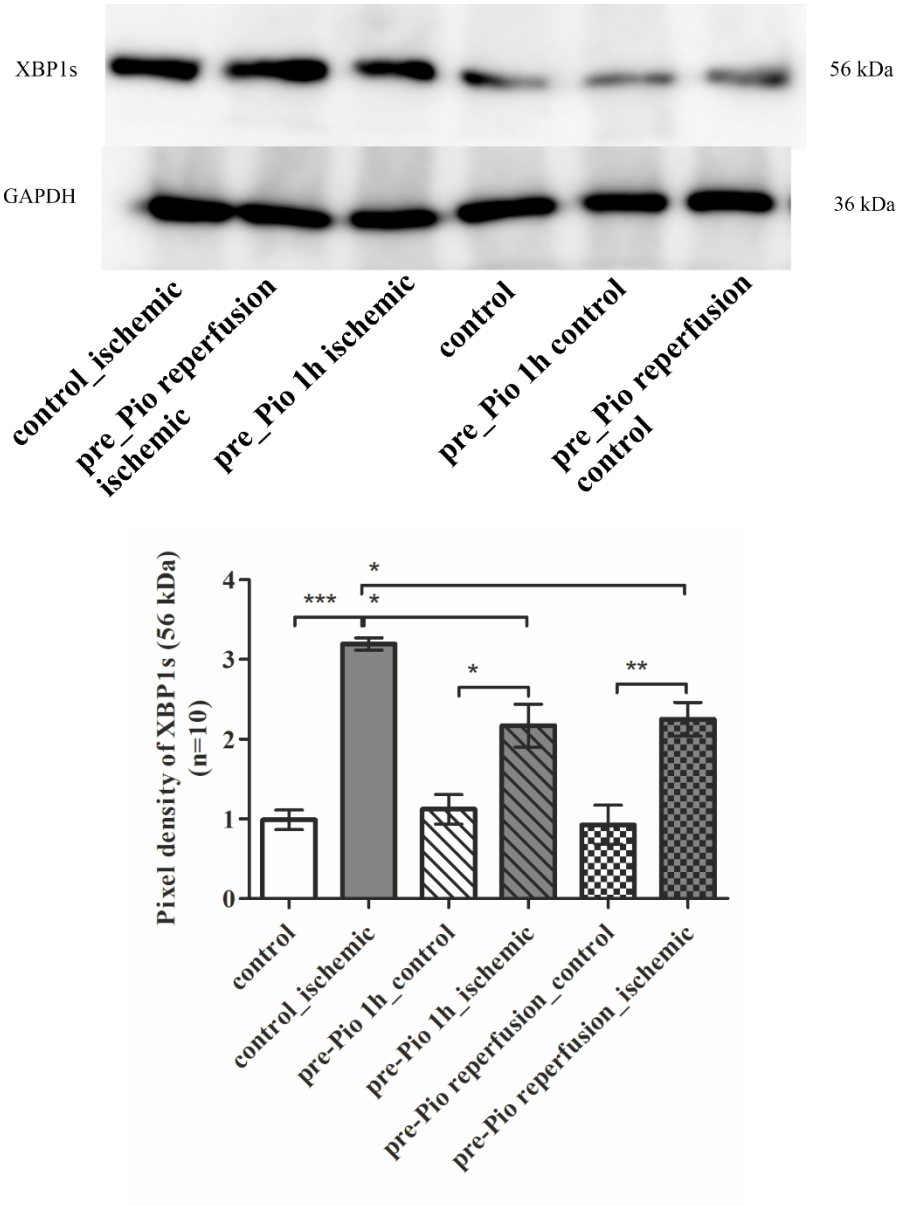

Figure 13: Pixel density of XBP1s (56 kDa) Western blots. XBP1s protein's expression are represented from kidney samples. GAPDH serves as a normalization control.

The protein expression of XBP1u (29 kDa) is represented in *Fig.14*. Control groups show significant deviation from non-treated but ischemic (control ischemic) and treated groups. The most effective time point was the Pio administration one-hour before the initiation of ischemia compared to control ischemic group in decreasing XBP1u expression. However, the pattern of the bands depicts as in *Fig.13*., any significantly between control ischemic

and pre-Pio reperfusion ischemic groups were not ascertained by statistical analysis. (control: 0.996935 ± 0.08777 vs. control ischemic: 2.2 ± 0.14142 $p<0.0001$; control ischemic: 2.2 ± 0.14142 vs. pre-Pio 1h ischemic: 1.57 ± 0.04243 $p<0.005$; pre-Pio 1h control: 0.925 ± 0.10607 vs. pre-Pio 1h ischemic: 1.57 ± 0.04243 $p<0.005$; pre-Pio reperfusion control: 0.876 ± 0.17819 vs. pre-Pio reperfusion ischemic: 1.715 ± 0.09192 $p<0.001$)

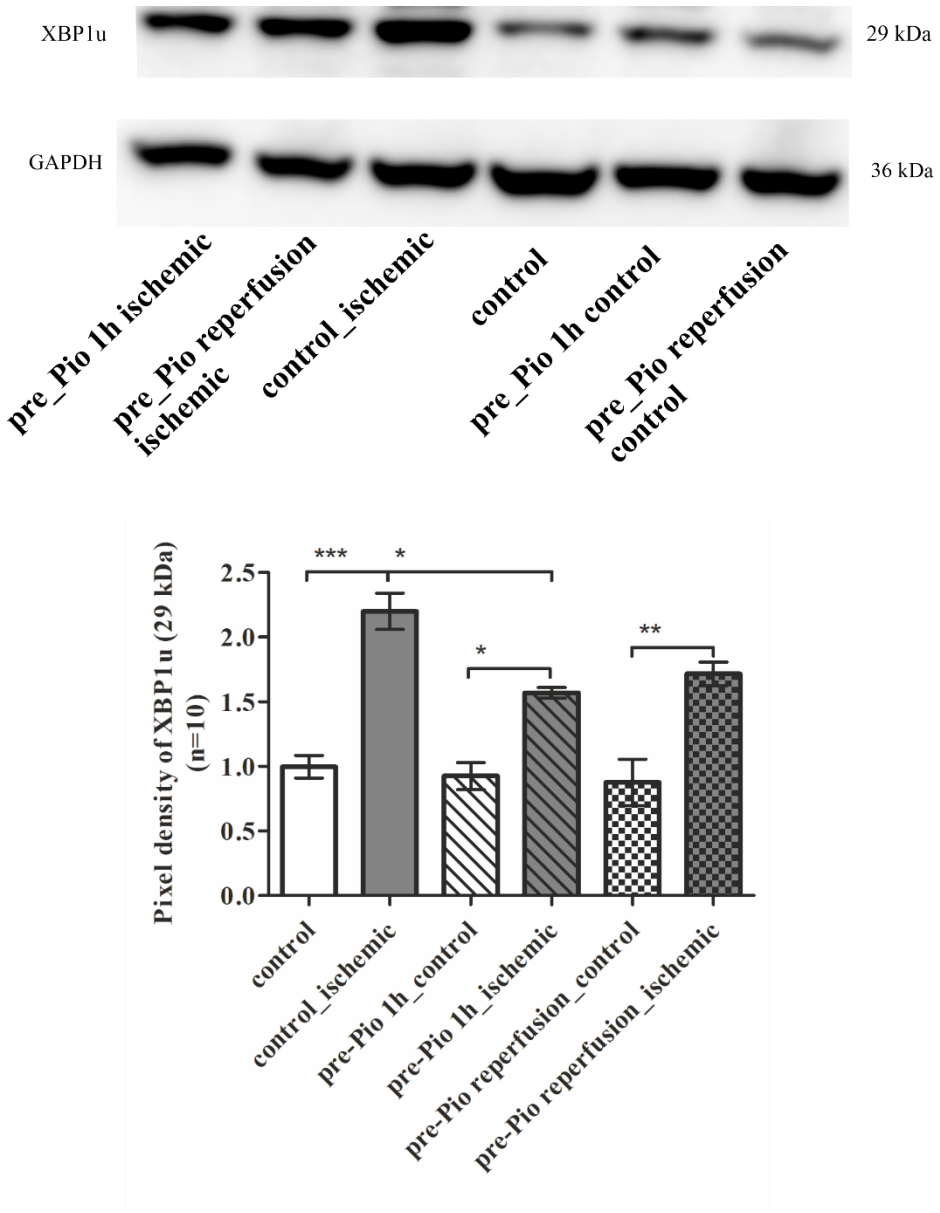

Figure 14: Pixel density of XBP1u (29 kDa) Western blots. Expression of XBP1u protein is displayed, where GAPDH serves as a normalization control.

5.1.2. Discussion

IRI can cause severe problems in microcirculation and it may lead to patient's higher morbidity and prolonged hospitalization. Cellular dysfunction, interstitial oedema, inflammatory cytokine expression can lead to cell death. The length of the ischemic period has a great importance on the caused damage. In case of our IRI model, the 45 mins ischemic and 90 mins reperfusion periods were used, since in international literature it is recommended. A longer ischemic period (over 60 minutes) causes irreversible injury and significant cell death, which has adverse consequences on the organ function and can lead to renal failure. [82, 83]

Based on international literature, gender and/or sexual steroids may play a role in the recovery from ischemic injury in non-renal organs, and postischemic organ dysfunction is influenced by gender and sexual steroids. Müller et al. published an article about this issue and according to the published papers' conclusions, male Wistar rats were chosen in all experiments presented in this thesis. They concluded that female rats have relative protection against postischemic renal failure, furthermore, in intact males the effects of androgens upon ischemic kidney damage seemed to be mediated by endothelin-induced vascular changes. [84] Robert et al. examined the gender difference and sex hormone production in rodent renal ischemia reperfusion injury and repair. Overall, after ischemia, renal function recovery and tissue injury was gender-dependent and the differences were associated with a modulation of sex hormone production and a modification of tissue remodeling and proliferative cell processes. [85]

IRI method has a wide variety in application. Huge number of drugs were tested whether they antioxidant, anti-inflammatory or kidney protective agents are or not. Our aim was to characterize the effect of Pio administration in a single dose but different time point. Therefore, SOD and catalase activity, inflammatory cytokines (IL1-beta, IL6, TNF-alpha) were measured, histopathological changes and endoplasmic reticulum stress markers (Caspase 12, XBP1s and XBP1u) were analyzed. For further experiments, first the conclusion was made and the Pio treatment one-hour before initiation of ischemic period was preferred, since this experimental group represented our expectations and served as answer to hypotheses. The pre-Pio 1h ischemic group could decrease not only the oxidative stress markers and inflammatory cytokines, but also the ERS markers. Thus, we hypothesize that Pio has a preventive effect in IRI against oxidative stress, inflammation and ERS, and the consequent cell death.

IRI method has been used since 1980's and several drugs and agents were applied to determine their effects and applicability. Our department has numerous publications and contribution with other researchers among IRI induction and pre- and post-conditional methods. [86-88]

According to international literature, Pio's anti-inflammatory, antioxidant, and kidney-protective effects were proven (*Table 1.*). However, the beneficial function in ERS regarding IRI rat kidney model was not examined yet. Therefore, to compare the two treated groups' influence on above mentioned markers, as a pilot study, we considered it important to compare their effects, the results of which served as a basis for further experiments such as in situ perfusion model and in situ perfusion-reperfusion model.

Previously as above was mentioned, Pio's protective effect against oxidative stress and inflammation were examined and proven, however, ERS markers were not examined in IRI setting with Pio yet. However, NRK-52E cells were exposed by hypoxia/reoxygenation injury and the cytoprotective effect of Pio was declared. [89]

In conclusion, histopathological findings correlate to the ELISA and Western blot results since Pio was not depicted any toxic effects in the administered dose and decreased the inflammation by diminishing the expression of the examined cytokines and reduced the oxidative stress. ERS markers depicted that Pio has a protective impact against the organelle's stress upon IRE1 pathway. However, further experiments are needed to determine the most effective quantity of Pio regarding IRI and our other models.

5.2. *In situ* whole body perfusion model

5.2.1. Results

5.2.1.1. Rat kidney results

SOD and catalase activity ELISA's were performed to specify the most effective dosage of administered Pio regarding in situ perfusion rat model. In *Fig.15*. a dose dependent manner can be observed. Except the 10 mg/kg Pio group, a significant difference was not only between the KH (perfused without Pio) and treated groups (20, 30, 40 mg/kg Pio), but also in 10 mg/kg Pio and 30, 40 mg/kg Pio groups (*Fig.15. A.*), furthermore, in *Fig. 15. B.,* 10 and 20 mg/kg Pio groups depict significantly higher SOD and catalase activity compared to 40 mg/kg Pio group. *Fig.15. A.* (control $p<0.0001$ compared to all groups; KH: 58.19 ± 1.6546 vs. KH + 20 mg/kg Pio: 49.16 ± 1.6971 and KH + 30 mg/kg Pio: 44.992925 ± 1.4101 and KH + 40 mg/kg Pio: 42.6995 ± 2.4035 $p<0.005$, $p<0.001$, $p<0.001$; KH + 10 mg/kg Pio: 54.185 ± 1.6617 vs. KH + 30 mg/kg Pio: 44.992925 ± 1.4101 and KH + 40 mg/kg Pio: 42.6995 ± 2.4035 $p<0.005$, $p<0.001$) *Fig.15. B.* (control: 3.4503 ± 0.2408 vs. KH: 6.2016 ± 0.1674 and KH + 10 mg/kg Pio: 5.64 ± 0.2121 and KH + 20 mg/kg Pio: 5.1884 ± 0.1391 and KH + 30 mg/kg Pio: 4.835 ± 0.2051 and KH + 40 mg/kg Pio: 4.2435 ± 0.1747 $p<0.0001$, $p<0.0001$, $p<0.001$, $p<0.001$, $p<0.005$; KH: 6.2016 ± 0.1674 vs. KH + 20 mg/kg Pio: 5.1884 ± 0.1391 and KH + 30 mg/kg Pio: 4.835 ± 0.2051 and KH + 40 mg/kg Pio: 4.2435 ± 0.1747 $p<0.005$, $p<0.001$, $p<0.0001$; KH + 10 mg/kg Pio: 5.64 ± 0.2121 vs. KH + 40 mg/kg Pio: 4.2435 ± 0.1747 $p<0.001$; KH + 20 mg/kg Pio: 5.1884 ± 0.1391 vs. KH + 40 mg/kg Pio: 4.2435 ± 0.1747 $p<0.05$)

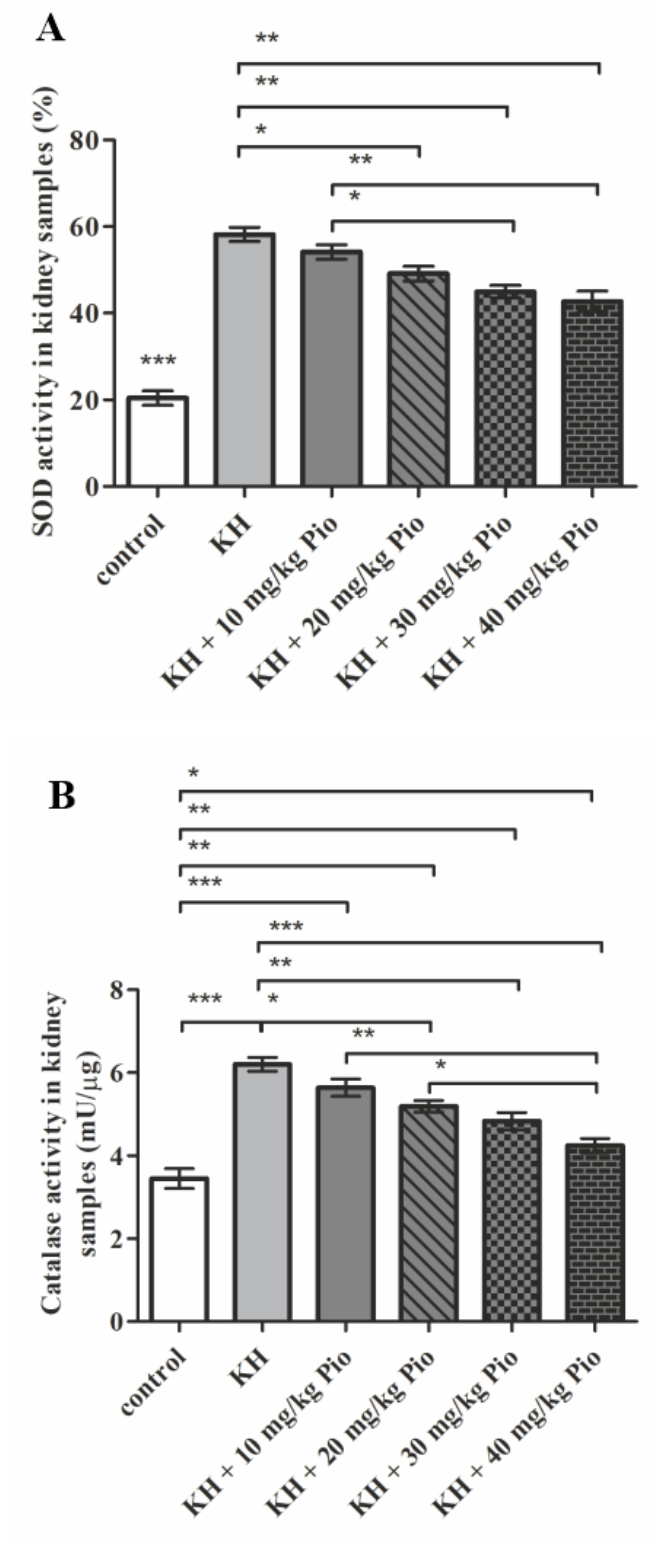

Figure 15: SOD (%) and catalase (mU/µg tissue) activity regarding kidney samples (n=10). Superoxide dismutase and catalase activity ELISA assay were performed. In a dose-dependent manner, the decrease of SOD and catalase activity can be observed compared to KH group. Data is represented in mean ± SD. ($p<0.005$ - *; $p<0.001$ - **; $p<0.0001$ - ***)

In the hematoxylin-eosin-stained histopathological analyses demonstrates, that the control group's main tissue structure was kept, and we cannot detect any signs of apoptosis or swelling the tubules or Bowman's capsules. However, in the Krebs-Henseleit-treated group (KH), the swelling of tubules and Bowman's capsule can be seen. In a dosage dependent manner, we can observe a positive effect of the drug, since in the KH+40 mg/kg Pio group, the tissue structure correlates to the control's sample. (*Fig. 16.)*

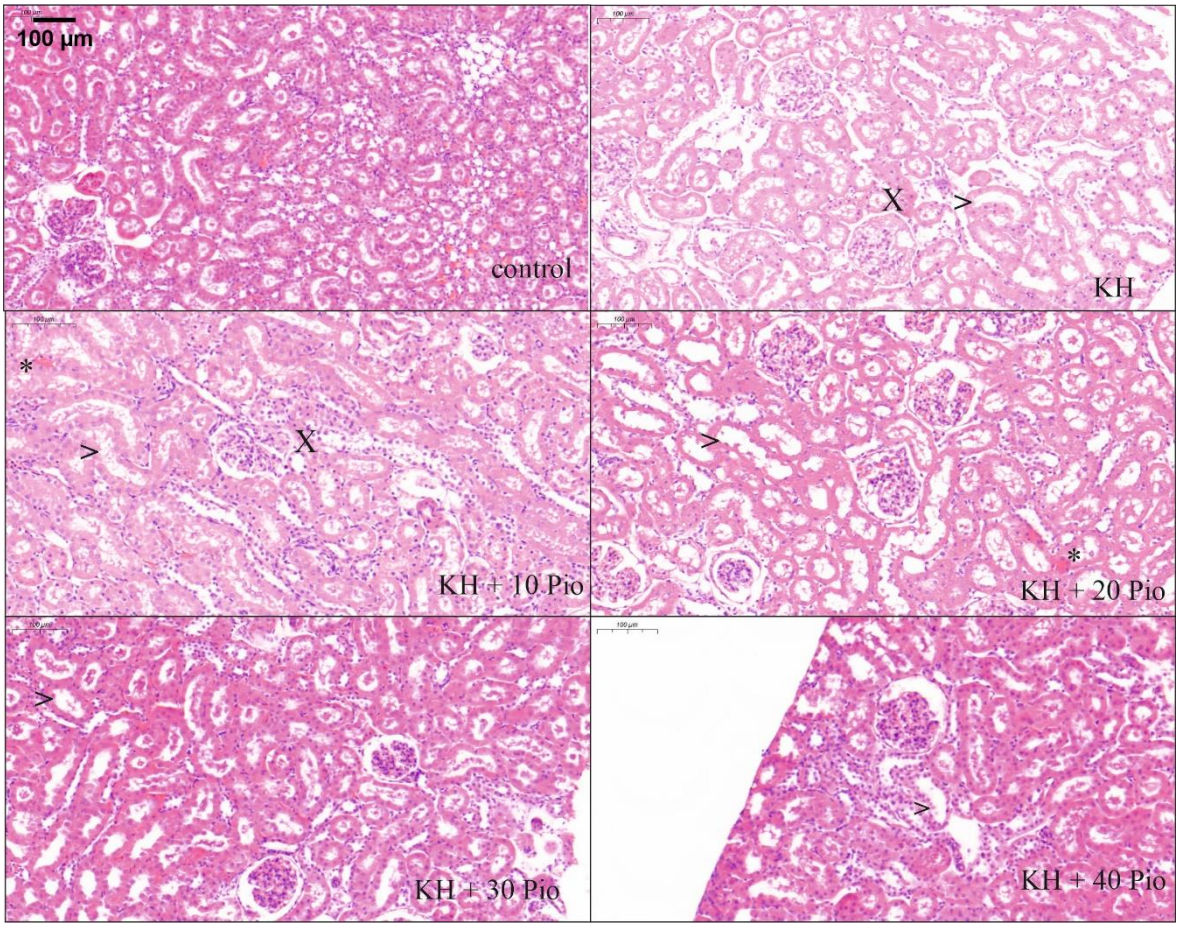

Figure 16: Hematoxylin-eosin staining, magnification: 11.3x. In the control group the tissue structure was kept. In KH and Pio treated groups, the damages are labeled with X's, which show the swelling of Bowman's capsule, the arrowhead (>) shows the swelling of endothelial tubules and the asterisk (*) represents eosinophilia.

To conclude the ERS decreasing effect of Pio, we performed Caspase-12 and XBP1 Western blots. In *Fig. 17.*, the positive effect of Pio can be detected in a dose-dependent manner. Western blot analysis was performed to examine the expressions regarding Caspase 12 and XBP1, both from liver and kidney samples, and explore the effect of the different doses regarding Pio. Expression of Caspase 12 was lower, dependent on the dosage of the drug regarding kidney samples. Pio was efficient in all the four administered

doses (control: 1.000 ± 0.1114 vs. KH: 3.3614 ± 0.4694 and KH + 10 Pio: 2.6794 ± 0.2788 p=0.0001 and p=0.05; KH: 3.3614 ± 0.4694 vs. KH + 20 Pio: 1.7900 ± 0.1420 and KH + 30 Pio: 1.5439 ± 0.3233 and KH + 40 Pio: 1.4373 ± 0.1519 p=0.0001; KH + 10 Pio: 2.6794 ± 0.2788 vs. KH + 20 Pio: 1.7900 ± 0.1420 and KH + 30 Pio: 1.5439 ± 0.3233 and KH + 40 Pio: 1.4373 ± 0.1519 p=0.0001).

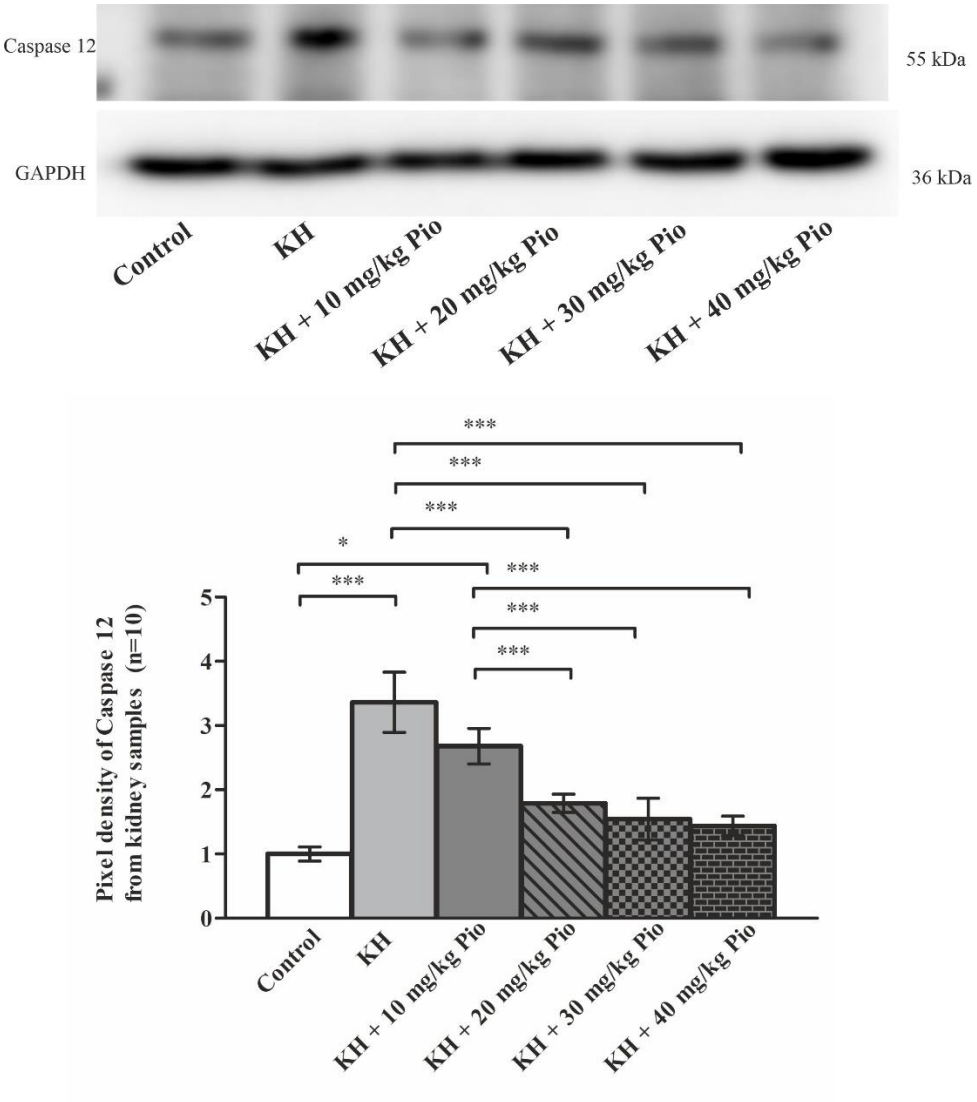

Figure 17: Western blot results for expression of Caspase 12 from kidney samples. GAPDH served as a normalization control. Blots and relative quantities of Caspase 12 are presented.

The Western blot analysis exhibited the significant differences in the case of XBP1 expression in kidney samples. The pattern of the pixel density appears similar in the case of XBP1s and XBP1u, however, the XBP1u had weaker bands and the expression of these proteins was lower. Nevertheless, the 40 mg/kg dose of Pio was significantly effective in

reducing the expression of both of the XBP1s and XBP1u (*XBP1s*: control: 1.0000 ± 0.1405 vs. KH: 5.6946 ± 0.8711 *p*=0.001; KH: 5.6946 ± 0.8711 vs. KH + 30 Pio: 2.0773 ± 0.3394 and KH + 40 Pio: 1.5163 ± 0.2277 p=0.5 and *p*=0.0001) (*XBP1u*: KH: 2.9561 ± 0.6434 vs. KH + 40 Pio: 1.5087 ± 0.3540 *p*=0.05; KH + 10 Pio: 2.8705 ± 0.7607 vs. KH + 40 Pio: 1.5087 ± 0.3540 *p*=0.05) (*Fig.18, 19.*).

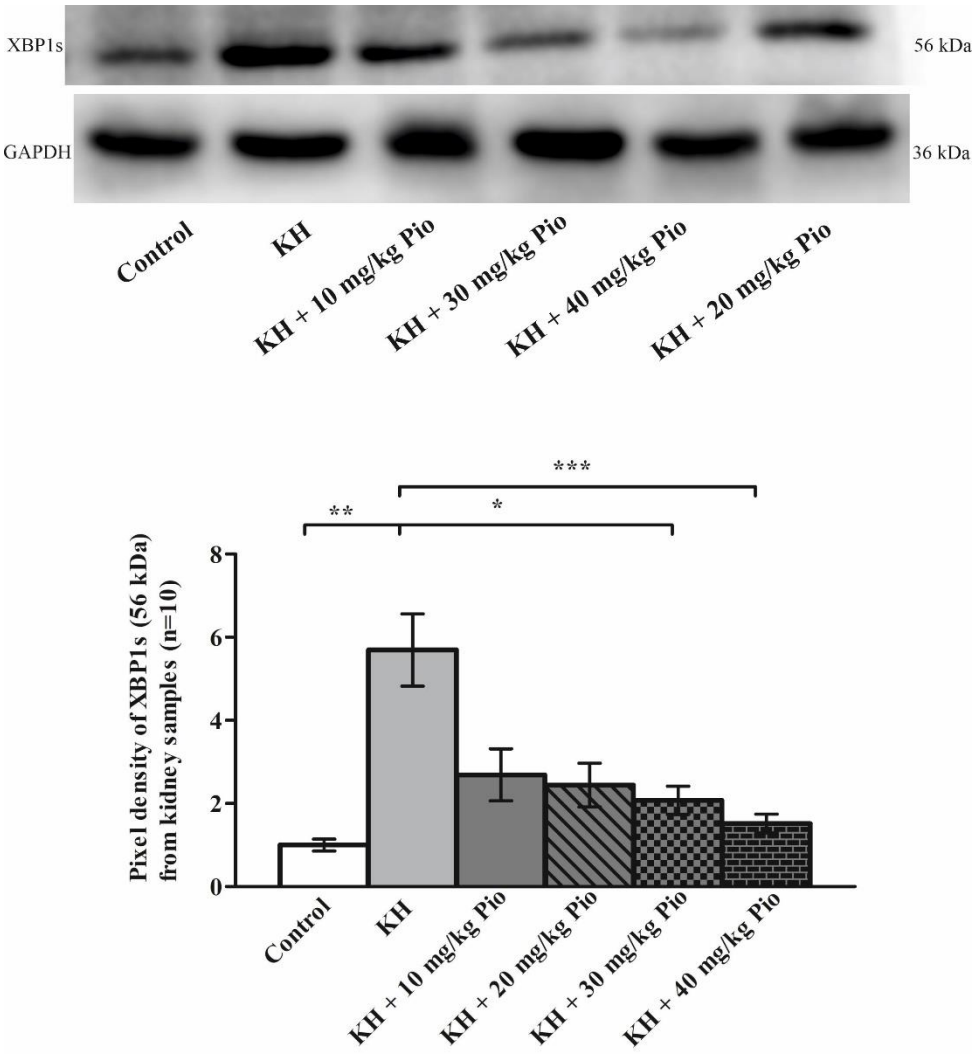

Figure 18: Protein expression of XBP1s (56 kDa) in pixel density. GAPDH served as a normalization control.

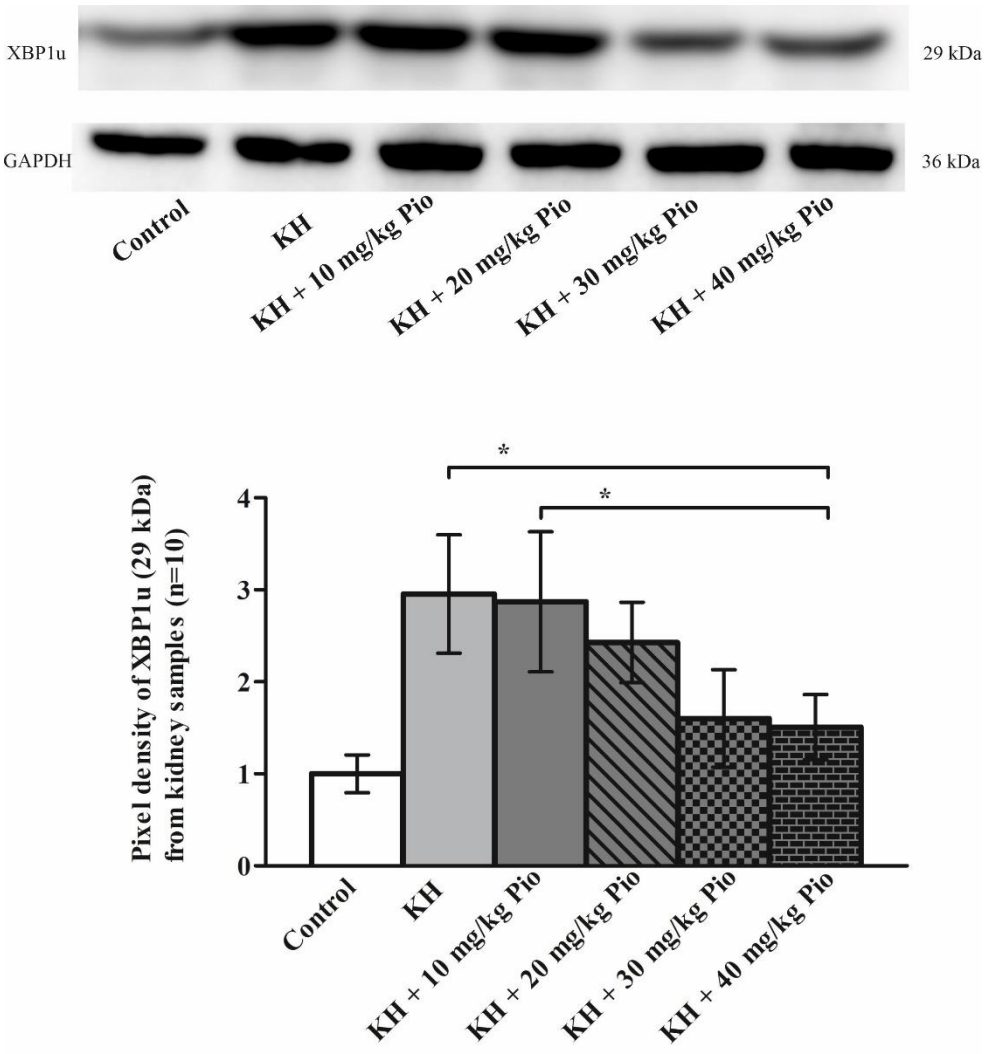

Figure 19: Protein expression of XBP1u (29 kDa) in pixel density from densitometry analyses. GAPDH served as a normalization control.

5.2.1.2. Rat liver results

Rat liver samples were also analyzed, and the effect of Pio regarding SOD and catalase activity was measured (*Fig.20*.) The above-mentioned dose-dependent manner can be observed. Control group depict significantly lower SOD (*Fig.20. A*.) and catalase (*Fig.20. B*.) activity compared to all other experimental groups. KH + 30 and 40 mg/kg Pio dosages significantly decreased the oxidative stress markers' activity compared to KH group. KH + 10 mg/kg Pio group similarly as KH group, had significantly higher SOD and catalase activity compared to KH + 40 mg/kg Pio group. *Fig.20. A.* (control: 21.421 ± 1.7946 vs. KH: 57.8 ± 3.1113 and KH + 10 mg/kg Pio: 53.65 ± 2.1921 and KH + 20 mg/kg Pio: 48.8 ± 2.5456 and KH + 30 mg/kg Pio: 44 ± 1.5556 and KH + 40 mg/kg Pio: 41.3 ± 1.4142 $p<0.0001$ in all cases except the last one where $p<0.001$; KH: 57.8 ± 3.111 vs. KH + 30 mg/kg Pio: 44 ± 1.5556 and KH + 40 mg/kg Pio: 41.3 ± 1.4142 $p<0.005$ and $p<0.001$; KH + 10 mg/kg Pio: 53.65 ± 2.1921 vs. KH + 40 mg/kg Pio: 41.3 ± 1.4142 $p<0.005$) *Fig.20. B.* (control: 4.05 ± 0.2121 vs. KH: 6.1874 ± 0.1593 and KH + 10 mg/kg Pio: 5.9263 ± 0.1042 and KH + 20 mg/kg Pio: 5.5951 ± 0.0921 and KH + 30 mg/kg Pio: 5.4467 ± 0.0802 and KH + 40 mg/kg Pio: 5.03 ± 0.2404 $p<0.0001$, $p<0.0001$, $p<0.001$, $p<0.001$, $p<0.005$; KH: 6.1874 ± 0.1593 vs. KH + 40 mg/kg Pio: 5.03 ± 0.2404 $p<0.001$; KH + 10 mg/kg Pio: 5.9263 ± 0.1042 vs. KH + 40 mg/kg Pio: 5.03 ± 0.2404 $p<0.005$)

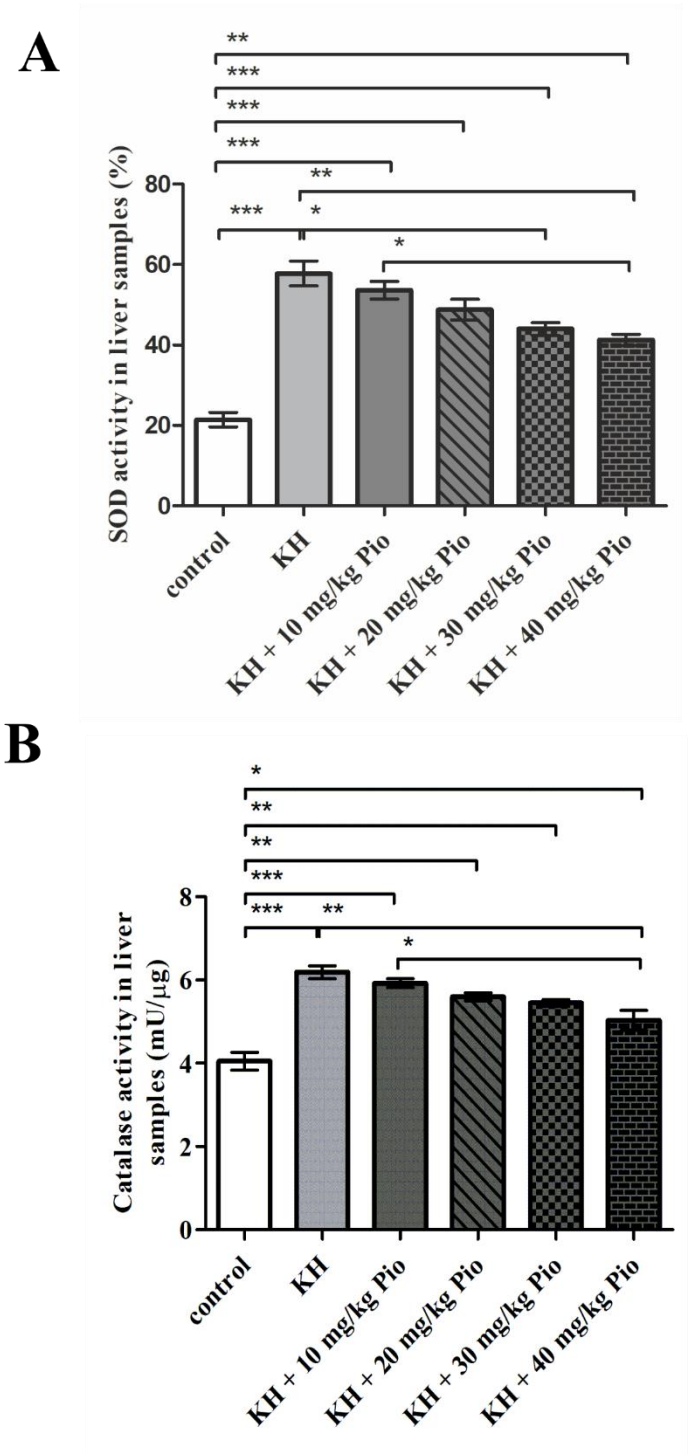

Figure 20: SOD (%) and catalase (mU/μg tissue) activity in liver samples (n=10). A dose dependent manner can be detected, both the SOD and catalase activity was decreased in the highest dosages of Pio, compared to KH group. Data is represented in mean ± SD. ($p<0.005$ - *; $p<0.001$ - **; $p<0.0001$ - ***)

Sections of rat livers from different treated groups were stained with hematoxylin and eosin and are presented in *Fig. 21*. The control group depicted a normal appearance. In the non-treated ischemic group (KH), we can detect pronounced nodular fibrosis of the parenchyma with hypertrophic hepatocytes and a swelling of the liver cells. In KH + 20

Pio and KH + 30 Pio groups, the basic tissue structure was mainly kept. We cannot detect any signs of oncosis or apoptosis among the treated groups. However, the changes are not significant, but viewing all the samples from the liver, the tendency of the protective effect of the administered drug can be very well detected.

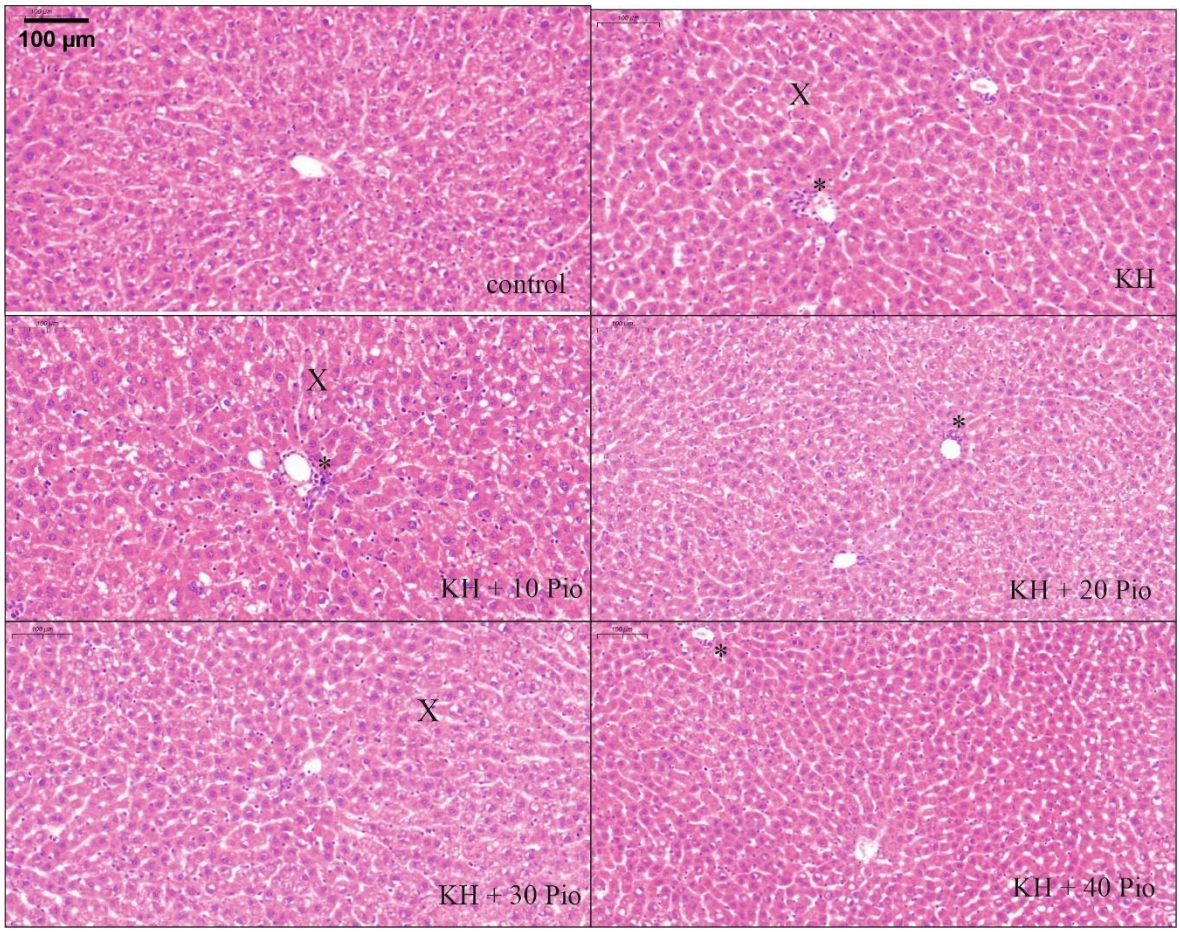

Figure 21: Staining: HE, magnification: 11.3x. The control group depicted a normal appearance. In the non-treated ischemic group, we detect pronounced nodular fibrosis of the parenchyma with hypertrophic hepatocytes. In the KH+20 Pio and KH+30 Pio groups, the basic tissue structure was mainly kept, and it is correlated to the control group. The X's point represents the swollen liver cells. The asterisk (*) shows nodular fibrosis of the parenchyma. We cannot detect any signs of oncosis nor apoptosis.

The expression of Caspase 12 regarding liver samples was significantly lower at 10 and 20 mg/kg Pio concentrations compared to the KH group (control: 1.0000 ± 0.0668 vs. KH: 3.0578 ± 0.4240 p=0.05; KH: 3.0578 ± 0.4240 vs. KH + 10 Pio: 2.0768 ± 0.2354 and KH + 20 Pio: 2.0591 ±0.4795 p=0.05) (*Fig.22).*

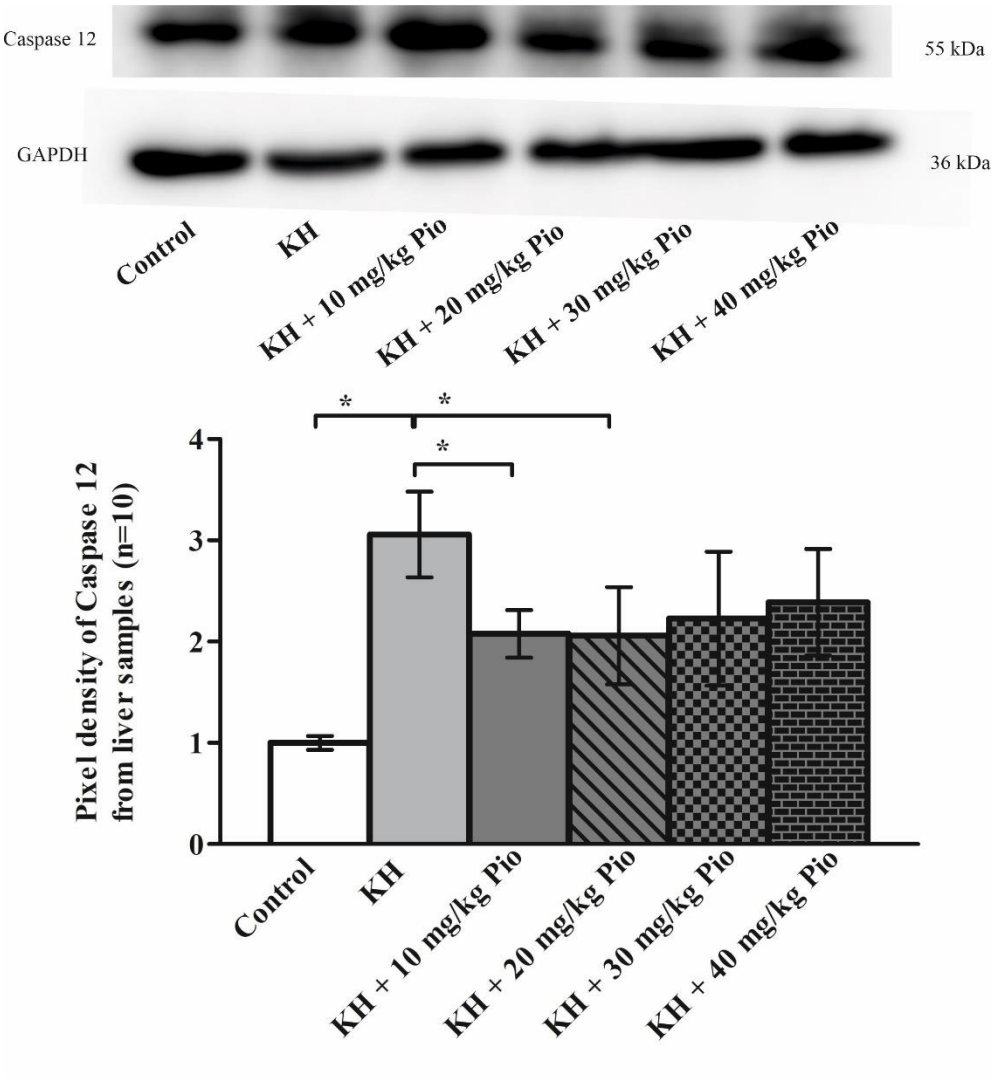

Figure 22: Drug treatment effect on expression of Caspase 12 from liver samples. GAPDH served as a normalization control.

In regards to the liver samples, the pattern of the bands appeared similar, however, the significantly effective dosages of Pio were the 30 and the 40 mg/kg analyzing XBP1s and XBP1u (*XBP1s:* control: 1.0000 ± 0.3736 vs. KH: 5.1087 ± 0.9549 *p*=0.001; KH: 5.1087 ± 0.9549 vs. KH + 30 Pio: 1.6936 ± 0.6389 and KH + 40 Pio: 1.6460 ± 0.3627 *p*=0.05) (*XBP1u*: control: 1.0000 ± 0.3655 vs. KH: 5.5834 ± 0.4024 *p*=0.01; KH: 5.5834 ± 0.4024 vs. KH + 30 Pio: 2.1226 ± 0.5372 and KH + 40 Pio: 1.9820 ± 0.5670 *p*=0.05) (*Fig.23, 24.).*

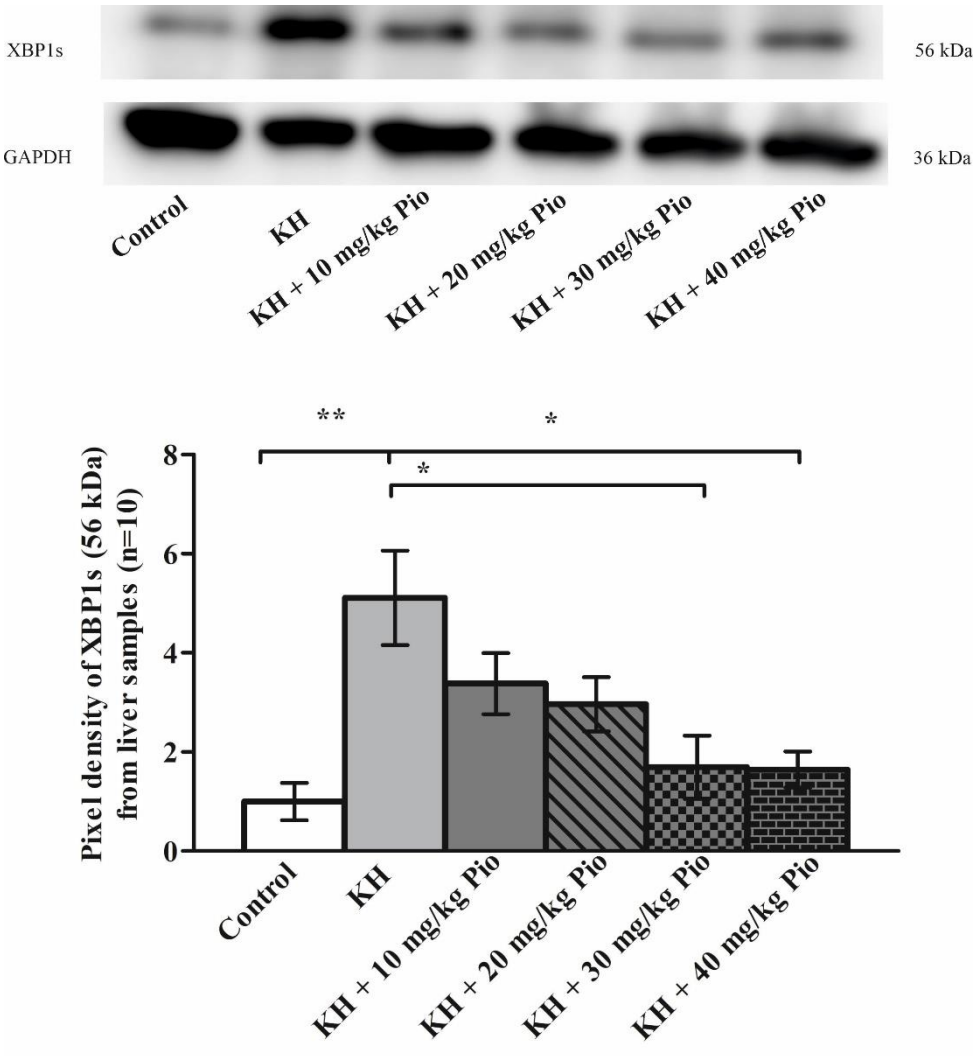

Figure 23: Validation of proteomic results using Western blot analysis of protein extracts from liver samples with antibodies against XBP1s (56 kDa). GAPDH was used as a normalization control

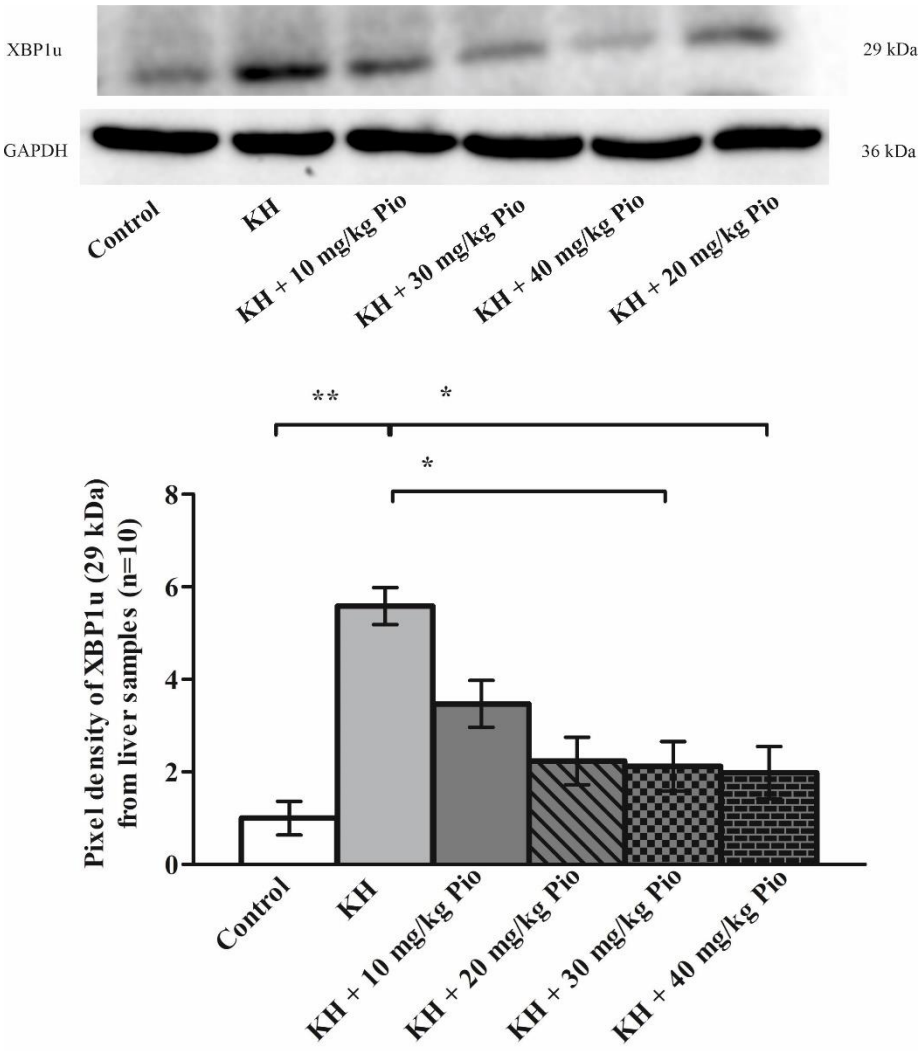

Figure 24: Protein expression of XBP1u (29 kDa). GAPDH was used as a normalization control.

5.2.2. Discussion

The use of a proper drug to decrease the damage caused by IRI plays a crucial role in transplantation and surgery. Approximately 30% of DGF following kidney transplantation is linked to IRI. [89] In our experiment, we chose a drug, Pio, which is used as an insulin sensitizer agent in treatment of type 2 diabetes and according to published literature, it has anti-inflammatory and antioxidant effects, and can decrease the amount of cell damage and apoptosis. The initial ERS response is a defensive mechanism to detect unfolded and misfolded proteins and maintain ER homeostasis. Prolonged perturbation of ER triggers the activation of an adaptive signaling pathway referred to as UPR. Long-term UPR activation can lead to apoptotic programmed cell death. [90, 92] In the present study, we demonstrated the use of Pio as an antioxidant agent can suppress the expression of ERS markers. Activation of IRE1 induces altered communication between ER and mitochondria, leading to dysfunction in mitochondria, metabolic imbalance, and cell death.

According to the results of SOD and catalase activity both from kidney and liver samples, a dose-dependent manner can be observed. Therefore, Pio in our novel in situ perfusion setting kept its antioxidant activity and protected kidneys and livers from cell death.

In the control group, we observed an enhanced expression of XBP1 and Caspase 12 and in a dose-dependent manner, Pio decreased the level of these ERS markers. These findings implicate Pio as a therapeutic target for the protection of ERS and ultimately cell death. The ratio of the XBP1s/XBP1u presents the activity of IRE1 pathways, however, different gels and membranes were used to detect XBP1s and XBP1u. Therefore, the calculation of the ratio is not necessarily reliable.

In our experimental model, we used the *in situ* whole body perfusion system to perfuse the kidneys and liver with Krebs-Henseleit solution modified with different dosages of Pio. Dosages used were 10, 20, 30 and 40 mg/kg Pio. The literature stated these concentrations can be protective against cell damage and apoptosis, and a higher dose level is more effective. [60, 64, 65, 91] This *in situ* perfusion model is suitable for mimicking the kidney or liver transplantation, when clinicians perfuse the organ with organ preservative solution, which helps to keep the organ functional and does not modify the cell structure. This process is inevitably necessary to decrease DGF and the consequently repeated transplantation. According to our results, we conclude Pio is suitable for reducing the cell damage and decreasing potential ERS and apoptosis.

Concentrations used were based on published literature. [60, 91] *Singh et al.* used in their experiment, 20 and 40 mg/kg Pio orally 1 h prior to IRI induction. According to their results, the 40 mg/kg dosage decreased the serum urine acid, blood urea nitrogen, serum nitrogen and microproteinuria concentrations. Furthermore, Pio in higher concentrations lowers the myeloperoxidase activity regarding tissue. They highlight the renoprotective effect of Pio in diabetic and non-diabetic models in reference to a kidney injury. [48, 50]

To set the perfusion time and perfusate volume, we used a perfusion fixation protocol and modified it since we used the vena cava as inflow and abdominal aorta section as outflow. The protocol recommended, passing through the abdominal aorta of the rat, we need 100 ml/h flow rate, thus, in our experiment, we initiated perfusion from 100 ml/h and then slowly increased the flow rate until the kidney and the liver became opalescent/white. According to the protocol, 250-300 ml of perfusate solution is optimal for one rat. [93]

The group of thiazolidinediones (TZDs) is the most widely studied PPARγ ligands. [42] Activation of PPARγ results in insulin sensitization by opposing the effect of TNFα in adipocytes and enhances glucose metabolism. Recent studies show Pio protects kidneys, myocardium, and the brain against IRI. [44-47] The potential role of Pio and other PPARγ agonists are nephroprotective agents and is demonstrated in non-diabetic models of renal injury (such as IRI and induced renal toxicity by a drug or chemical). [48, 93, 50] Renoprotective properties of Pio exhibits via facilitation of endothelium-dependent vasodilatation through amending abnormalities in NO production, [51] developing the antioxidant profile [52] and control of the expression of inflammatory mediators [53, 54] and apoptotic factors. [55] Additionally, with regards to the insulin sensitizing effect of Pio, it can reduce inflammation and consequences of oxidative stress in IRI model. [56] Experiments under hypoxic conditions on NRK-52 cells proved Pio increased the rate of cell survival and decreased the injury caused by hypoxia/reperfusion. According to TUNEL assay, they ascertain Pio can reduce the rate of apoptotised cells in treated groups compared with the untreated, hypoxia/reperfusion control group. [57] Furthermore, Pio has endothelial protective functionality which can be used beside methotrexate (MTX) therapy. [58]

Previously, the effect of Pio was studied in IRI rat models, yet, in an *in situ* perfusion set, we cannot find any results. To the best of our knowledge, this is the first study in which Pio effects were thoroughly examined regarding an *in situ* perfusion model in reference to ERS and histological changes. We conclude Pio is most effective in acute use and in higher concentrations.

5.3. *In situ* perfusion-reperfusion model

5.3.1. Results

A novel in-situ perfusion-reperfusion model was performed to test the effect of Pio in different dosages. As in the case of the other experimental models of this PhD thesis, the oxidative stress markers' activity and inflammatory cytokines' expression were measured and analyzed comparing the controls and perfused groups. *Figure 25* represents SOD (*A*) and catalase (*B*) activity and the degree of significance. KH + 40 Pio perf. group was the most effective and had the lowest SOD and catalase activity. *Fig.25. A.* (KH control: 20.7638 ± 1.2802 vs. KH perf: 78.16 ± 2.0789 $p<0.0001$; KH-perf: 78.16 ± 2.0789 vs. KH + 40 Pio perf: 59.645 ± 1.8597 $p<0.001$; KH + 10 Pio control: 20.55 ± 2.8991 vs. KH + 10 Pio perf: 75.495 ± 2.1284 $p<0,0001$; KH + 10 Pio perf: 75.495 ± 2.1284 vs. KH + 40 Pio perf: 59.645 ± 1.8597 $p<0.001$; KH + 20 Pio control: 22.0313 ± 1.5114 vs. KH + 20 Pio perf: 71.13 ± 2.6588 $p<0.0001$; KH + 30 Pio control: 19.345 ± 1.9163 vs. KH + 30 Pio perf: 67.9713 ± 2.855 $p<0.0001$; KH + 40 Pio control: 21.6495 ± 5.2050 vs. KH + 40 Pio perf: 59.645 ± 1.8597 $p<0.0001$) *Fig.25. B.* (KH control: 2.825 ± 0.1061 vs. KH perf: 5.04 ± 0.0849 $p<0.0001$; KH perf: 5.04 ± 0.0849 vs. KH + 30 Pio perf: 4.395 ± 0.1485 and KH + 40 Pio perf: 4.04 ± 0.0848 $p<0.001$ and $p<0.0001$; KH + 10 Pio control: 3.095 ± 0.1344 vs. KH + 10 Pio perf: 4.765 ± 0.1202 $p<0.0001$; KH + 10 Pio perf: 4.765 ± 0.1202 vs. KH + 40 Pio perf: 4.04 ± 0.0848 $p<0.001$; KH + 20 Pio control: 3.25 ± 0.1131 vs. KH + 20 Pio perf: 4.66 ± 0.1273 $p<0.0001$; KH + 20 Pio perf: 4.66 ± 0.1273 vs. KH + 40 Pio perf: 4.04 ± 0.0848 $p<0.005$; KH + 30 Pio control: 3.175 ± 0.1061 vs. KH + 30 Pio perf: 4.395 ± 0.1485 $p<0.0001$; KH + 40 Pio control: 3.245 ± 0.0849 vs. KH + 40 Pio perf: 4.04 ± 0.0861 $p<0.001$)

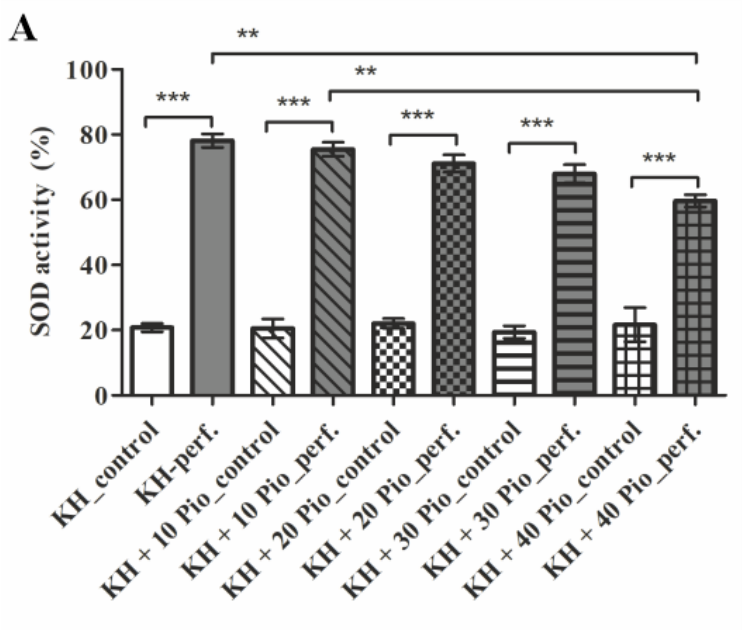

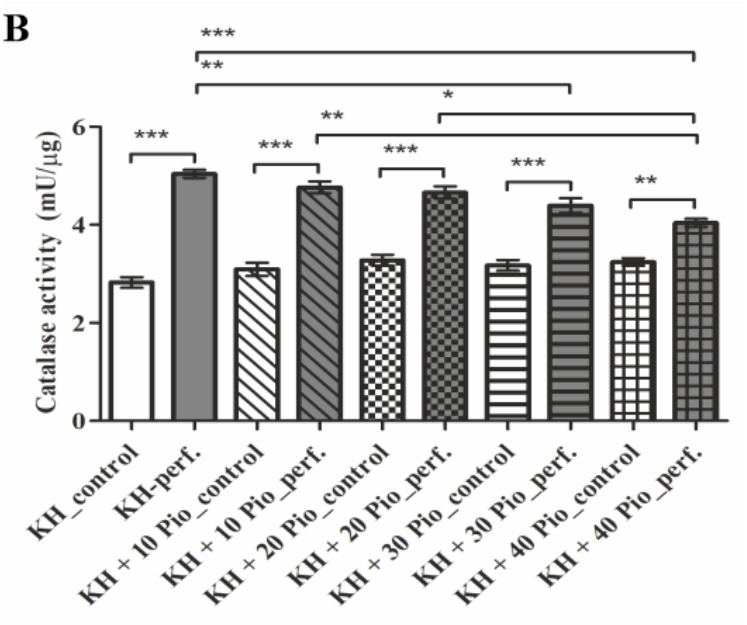

Figure 25: SOD (%) and catalase (mU/µg tissue) activity (n=10). The dose dependent tendence can be detected, like previous result with other experimental models. Data is represented in mean ± SD. ($p<0.005$ - *; $p<0.001$ - **; $p<0.0001$ - ***)

Inflammatory cytokines' expressions were measured by ELISA, and the groups were compared to each other (*Fig.26.*) We focused on the difference between the perfused but not treated and the treated groups' statistical relation. According to the results, all the three graphs depict a dose dependent manner of Pio, since the highest concentration diminished to the greatest extent the expression of IL1-beta (A), IL6 (B) and TNF-alpha (C). *Fig.26.*

A. (KH control: 190 ± 14.1421 vs. KH perf: 639 ± 12.7279 p<0.0001; KH perf: 639 ± 12.7279 vs. KH + 30 Pio perf: 527.5 ± 17.6777 p<0.001; KH perf: 639 ± 12.7279 vs. KH + 40 Pio perf: 500 ± 14.1421 p<0.0001; KH + 10 Pio control: 211 ± 16.9701 vs. KH + 10 Pio perf: 580 ± 14.1142 p<0.0001; KH + 10 Pio perf: 580 ± 14.1142 vs. KH + 40 Pio perf: 500 ± 14.1421 p<0.005; KH + 20 Pio control: 207.5 ±31.8198 vs. KH + 20 Pio perf: 568 ± 11.3137 p<0.0001; KH + 30 Pio control: 209.5 ± 14.8492 vs. KH + 30 Pio perf: 527.5 ± 17.6777 p<0.0001; KH + 40 Pio control: 215.5 ± 20.5061 vs. KH + 40 Pio perf: 500 ± 14.1421 p<0.0001) *Fig.26. B.* (KH control: 103.5 ± 12.0208 vs. KH perf: 523 ± 18.3848 p<0.0001; KH perf: 523 ± 18.3848 vs. KH + 40 Pio perf: 419.5 ± 14.8492 p<0.001; KH + 10 Pio control: 122 ± 19.799 vs. KH + 10 Pio perf: 514.5 ± 7.7781 p<0.0001; KH + 10 Pio perf: 514.5 ± 7.7781 vs. KH + 40 Pio perf: 419.5 ± 14.8492 p<0.001; KH + 20 Pio control: 112.5 ± 17.6777 vs. KH + 20 Pio perf: 492 ± 11.3137 p<0.0001; KH + 20 Pio perf: 492 ± 11.3137 vs. KH + 40 Pio perf: 419.5 ± 14.8492 p<0.005; KH + 30 Pio control: 124 ± 16.9701 vs. KH + 30 Pio perf: 461 ± 12.7279 p<0.0001; KH + 40 Pio control: 135 ± 21.2132 vs. KH + 40 Pio perf: 419.5 ± 14.8492 p<0.0001) *Fig.26. C.* (KH control:22 ± 4.2426 vs. KH perf: 180 ± 7.071 p<0.0001; KH perf: 180 ± 7.071 vs. KH + 30 Pio perf: 126.5 ± 13.435 and KH + 40 Pio perf: 104.5 ± 10.6067 p<0.001 and p<0.0001; KH + 10 Pio control: 26 ± 5.6569 vs. KH + 10 Pio perf: 154.5 ± 7.7782 p<0.0001; KH + 10 Pio perf: 154.5 ± 7.7782 vs. KH + 40 Pio perf: 104.5 ± 10.6067 p<0.001; KH + 20 Pio control: 22 ± 9.8995 vs. KH + 20 Pio perf: 148 ± 11.3137 p<0.0001; KH + 20 Pio perf: 148 ± 11.3137 vs. KH + 40 Pio perf: 104.5 ± 10.6067 p<0.005; KH + 30 Pio control: 25.5 ± 9.1924 vs. KH + 30 Pio perf: 126.5 ± 13.435 p<0.0001; KH + 40 Pio control: 26.5 ± 9.1924 vs. KH + 40 Pio perf: 104.5 ± 10.6067 p<0.0001)

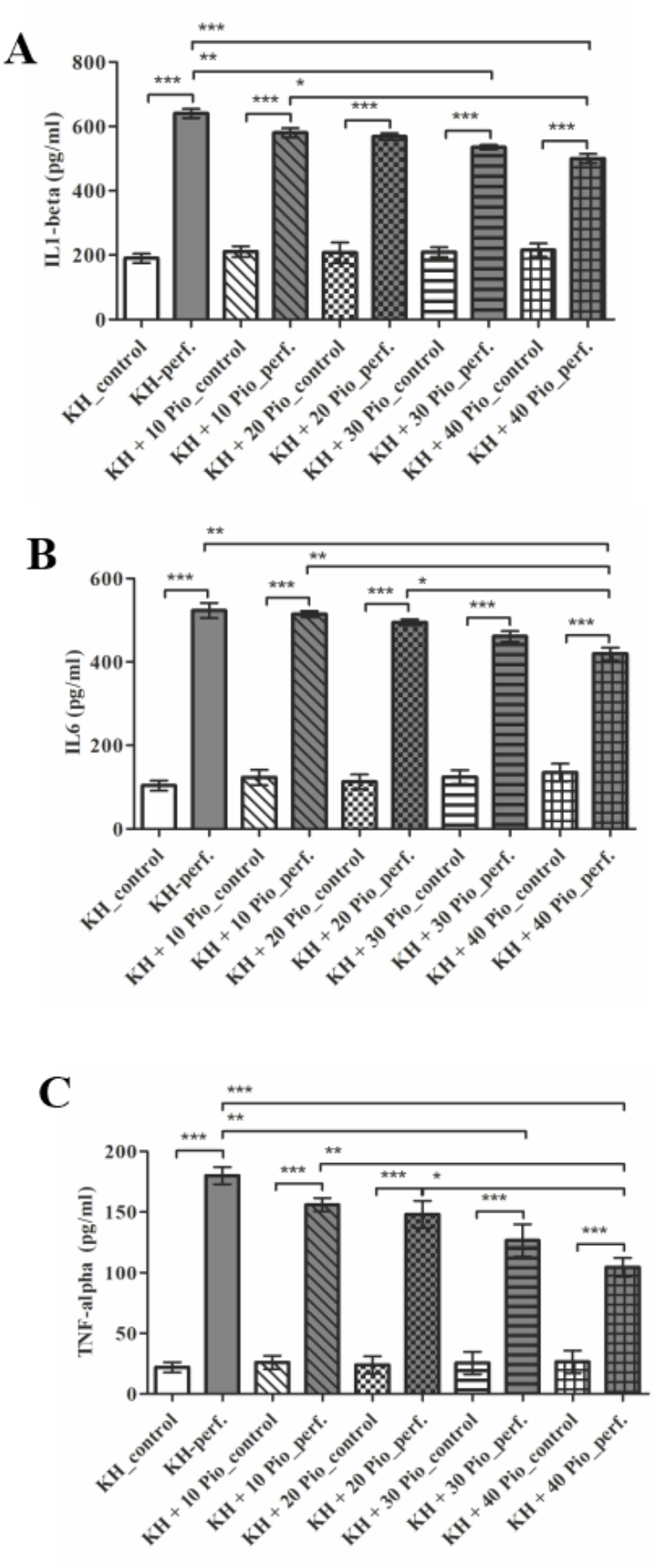

Figure 26: Expression of inflammatory cytokines; IL1-beta, IL6 and TNF-alpha (n=10). KH + 40 Pio perf. was the most effective in reducing the inflammatory cytokines among Pio treated groups, compared to KH perf. group. Data is represented in mean ± SD. ($p<0.005$ - *; $p<0.001$ - **; $p<0.0001$ - ***)

Figure 27 represents the HE-staining from kidney samples in all experimental groups. In control histological sections any oncosis or apoptosis cannot be detected, the basic tissue structure is kept. However, in KH perf. group, swelled Bowman's capsules and endothelial tubules and eosinophilia can be observed. According to the sections on *Fig.27.*, the perfusion with KH + 20 and 30 mg/kg Pio depict less histological abnormality and their tissue structure correlate to the control groups'.

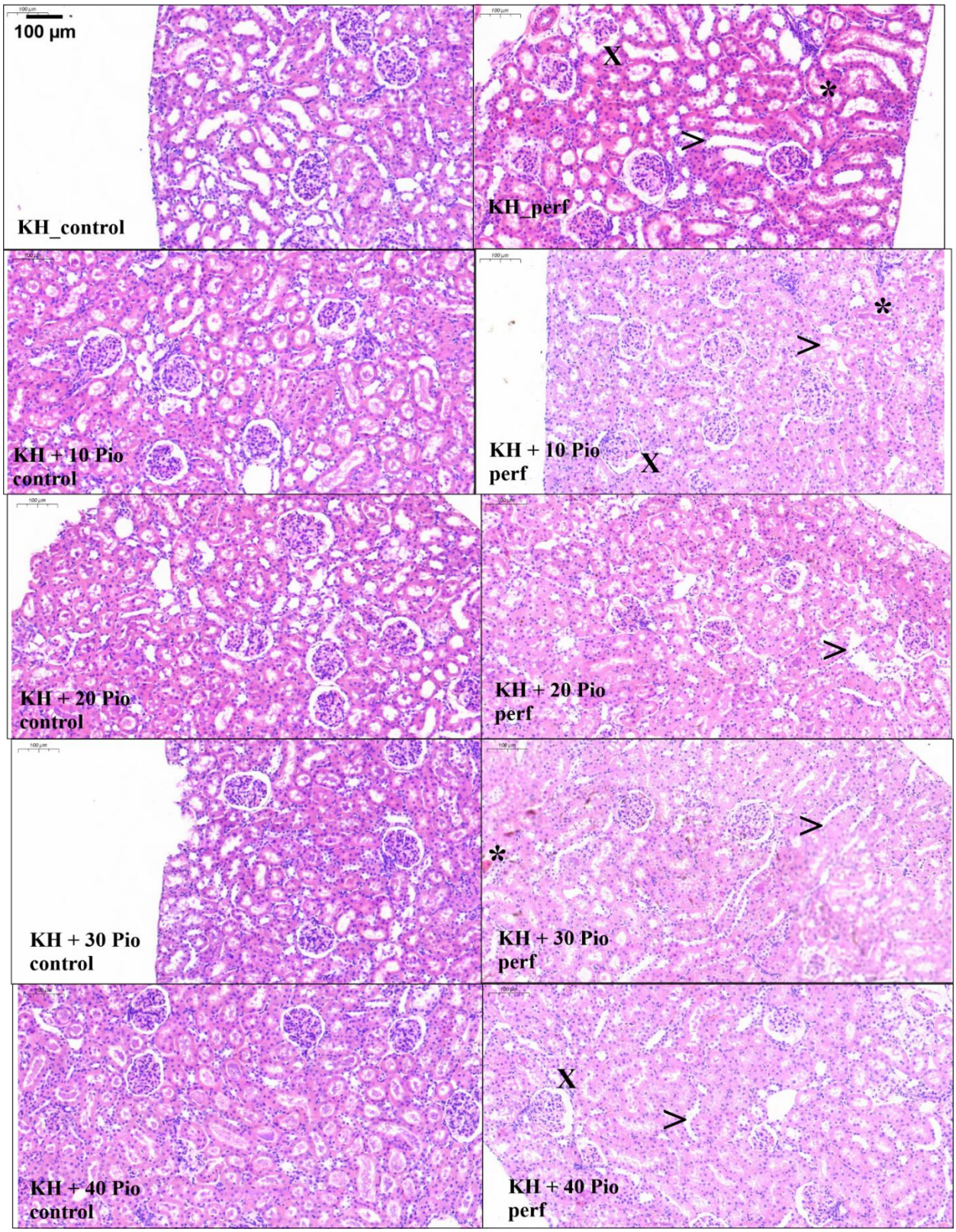

Figure 27: Hematoxylin-eosin staining of kidney samples. Magnification: 11.3x. According to the control group's samples, any oncosis or apoptosis cannot be detected, the basic tissue structure was kept. Mostly KH + 40 Pio perf. group correlates to the control. In other perfused groups, eosinophilia, swelling of endothelial tubules and Bowman's capsule can be detected. Asterisk (*) represents the eosinophilia, arrowhead (>) depicts swelling of endothelial tubules and X's show swelled Bowman's capsules.

The protein expression of Caspase 12 was measured by Western blot. In *Figure 28* the bands of the samples' blots and the normalization controls are presented. According to previous results, the KH + 40 Pio perf group diminished the expression of Caspase 12, however, significant difference can be observed between KH perf and KH 20, 30 and 40 Pio perf. groups, and between KH + 10 Pio perf. and KH 30 and 40 Pio perf. groups. (KH control: 0.89 ± 0.1556 vs. KH perf: 5.4 ± 0.2828 $p<0.0001$; KH perf: 5.4 ± 0.2828 vs. KH + 20 Pio perf: 4.1263 ± 0.1043 and KH + 30 Pio perf: 3.82 ± 0.198 and KH + 40 Pio perf: 3.335 ± 0.1201 $p<0.001$, $p<0.0001$, $p<0.0001$; KH + 10 Pio control: 1.125 ± 0.1061 vs. KH + 10 Pio perf: 4.825 ± 0.1909 $p<0.0001$; KH + 10 Pio perf: 4.825 ± 0.1909 vs. KH + 30 Pio perf: 3.82 ± 0.198 and KH + 40 Pio perf: 3.335 ± 0.1201 $p<0.005$ and $p<0.0001$; KH + 20 Pio control: 1.1493 ± 0.2132 vs. KH + 20 Pio perf: 4.1263 ± 0.1043 $p<0.0001$; KH + 30 Pio control: 1.1 ± 0.1414 vs. KH + 30 Pio perf: 3.82 ± 0.198 $p<0.0001$; KH + 40 Pio control: 1.1913 ± 0.2245 vs. KH + 40 Pio perf: 3.335 ± 0.1201 $p<0.0001$)

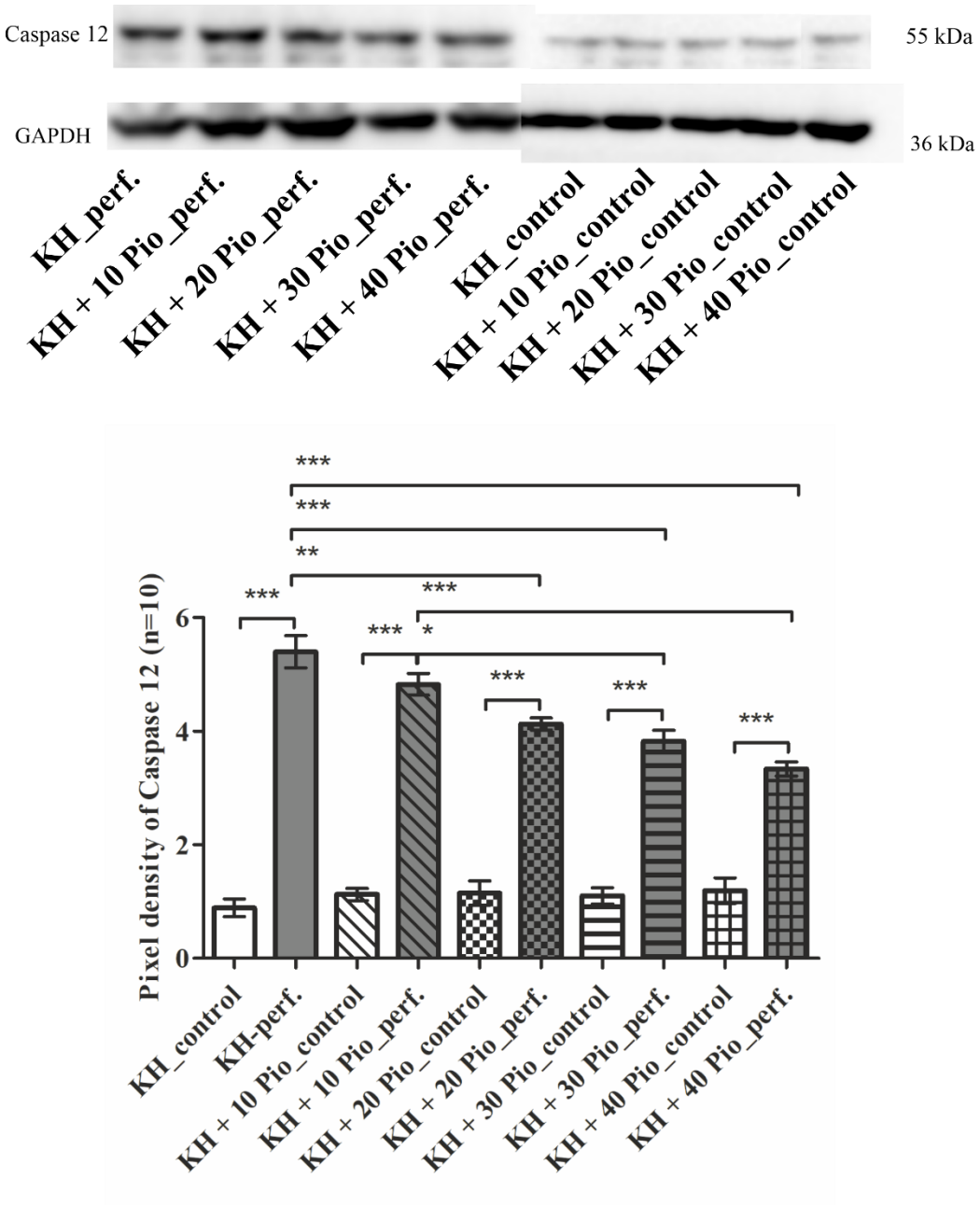

Figure 28: Expression rate of Caspase 12 protein among kidney samples. GAPDH serves as a normalization control.

Protein expression of XBP1s (56 kDa) is demonstrated in *Fig.29*. Compared to KH perf. group, the KH + 30 and 40 mg/kg Pio perf. groups significantly diminished the expression of XBP1s. (KH control: 0.9083 ± 0.1587 vs. KH perf: 4.5518 ± 0.7208 $p<0.0001$; KH perf: 4.5518 ± 0.7208 vs. KH + 30 Pio perf: 2.7472 ± 0.3951 and KH + 40 Pio perf: 2.39 ± 0.2812 $p<0.001$ and $p<0.0001$; KH + 10 Pio control: 0.9794 ± 0.3081 vs. KH + 10 Pio perf: 3.6263 ± 0.9587 $p<0.0001$; KH + 20 Pio control: 1.0149 ± 0.0404 vs. KH + 20 Pio perf: 3.0533 ± 0.2216 $p<0.001$; KH + 30 Pio control: 1.0686 ± 0.133 vs. KH + 30 Pio perf:

2.7472 ± 0.3951 p<0.001; KH + 40 Pio control: 0.9342 ± 0.2261 vs. KH + 40 Pio perf: 2.39 ± 0.2812 p<0.005)

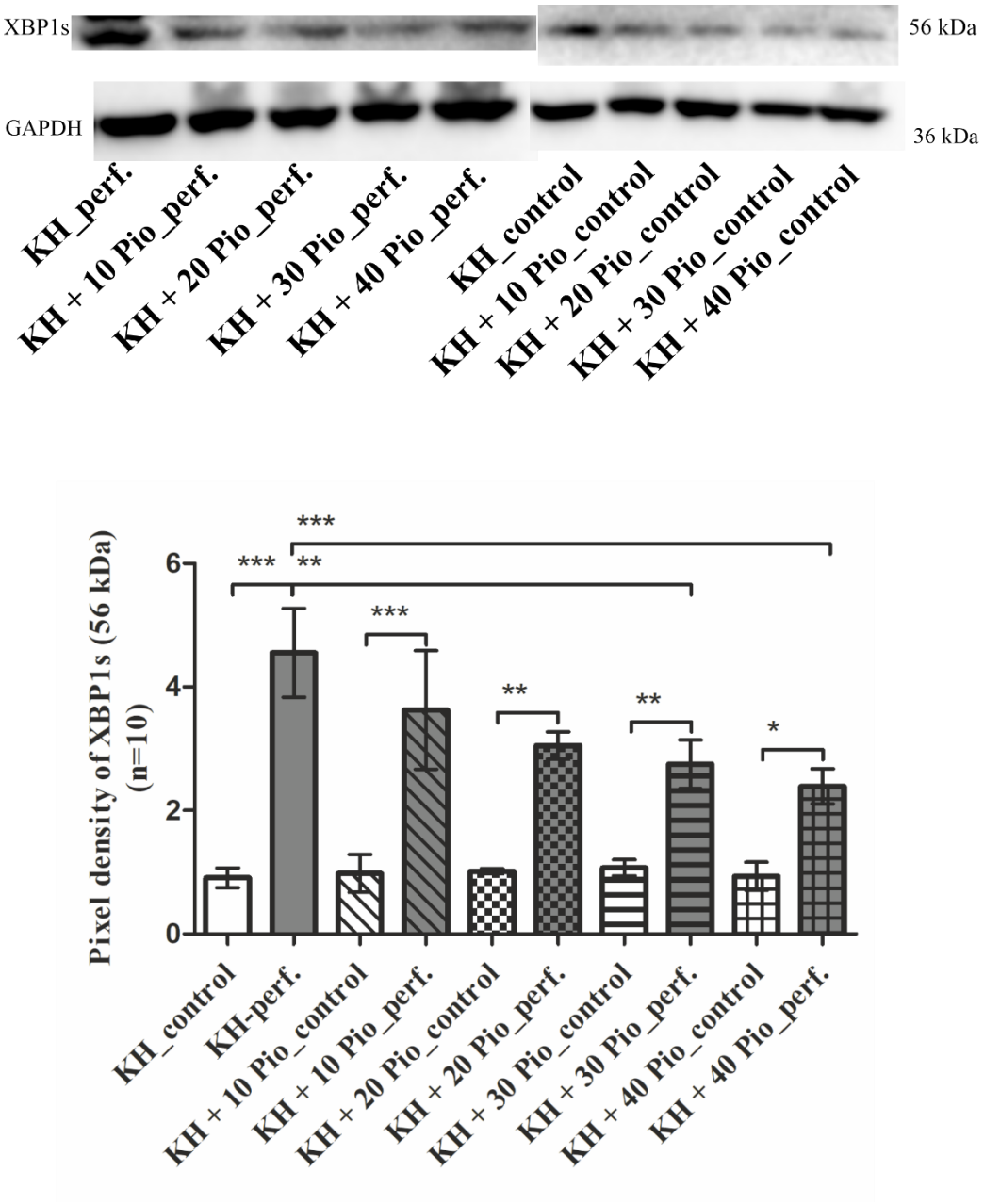

Figure 29: Pixel density of XBP1s (56 kDa) protein expression in kidney samples. GAPDH serves as a normalization control.

The pixel density of XBP1u's (29 kDa) protein expression can be seen in *Fig.30*. All treated groups, except KH + 10 Pio perf., could decrease the XBP1s' protein expression, and the KH + 40 Pio perf. performed it to the greatest extent compared to KH perf. group. (KH control: 0.87 ± 0.1833 vs. KH perf: 4.73 ± 0.4487 p<0.0001; KH perf: 4.73 ± 0.4487 vs. KH + 20 Pio perf: 3.83 ± 0.1839 and KH + 30 Pio perf: 3.3009 ± 0.1568 and KH + 40

Pio perf: 2.9999 ± 0.1192 p<0.001, p<0.0001 and p<0.0001; KH + 10 Pio control: 1.3529 ± 0.5274 vs. KH + 10 Pio perf: 4.205 ± 0.2192 p<0.0001; KH + 10 Pio perf: 4.205 ± 0.2192 vs. KH + 30 Pio perf: 3.3009 ± 0.1568 and KH + 40 Pio perf: 2.9999 ± 0.1192 p<0.005 and p<0.0001; KH + 20 Pio control: 1.2904 ± 0.2693 vs. KH + 20 Pio perf: 3.83 ± 0.1839 p<0.0001; KH + 30 Pio control: 1.2175 ± 0.3612 vs. KH + 30 Pio perf: 3.3009 ± 0.1568 p<0.0001; KH + 40 Pio control: 1.3773 ± 0.7203 vs. KH + 40 Pio perf: 2.9999 ± 0.1192 p<0.0001)

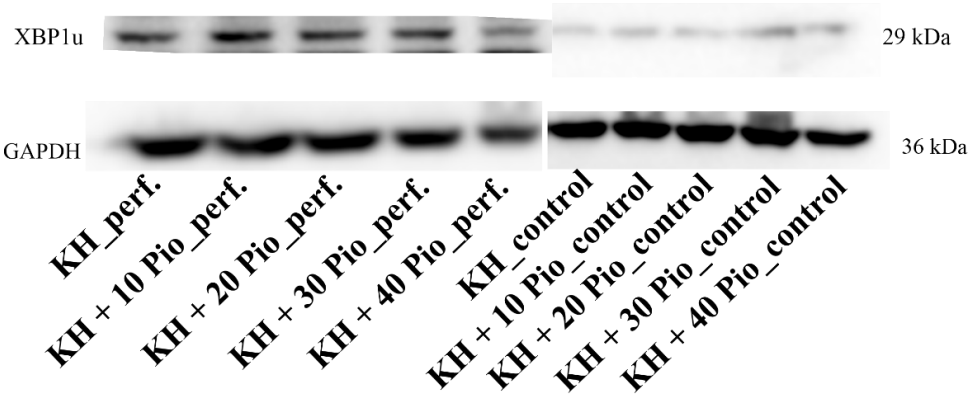

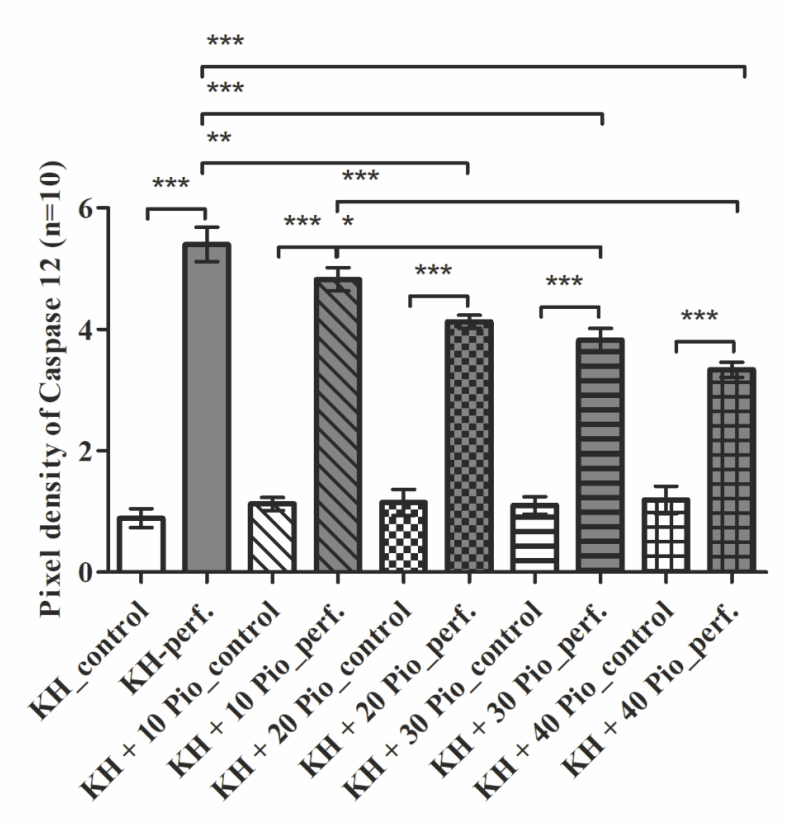

Figure 30: Pixel density of XBP1u protein expression regarding kidney tissue samples from different experimental groups. GAPDH serves as a normalization control.

5.3.2. Discussion

The importance of diminishing IRI is unquestionable, considered as a relevant factor in determining high morbidity and mortality in several diseases such as myocardial infarction, ischemic stroke, AKI, and trauma. Especially, in organ transplantation as well as in major surgery IRI cause severe complication and influences the clinical outcome. As above was mentioned, ischemic period results in reduces metabolic supply with respect to the demand within an ischemic organ. Due to severe hypoxia microvascular dysfunction develops. Furthermore, in reperfusion phase, instead of restoring the normal conditions, further damages cause the activation of several mechanisms (innate and adaptive immune response and cell death program). [96-98]

In modeling the human transplantation protocol, these findings are important, since a preservation solution can be perfused, and it could maintain the cell and tissue structure under reperfusion period. By this method, the incidence of DGF could be diminished and the survival rate could be increased.

For more than 5 decades, the cold storage (a preservation solution is perfused into the organ and the organ is stored at hypothermic conditions) in organ preservation was successfully used and decreased the organ failure since the method reduced the metabolic requirements of organs and attenuated ischemic injury. [99-100] Several preservation solutions are available in the clinic and the effectivity is getting better. University of Wisconsin Solution (UW)/Viaspan and Histidine-tryptophan-ketoglutarate (HTK)/Custodiol solution are the most common preservation solutions and the perspectives on abdominal organ preservation are similar. However, HTK shows conflicting results with respect to pancreatic cellular edema, several studies were noted its advantageous effect in liver transplant against biliary complications than UW. In case of kidney, HTK is associated with higher graft loss and increased DGF in marginal deceased donors. UW serves as a reference standard for use during multiorgan recoveries but has its own competitors, especially HTK solution. [101]

Mitochondria plays important roles in oxidative stress and crosstalk in ERS, inflammasome and autophagy in type 2 diabetes. ER is an organelle with essential functions, including protein synthesis and processing. After the initiation of UPR, ERS is activated through three major signaling pathways: IRE1, ATF6 and PERK pathways.

According to our knowledge, ERS is involved in several types of kidney diseases, such as renal fibrosis, diabetic nephropathy, AKI, CKD. [102, 103]

This is the first study, where kidney perfusion was performed *in situ* using subnormothermic (20 °C) KH solution modified with Pio in different dosages. *In situ* perfusion-reperfusion model is a combination of IRI and our novel *in situ* perfusion rat model. Our aim was to determine the optimal dosage of Pio, which were the same as in the second chapter of the thesis. The hypothesis was, that does the reperfusion phase modify the effect of Pio and how. According to the results, the highest dosage of the drug (KH + 40 mg/kg Pio perf. group) was an effective decreasing factor of oxidative stress, inflammatory cytokines and ERS markers. Histopathological findings correlate to the ELISA and Western blot results, however, on HE stained kidney sections the 20 and 30 mg/kg Pio perf. groups depicted less tissue damage (*Fig.27.*).

6. Conclusion

Pio is a clinically applicable and non-toxic agent, which can increase the ischemic tolerance of tissues in decreasing the endoplasmic reticulum stress and consequent apoptosis. The results support the finding in which Pio has an ERS decreasing effect in higher dosage levels, both in the case of kidney and liver perfusion. Furthermore, we could not detect any necrotic effect regarding Pio, which may indicate for a short period of time, an acute administered higher dosage of this PPARγ agonist Pioglitazone can help in maintaining the basic organ structure in the case of both the kidney and liver. Further experiments are needed to examine other PPARγ agonists referenced this methodological set and prove their potential role in ischemia and organ preservation by in situ perfusion. In our preliminary study, we aimed to confirm the protective effect of Pio in our novel in situ perfused rat model. Other ERS pathways should be examined in this experimental set to get a broader knowledge of ERS reducing activity of Pio. We can conclude that the highest dosage has anti-inflammatory, anti-oxidative and ERS inhibitory effects, furthermore, histopathological results prove Pio's effectiveness.

Our third aim was, to compare the second and the third experimental set of this study, however, the administered dosages of Pio was similar, but the periods of perfusion not. Therefore, we should carefully conclude any correlation between the two methods.

Due to enzyme polymorphism, application on humans differs from the applied protocols, dosages, and time periods of Pio. Therefore, the modeling of a real-time rat kidney transplantation is planned, where our experiments will be merged and the time periods, administered dosages of Pio and the surgical procedure will be tested and improved.

7. Novel findings

1. In our **first study**, we investigated and proved the protective effect of Pio in inflammation, oxidative stress and ERS which was dedicated to the group of 1h before the initiation of ischemic period. In the traditional IRI experimental setting ERS markers were analyzed for the first time and established a basis to the other experimental sets.
2. Based on the **second chapter**, there was a difference between kidney and liver samples regarding Pio metabolism, since in case of kidney tissue, higher dosage was most preventive, however, the liver sections represented in middle dosages (20 and 30 mg/kg Pio) the similar improvement. According to our knowledge and compared to the international literature, a novel in situ perfusion system was examined and raises the question of the use of Pio in clinical transplantation protocol.
3. In the **third part** of the study, the results were correlated to the other two performed protocols', and the 40 mg/kg Pio dosage depicted a protective effect against IRI compared to the KH-perfused group. On the basis of our knowledge, this novel experimental setting is suitable for preclinical drug testing and improving of our tool against IRI.
4. Overall, we can conclude, that Pio is applicable in higher dosages and has an advantageous effect on kidney and liver samples in IRI, *in situ* perfusion and *in situ* perfusion-reperfusion models.

8. Bibliography

[1] Philipponnet C, Aniort J, Garrouste C, Kemeny J, Heng A. Ischemia reperfusion injury in kidney transplantation. Medicine (Baltimore). 2018; 97(52): e13650. DOI: 10.1097/MD.0000000000013650

[2] Womer KL, Vella JP, Sajegh MH. Chronic allograft dysfunction: mechanisms and new approaches to therapy. Semin Nephrol. 2000; (20): 126-147. ISSN 0270-9295.

[3] Torras J, Cruzado JM, Grinyo JM. Ischemia and reperfusion injury in transplantation. Transplantation Proceedings. 1999; (31): 2217-2218. ISSN 0041-1345.

[4] M., Crompton. The mitochondrial permeability transition pore and its role in cell death. Biochem J. 1999; 2(341): 233-249.

[5] Kersten JR, Schmeling TJ, Pagel PS, Gross GJ, Warltier DC. Isoflurane mimics ischemic preconditioning via activation of K(ATP) channels: reduction of myocardial infarct size with an acute memory phase. Anesthesiology. 1997; 2(87): 361-370.

[6] Gulec, Bulent. Ischemia reperfusion injury in kidney transplantation. Kidney Transplantation - New Perspectives. 2011; 213-222. ISBN 978-953-307-684-3.

[7] Yellon DM, Hausenloy DJ. Myocardial reperfusion injury. N Engl J Med. 2007; 11(357): 1121-1135.

[8] Robert Meller, Roger P. Simon. Tolerance to ischemia - an increasingly complex biology. Trans Stroke Res. 2014; 1(4): 40-50. DOI: 10.1007/s12975-012-0246-x

[9] Horvath KA, Torchiana DF, Daggett WM, Nishioka NS. Monitoring myocardial reperfusion injury with NADH fluorometry. Lasers in Surgery and Medicine. 1992; 1(12): 2-6.

[10] Takeo S, Tanonaka K, Liu JX, Kamiyama T, Ohio I, Kajiwara H, Kameda H, Takasaki A. Ischemia/reperfusion injury and ion channel blockade. Protection Against ISchemia/Reperfusion Damage of the Heart. 1998; 195-214. ISBN 978-4-431-68484-8.

[11] Sanada S, Komuro I, Kitakaze M. Patophysiology of myocardial reperfusion injury: preconditioning, postconditioning and translational aspets of protective measures. Am. J. Physiol. 2011; H1723-H1741: 301. DOI: 10.1152/ajpheart.00553.2011

[12] Yellon DM, Hausenloy DJ. Myocardial reperfusion injury.. [PubMed: 17855673], N. Engl. J. Med. 2007; 357(11): 1121-1135.DOI: 10.1056/NEJMra071667

[13] Grisotto PC et al. Indications of oxidative injury and alterations of the cell membrane in the skeletal muscle of rats submitted to ischemia reperfusion. J Surg Res. 2000; 92(1): 1-6. DOI: 10.1006/jsre.2000.5823

[14] Baines CP. The mitochondrial permeability transition pore and ischemia-reperfusion injury. Basic Res Cardiol. PubMed: 19242640, 2009a; (104): 181-188. DOI: 10.1007/s00395-009-0004-8

[15] Kalogeries T, Baines CP, Krenz M, Korthuis RJ. Ischemia/Reperfusion. Compr Physiol. 2016; 1(7): 113-170. DOI: 10.1002/cphy.c160006

[16] Coulter SA, Cannon CP, Ault KA, Antman EM, Van de Werf F, Adgey AA, Gibson CM, Giugliano RP, Mascelli MA, Scherer J, Barnathan ES, Braunwald E, Kleiman NS. High levels of platelet inhibition with abciximab despite heightened platelet activation and aggregation during thromboslysis for acute myocardial infarction: results from TIMI (thrombolysis in myocardial infarction). Circulation. 2000; (101): 2690-2695. DOI: 10.1161/01.cir.101.23.2690

[17] Davies MG, Juynh TTT, O. HP. Endothelial physiology. In: Grace PA, Mathie RT (eds). Ischemia-reperfusion injury. Blackwell Science: London. 1999; 157-179.

[18] Reffelmann T, Kloner RA. The "no-reflow" phenomenon: basic science and clinical correlates. Heart. 2002; 2(87): 162-168. DOI: 10.1136/heart.87.2.162

[19] Holzheimer RG, Gross J, Schein M. Pro- and anti-inflammatory cytokine-response in abdominal aortic aneurysm repair: a clinical model of ischemia-reperfusion. Shock. 1999; 5(11): 305-310.

[20] Ley K, Tedder TF. Leukocyte interactions with vascular endothelium. J. Immunol. 1995; (155): 525-528.

[21] McEver RP, Moor KL, Cummings RD. Leukocyte trafficking mediated by selectin carbohydrate interactions. J. Biol. Chem. 1995; (270): 11025-11028.

[22] Berman CL, Yeo EL, Wencel-Drake JD, Furie BC, Ginsberg MH, Furie B. A platelet alpha granule memrbane protein that is associated with the plasma membrane after activation. J. Clin. Invest. 1986; (78): 130-137.

[23] McEver RP, Beckstead JH, Moore KL, Marshall-Carlson L, Bainton DF. GMP-140, a platelet alpha-granule memrbane protein, is also synthetised by vascular endothelial cells and is located in Weibel-Palade bodies. J. Clin.Invest. 1989; (84): 92-99.

[24] Weyrich AS, Ma XY, Lefer DJ, Albertine KH, Lefer AM. In vivo neutralization of P-selectin protects feline heart and endothelium in myocardial ischemia and reperfusion. J. Clin. Invest. 1993; (91): 2620-2629.

[25] Garcia-Criado FJ, Toledo-Pereyra LH, Lopez-Neblina F, Phillips ML, Paez-Rollys A, Misawa K. Role of P-selectin in total hepatic ischemia and reperfusion. J. Am. Coll. Surg. 1995; (181): 327-334.

[26] Weller A, Isenmann S, Vestweber D. Cloning of the mouse endothelial selectins: expression of both E- and P-selectin is inducible by tumor necrosis factor alpha. J. Biol. Chem. 1992; (267): 15176-15183.

[27] Sasaki K, Joshida H. Organelle autoregulation-stress responses in the ER, Golgi, mitochondria and lysosome. J. Biochem. 2015; 157(4): 185-195. DOI: 10.1093/jb/mvv010

[28] Helenius A, Aebi M. Roles of N-linked glycans in the endoplasmic reticulum. Annu. Rev. Biochem. 2004; (73): 1-12. DOI: 10.1146/annurev.biochem.73.011303.073752

[29] Otero JH, Lizak B, Hendershot LM. Life and death of a BiP substrate. Semin. Cell Develop. Biol. 2010; (21): 472-478. DOI: 10.1016/j.semcdb.2009.12.008

[30] Gething MJ. Role and regulation of the ER chaperone BiP. Semin. Cell Develop. Biol. 1999; (10): 465-472.

[31] Hampton RY, Sommer T. Finding the will and the way of ERAD substrate retrotranslocation. Curr. Opin. Cell Biol. 2012; (24): 460-466. DOI: 10.1016/j.ceb.2012.05.010

[32] Merulla J, Fasana E, Solda T, Molinari M. Specificity and regulation of the endoplasmic reticulum-associated degradation machinery. Traffic. 2013; (14): 767-777. DOI: 10.1111/tra.12068

[33] Lin JH, Walter P, Yen TSB. Endoplasmic reticulum stress in disease pathogenesis. Annu Rev Pathol. 2008; (3): 399-425. DOI: 10.1146/annurev.pathmechdis.3.121806.151434

[34] Shaffer AL, Shapiro-Shelef M, Iwakoshi NN, Lee AH, Qian SB et al. XBP1, downstream of Blimp-1, expands the secretory apparatus and other organelles, and increases protein synthesis in plasma cell differentation. Immunity. 2004; (21): 81-93. DOI: 10.1016/j.immuni.2004.06.010

[35] Lee AH, Iwakoshi NN, Glimcher LH. XBP-1 regulates a subset of endoplasmic reticulum resident chaperone genes in the unfolded protein response. Mol Cell Biol 2003; (23): 7448-59. DOI: 10.1128/mcb.23.21.7448-7459.2003

[36] Oda Y, Okada T, Yoshida H, Kaufman RJ, Nagata K et al. Derlin-2 and Derlin-3 are regulated by the mammalian unfolded protein response nad are required for ER-associated degradation. J Cell Biol. 2006; (172): 383-93. DOI: 10.1083/jcb.200507057

[37] Urano F, Wang X, Bertolotti A, Zhang Y, Chung P et al. Coupling of stress in the ER to activation of JNK protein kinases by transmembrane protein kinase IRE1. Science 2000; (287): 664-66.

[38] Nishitoh H, Matsuzawa A, Tobiume K, Saegusa K, Takeda K et al. ASK1 is essential for endoplasmic reticulum stress-induced neuronal cell death triggered by expanded polyglutamine repeats. Genes Dev 2002; (16): 1345-55. DOI: 10.1101/gad.992302

[39] Barr RK, Bogoyevitsh MA. The c-Jun N-terminal protein kinase family of mitogen-activated protein kinases (JNK MAPKs). Int Biochem Cell Biol. 2001; (33): 1047-63. DOI: 10.1016/s1357-2725(01)00093-0

[40] Nakagawa T, Zhu H, Morishima N, Li E, Xu J, Yankner B, et al. Caspase-12 mediates endoplasmic-reticulum-specific apoptosis and cytotoxicity by amyloid-beta. Nature. 2000; 403: 98-103. DOI: 10.1038/47513

[41] Saleh M, Mathison JC, Wolinski MK, Bensinger SJ, Fitzerald P et al. Enhances bacterial clearance and sepsis resistance in caspase-12-deficient mice. Nature. 2006; (440): 1064-68. DOI: 10.1038/nature04656

[42] Michalik L, Wahli W. Involvement of PPAR nuclear receptors in tissue injury and wound repair. J Clin Invest. 2006; 3(116): 598-606. DOI: 10.1172/JCI27958

[43] Evans RM, Barish GD, Wang YX. PPARs and the complex journey to obesity. Nat Med. 2004; (10): 355-61. DOI: 10.1038/nm1025

[44] Ahmed LA, Salem HA, Attia AS, Agha AM. Pharmacological preconditioning with nicorandil and pioglitazone attenuates myocardial ischemia/reperfusion injury in rats. Eur. J. Pharmacol. 2011; (663): 51-58. DOI: 10.1016/j.ephar.2011.04.038

[45] Zhang H, Xu M, Qin A, Liu C, Hong L, Zhao X, et al. Neuroprotective effects of pioglitazone in a rat model of permament focal cerebral ischemia are associated with peroxisome proliferator-activated receptor gamma-mediated suppression of nuclear factor-kB signaling pathway. Neuroscience. 2011; 176: 381-395. DOI: 10.16/j.neuroscience.2010.12.029

[46] Zhang X, Xiao Y, Zhang Y, Ye W. Protective effect of pioglitazone on retinal ischemia/reperfusion injury in rats. Ophtalmol. Vis. Sci. 2013; 54: 3912-3921. DOI: 10.1167/iovs.13-11614

[47] Zou X, Hu H, Xi X, Shi Z, Wang G, Huang X. Pioglitazone protects against renal ischemia-reperfusion injury by enhancing antioxidant capacity. J. Surg. Res. 2013; 184: 1092-1095. DOI: 10.1016/j.jss.2013.03.027

[48] Sivarajah A, Chatterjee P, Patel N, Todorovic Z, Hattori Y, Brown P, et al. Agonists of peroxisome proliferator activated receptor-gamma reduce renal ischemia/referfusion injury. Am J Nephrol. 2003; 23: 267-276. DOI: 10.1159/000072088

[49] Chung B. Protective effect of peroxisome proliferator activated receptor gamma agonists on diabetic and non-diabetic renal diseases. Nephrology. 2005; 10: 40-43. DOI: 10.1111/j.1440-1797.2005.00456.x

[50] Pereira M, Camara N, Campaholle G, Cenedeze M, Teixeira V, Antonia dos Reis M, Pacheco-Silva A. Pioglitazone limits cyclosporine nephrotoxicity in rats. Int Immunopharmacol. 2006; 6: 1943-1951. DOI: 10.1016/j.intimp.2006.07.024

[51] Abd-Elrahman K, El-Gowelli H, Saad E, Abdel-Galil A, El-Mas M. Role of PPAR gamma/nitric oxide synthase signaling in the cyclosporine-induced attenuation of endothelium-dependent renovascular vasodilatation. J Cardiovasc Pharmacol. 2010; 56: 195-202. DOI: 10.1097/FJC.0b013e3181e74d83

[52] El-Mas M, El-Gowelli H, Adb-Elrahman K, Saad E, Abdel-Galil A, Abdel-Rahman A. Pioglitazone abrogates cyclosporine-evoked hypertension via rectifying abnormalities in vascular endothelial function. Biovhem Pharmacol. 2011; 81: 526-533. DOI: 10.1016/j.bcp.2010.11.013

[53] Ibrahim M, El-Sheikh A, Khalaf H, Abdelrahman A. Protective effect of peroxisome proliferator activator receptor (PPAR)-alpha and gamma ligands against methotrexate-induced nephrotoxicity. Immunopharmacol. Immunotoxicol. 2014;(36): 130-137. DOI: 10.3109/08923973.2014.884135

[54] Vijay S, Mishra M, Kumar H, Tripathi K. Effect of pioglitazone and rosiglitazone on mediators of endothelial dysfunction, markers of angiogenesis and inflammatory cytokines in type-2 diabetes. Acta Diabetol. 2009; 46: 27-33. DOI: 10.1007/s00592-008-0054-7

[55] Chen J, Li D, Zhang X, Mehta J. Tumor necrosis factor-alpha-induced apoptosis of human coronary artery endothelial cells: modulation by the peroxisome proliferator-activated receptor-gamma ligand pioglitazone. J. Cardiovasc. Pharmacol. 2004;(9): 35-41. DOI: 10.1177/107424840400900i106

[56] Cao Z, Ye P, Long C, Chen K, Li X, Wang H. Effect of pioglitazone a peroxisome proliferator-activated receptor gamma agonist, on ischemia reperfusion injury in rats. Pharmacology. 2007; 79: 184. DOI: 10.1159/000100870

[57] Xi X, Zou C, Ye Z, Huang Y, Chen T, Hu H. Pioglitazone protects tubular cells against hypoxia/reoxygenation injury through enhancing autophagy via AMPK-mTOR signaling pathway. European Journal of Pharmacology. 2019; 863: 172695. DOI: 10.1016/j.ejphar.2019.172695

[58] El-Gowilly S, Helmy M, El-Gowelli H. Pioglitazone ameliorates methotrexate-induced renal endothelial dysfunction via amending detrimental changes is some antioxidant parameters, systemic cytokines and Fas production. Vascular Pharmacology. 2015; 74: 139-150. DOI: 10.1016/j.vph.2015.07.002

[59] Chen W, Xi X, Zhang S, Zou C, Kuang R, Ye Z, et al. Pioglitazone protects against renal ischemia/reperfusion injury via the AMP-activated protein kinase-regulated autophagy pathway. Front. Pharmacol. 2018; 9(851): 1-12. DOI: 10.3389/fphar.2018.00851

[60] Singh A, Singh N, Bedi P. Pioglitazone ameliorates renal ischemia reperfusion injury through NMDA receptor antagonism in rats. Mol Cell Biochem. 2016; 417: 111-118. DOI: 10.1007/s11010-016-2718-x

[61] Reel B, Bagriyanik A, Atmaca S, Aykut K, Albaxrak G, Hazan E. The effect of PPAR-gamma agonist pioglitazone on renal ischemia/reperfusion injury in rats. 2013; 182: 176-184. DOI: 10.1016/j.jss.2012.08.020.

[62]. Zanchi A, Perregaux C, Maillard M, Cefai D, Nussberger J, Burnier M. The PPARgamma agonist pioglitazone modifies the vascular sodium-angiotensin II relationship in insulin-resistant rats. Am J Physiol Endocrinol Metab. 2006; 291: E1228-E1234. DOI: 10.1152/ajpendo.00171.2006

[63] Paciello F, Fetoni A, Roesi R, Wright M, Grassi C, Troiani D, et al. Pioglitazone represents an effective therapeutic target in preventing oxidative/inflammatory cochlear damage induced by noise exposure. Front Pharmacol. 2018; 9(1103): 1-15. DOI: 10.3389/fphar.2018.01103

[64] Medic B, Stojanovic M, Rovcanin B, Kekic D, Skodric S, Jovanovic G, et al. Pioglitazone attenuates kidney injury in an experimental model of gentamicin-induced nephrotoxicity in rats. Nature Scientific Reports. 2019; 9: 13689. DOI: 10.1038/s41598-019-49835-1

[65] Oliveira A, Bertollo C, Rocha L, Nascimento Jr. E, Costa K, Coelho M. Antinociceptive and antiedematogenic activities of fenofibrate, an agonist of PPAR alpha, and pioglitazone, an agonist of PPAR gamma. European Journal of Pharmacology. 2007; 561: 194-201. DOI: 10.1016/j.ejphar.2006.12.026

[66] Kaplan J, Nowell M, Chima R, Zingarelli B. Pioglitazone reduces inflammation through inhibition of nuclear factor kappa-B in polymicrobial sepsis. Innate Immun. 2014; 20(5): 519-528. DOI: 10.1177/1753425913501565

[67] Khooder D, Zaitone S, Farag N, Moustafa Y. Cardioprotective effect of pioglitazone in diabetic and non-diabetic rats subjected to acute myocardial infarction involves suppression of AGE-RAGE axis and inhibition apoptosis. Can. J. Physiol. Pharmacol. 2016; 94(5): 463-76. DOI: 10.1139/cjpp-2015-0135

[68] Elshazly S, Soliman E. PPAR gamma agonist, pioglitazone, rescues liver damage induced by renal ischemia/reperfusion injury. Toxicology and Applied Pharmacology. 2019; 362: 86-94. DOI: 10.16/j.taap.2018.10.022

[69] Adams M, Montague CT, Prins JB, Holder JC, Smith SA, Sanders L, et al. Activators of peroxisome proliferator-activated receptor gamma have depot-specific effects on human preadipocyte-differentation. J. Clin Invest. 1997; (100): 3149-3153.

[70] Akazawa S, Sun F, Ito M, Kawasaki E, Eguchi K. Efficacy of troglitazone on body fat distribution in type 2 diabetes. Diabetes Care. 2000; (23): 1067-1071.

[71] Mori Y, Murakawa Y, Okada K, Horikoshi H, Yokoyama J, Tajima N, et al. Effect of troglitazone on body fat distribution in type 2 diabetic patients. Diabetes Care. 1999; (22): 908-912.

[72] Anderson LA. The effects of androgens and estrogens on preadipocyte proliferation in human adipose tissue: influence of gender and sidte. J. Clin. Endocrinol. Metab. 2001; (86): 4045-5051. DOI: 10.1210/jcem.86.10.7955

[73] Dieudonne MN, Recquery R, Boumediene A, Leneveu MC, Guidicelli Y. Androgen receptors in human preadipocytes nad adipocytes: regional specificities and regulation by sex steroids. Am. J. Physiol. 1998; (274): C1645-1652.

[74] Dieudonne MN, Recquery R, Leneveu MC, Guidicelli Y. Opposite effects of androgens and estrogens on adipogenesis in rat preadipocytes: evidence for sex and site-related specificities and possible involvement of insulin-like growth factor 1 receptor and peroxisome proliferator-activated receptor gamma2. Endocrinology. 2000; (141): 649-656.

[75] Kiyota Y, Kondo T, Maeshiba Y, Hashimoto A, Yamashita K, Yoshimura Y et al. Studies on the metabolism of the new antidiabetic agent pioglitazone. Identification of metabolites in rats and dogs. Arzneim.-Forsch./Drug Res. 1997; (47): 22-28.

[76] Maeshiba Y, Kiyota Y, Yamashita K, Yoshimura Y, Motohashi M, Tanayama S. Disposition of the new antidiabetic agent pioglitazone in rats, dogs, and monkeys. Arzneim.-Forsch./Drug Res. 1997; (47): 29-35.

[77] Sohda T, Ikeda H, Meguro K. Studies on antidiabetic agents. XII. Synthesis and activity of the metabolites of (+/-)-5(-)[p(-)[2-(5-ethyl-2-pyridyl)ethoxy]benzyl]-2,4-thiazolidinedione (pioglitazone). Chem. Pharm. Bull. 1995; (43): 2168-2172.

[78] Tanis SP, Parker TT, Colca JR, Fisher RM, Kletzein RF. Synthesis and biological activity of metabolites of the antidiabetic, antihyperglycemic agent pioglitazone. J. Med. Chem. 1996; (39): 5053-5063.

[79] Fujita Y, Yamada Y, Kusama M, Yamauchi T, Kamon J, Kadowaki T, Iga T. Sex differences in the pharmacokinetics of pioglitazone in rats. Comparative Biochemistry and Physiology Part C: Toxicology & Pharmacology. 2003; 1(136): 85-94. DOI: 10.1080/09712119.2012.658061

[80] Bodwell W. Ischemia, reperfusion, and reperfusion injury: Role of oxygen free radicals and oxygen free eadical scavengers. J Cardiovasc Nurs. 1989; 1(4): 25-32.

[81] Ratych RE, Bulkley GB, Williams GM. Ischemia/reperfusion injury in the kidney. Prog Clin Biol Res 1986; (224): 263-89.

[82] Si, Y-N, et al. Dexmedetomidine protects against ischemia/reperfusion injury in rat kidney. Eur Rev Med Pharmacol Sci. 2014; 13(18): 1843-51.

[83] Kalbolandi, SM, et al. Luteolin confers renoprotection against ischemia-reperfusion injury via involving Nrf2 pathway regulating miR320. Mol Biol Rep. 2019; 4(46): 4039-4047. DOI: 10.1007/s11033-019-04853-0

[84] Müller, V, Losonczy, G, Heemann, U, Vannay, Á, Fekete, A, Reusz, G, Tulassy, T, Szabó, JA. Sexual dimorphism in renal ischemia-reperfusion injury in rats: Possible role of endothelin. Kidney Int. 2002; 62(4):1364-71. DOI: 10.1111/j.1523-1755.2002.kid590.x.

[85] Robert, R, Ghazali, DA, Favreau, F, Mauco, G, Hauet, T, Goujon, JM. Gender difference and sex hormone production in rodent renal ischemia reperfusion injury and repair. Journal of Inflammation. 2011; 8:14. DOI: 10.1186/1476-9255-8-14

[86] Laszlo, E, et al. Protective effect of PACAP on ischemia/reperfusion-induced kidney injury of male and female rats: gender differences. J Mol Neurosci. 2019; 3(68): 408-419. DOI: 10.1007/s12031-018-1207-y

[87] Hardi, P, et al. Sodium pentosan polysulfate reduced renal ischemia-reperfusion-induced oxidative stress and inflammatory responses in an experimental animal model. J Vasc Res. 2016; 3-4(53): 230-242. DOI: 10.1159/000452246

[88] Miklós, Z, et al. Ischaemic postconditioning reduces serum and tubular TNF-alpha expression in ischaemic-reperfused kidney in healthy rats. Clin Hemorheol Microcirc. 2012; 3(50): 167-78. DOI: 10.3233/CH-2011-1414

[89] Womer, K, Vela, J and Sajegh, M. Chronic allograft dysfunction: mechanisms and new approaches to therapy. Semin Nephrol. 2000; (20): 126-147.

[90] Ron, D and Walter, P. Signal integration in the endoplasmic reticulum unfolded protein response. Nat Rev Mol Cell Biol. 2007; (8): 219-529. DOI: 10.1038/nrm2199

[91] Zou, C, Zhou, Z, Tu, Y, Wang, W, Chen, T, Hu, H. Pioglitazone attenuates reoxygenation injury in renal tubular NRK-52E cells exposed to high glucose via inhibiting oxidative stress and endoplasmic reticulum stress. Front Pharmacol. 2020; 10:1067. DOI: 10.3389/fphar.2019.01607.

[92] Birnbaum, Y, et al. Pioglitazone limits myocardial infarct size, activates Akt, and upregulates cPLA2 and COX-2 in a PPAR-gamma-independent manner. Basic Res Cardiol. 2011; (106): 431-46. DOI: 10.1007/s00395-011-0162-3

[93] Gage, G, Kipke, D and Shain, W. Whole animal perfusion fixation for rodents. J Vis Exp. 2012; (30): 3564. DOI: 10.3791/3564

[94] Chung B. Protective effect of peroxisome proliferator activated receptor gamma agonists on diabetic and non-diabetic renal diseases. Nephrology. 2005; 10: 40-43. DOI: 10.1111/j.1440-1797.2005.00456.x

[95] [Online] https://www.drugs.com/monograph/pioglitazone.html.

[96] Bonventre, JV, Yang, L. Cellular pathophysiology of ischemic acute kidney injury. J Clin Invest. 2011; 121(11):4210-21. DOI: 10.1172/JCI45161

[97] Munshi, R, Hsu, C, Himmerfarb, J. Advances in understanding ischemic acute kidney injury. BMC Med. 2011; 9:11. DOI: 10.1186/1741-7015-9-11

[98] Yellon, DM, Hausenloy, DJ. Myocardial reperfusion injury. 2007; 357(11):1121-35. DOI: 10.1056/NEJMra071667

[99] O'Callaghan, JM, Knight, SR, Morgan, RD, Morris, PJ. Preservation solutions for static cold storage of kidney allografts: a systematic review and meta-analysis. Am J Transplant. 2012; 12(4):896-906. DOI: 10.1111/j.1600-6143.2011.03908.x

[100] Timsit, MO, Tullius, SG. Hypothermic kidney preservation: a remembrance of the past in the future? Curr Opin Organ Transplant. 2011; 16(2):162-8. DOI: 10.1097/MOT.0b013e3283446b07.

[101] Voigt, MR, DeLario, GT. Perspectives on abdominal organ preservation solutions: a comparative literature review. Prog Transplant. 2013; 23(4):383-91. DOI: 10.7182/pit2013100

[102] Chen, X, Karnovsky, A, Sans, MD, Andrews, PC, Williams, JA. Molecular characterization of the endoplasmic reticulum: insights from proteomic studies. Proteomics. 2010; 10(22):4040-4052. DOI: 10.1002/pmic.201000234

[103] Saito, A, Imaizumi, K. Unfolded protein response-dependent communication and contact among endoplasmic reticulum, mitochondria, and plasma membrane. Int J Mol Sci. 2018; 19(10):3215. DOI: 10.3390/ijms19103215

9. List of publication and presentation related to the thesis

Cumulative impact factor: **1.741**

Publication

Telek V, Erlitz L, Caleb I, Nagy T, Vecsernyés M, Balogh B, Sétáló G Jr, Hardi P, Jancsó G, Takács I. Effect of Pioglitazone on endoplasmic reticulum stress regarding in situ perfusion rat model. Clinical Hemorheology and Microcirculation. 2021. DOI: 10.3233/CH-211163. **IF 1.741 (Q2) /under publication/**

Presentations

Telek V, Erlitz L, Caleb I, Nagy T, Vecsernyés M, Balogh B, Sétáló G Jr, Hardi P, Jancsó G, Takács I. A novel treatment on endoplasmic reticulum stress regarding in situ perfused rat model. DOSZ Science and Innovation Conference 29-30th of January 2021

Telek V, Erlitz L, Caleb I, Nagy T, Vecsernyés M, Balogh B, Sétáló G Jr, Hardi P, Jancsó G, Takács I. Could Pioglitazone decrease endoplasmic reticulum stress regarding a novel in situ perfusion rat model? Magyar Haemorheologiai Társaság XXVII. Kongresszusa 23rd of April 2021.

9.1. Other publication and presentations

Cumulative impact factor: **1.901**

Publication

Borocz K, Csizmadia Z, Markovics A, Meszaros V, Farkas K, **Telek V**, Varga V, Maloba GO, Bodo K, Najbauer J, Berki T, Nemeth P. Development of a robust and standardized immunoserological assay for detection od anti-measles IgG antibodies in human sera. Journal of Immunological Methods. 2019. DOI: 10.1016/j.jim.2018.07.009 **IF 1.901 (Q2)**

Presentations

Telek V, Rapp J, Bognár A, Nagy G, Minier T, Czirják L, Berki T, Simon D. Analysis of PI3K pathway in B cells in early diffuse cutaneous systemic sclerosis. XVI. János Szentágothai Multidisciplinary Conference and Student Competition. 14-15th of February 2019. Pécs

Telek V, Rapp J, Balogh P, Minier T, Czirják L, Berki T, Simon D. PI3K jelátviteli útvonal aktivációjának vizsgálata autoreaktív B-sejtekben. 49. Membrán-Transzport Konferencia, 14-17th May 2019. Sümeg,

Telek V, Rapp J, Bognár A, Nagy G, Minier T, Czirják L, Berki T, Simon D. Innate immune activation of B cells in early diffuse cutaneous systemic sclerosis. Magyar Immunológiai Társaság 47. Vándorgyűlése 17-19th of October 2018 Bükfürdő

Telek V, Rapp J, Nagy G, Minier T, Czirják L, Berki T, Simon D. Alterations of PI3K pathway associated molecules in B cells in early diffuse cutaneous systemic sclerosis. 1st Medical Conference for PhD Students and Experts of Clinical Sciences. 27th of October 2018 Pécs

10.Acknowledgement

I would like to express my gratitude to all those who gave me the possibility to complete this thesis.

First of all, I owe a great debt of gratitude to Ildikó Takács MD and Gábor Jancsó MD for their excellent guidance, continuous support and irreplaceable help throughout my PhD studies.

I am grateful for the help of all the members of the Department of Surgical Research and Techniques, who contributed to my work.

I would also like to acknowledge the help of Mónika Vecsernyés, Bálint Balogh and György Sétáló Jr. MD at the Department of Medical Biology and Central Electron Microscope Laboratory of Pécs University.

I am also thankful to all my friends at the Department of Immunology and Biotechnology for providing me a researcher role model and an endless support.

Finally, I would like to give thanks to my parents and my family for their patience and love, and I appreciate that they supported me all the time.

Effect of Pioglitazone on endoplasmic reticulum stress regarding *in situ* perfusion rat model

Vivien Telek[1*], Luca Erlitz[1], Ibitamuno Caleb[1], Tibor Nagy[1], Mónika Vecsernyés[2], Bálint Balogh[2], György Sétáló Jr.[2,3], Péter Hardi[1], Gábor Jancsó[1], Ildikó Takács[1]

1 Department of Surgical Research and Techniques, Medical School, University of Pécs, 7624 Pécs, Hungary; telek.vivien@pte.hu (V.T.); lucaerlitz@gmail.com (L.E.); ibical@yahoo.com (I.C.); ntibor85@gmail.com (T.N.); hardipet@gmail.com (P.H.); jancsogabor@hotmail.com (G.J.); dr.takacsildi@gmail.com (I.T.)

2 Department of Medical Biology and Central Electron Microscope Laboratory, Medical School, University of Pécs, 7624 Pécs, Hungary; kali29@gmail.com (M.V.); balint.balogh@aok.pte.hu (B.B.); gyorgy.setalo.jr@aok.pte.hu (Gy.S.)

3 Signal Transduction Research Group, János Szentágothai Research Centre, 7624 Pécs, Hungary; gyorgy.setalo.jr@aok.pte.hu (Gy.S.)

* Correspondence: telek.vivien@pte.hu; Phone: +36-20-355-5191

Abstract

BACKGROUND: Ischemia-reperfusion injury (IRI) can cause insufficient microcirculation of the transplanted organ and results in a diminished and inferior graft survival rate.

OBJECTIVE: This study aimed to investigate the effect of different doses of an anti-diabetic drug, Pioglitazone (Pio), on endoplasmic reticulum stress and histopathological changes, using an *in-situ* perfusion rat model.

METHODS: Sixty male Wistar rats were used and were divided into six groups, consisting of the control group, vehicle-treated group and four Pio-treated groups (10, 20, 30 and 40 mg/kg Pio was administered). The rats were perfused through vena cava and an outflow on the abdominal aorta occurred. Following the experiment, kidneys and livers were collected. The level of the endoplasmic reticulum stress markers (XBP1 and Caspase 12) was analyzed using Western blot and histopathological changes were evaluated.

RESULTS: Histopathological findings were correlated with the Western blot results and depict a protective effect corresponding to the elevated dosage of Pioglitazone regarding in situ perfusion rat model.

CONCLUSIONS: In our study, Pioglitazone can reduce the endoplasmic reticulum stress, and the most effective dosage proved to be the 40 mg/kg Pio referencing the kidney and liver samples.

Keywords: endoplasmic reticulum stress, pioglitazone, in situ perfusion, cell damage

1. Introduction

Kidney transplantation is considered the best treatment for patients afflicted with an end stage renal disease. During surgical procedures, ischemia-reperfusion injury (IRI) can cause considerable problems. IRI is an evitable circumstance following donor transplantation and influences short term and long-term graft outcome. Following the effective transplant of a kidney, the main consequences include DGF (delayed graft function), acute and chronic graft rejection and chronic graft dysfunction [1-3]. A comprehensive understanding regarding IRI mechanisms will aid in discovering further improvements in donated organ survival. Around 30 % of DGF following a kidney transplantation is linked to IRI [4]. The mechanisms during IRI bear crucial relevance and more biomarkers are required in which one can predict the organ survival rate and proper function following transplantation. It is well known in which IRI can cause severe problems in microcirculation and it may lead to patient's higher morbidity and prolonged hospitalization. The intracellular biochemical changes which occur due to ischemia can cause cellular dysfunction, cellular and interstitial edema and inevitably result in cell death. As long the ischemia is prolonged, as severe the injury will be. During the reperfusion phase, following the ischemic period, reactive oxygen species are produced (oxygen ions, free radicals and peroxides) and all negatively impact ischemia-reperfusion damage. Additionally, this has an impact upon red blood cells micro-rheological parameters and may result in the disturbance of blood flow [5, 6, 7]. According to the paper of Varga et al., the optimal timing of remote ischemic preconditioning in renal IRI model has great importance. Delayed and early effect of preconditioning mechanisms were compared and hematological, microcirculatory and histomorphological parameters were analyzed. Based on histological findings, delayed effect of the used method was more effective. [8]

The endoplasmic reticulum (ER) is an important cell organelle responsible for the proper folding and sorting of proteins [9]. The functions of ER are disrupted when unfolded or misfolded proteins accumulate within it; characteristic of endoplasmic reticulum stress (ERS) [10]. ERS triggers the unfolded protein response (UPR) which improves cell survival by limiting ERS [11, 12]. ERS, in addition to mitochondrial changes, also play an important role in the processes of IRI. The two organelles are connected by signaling pathways and when ERS occurs in an uncontrolled means, several factors and mediators are released from the endoplasmic reticulum (ER) to mitochondria which results in the death of the cell [13]. X-box binding protein 1 (XBP1) is an inducible component of the

ERS response factor. Transcription of XBP1 messenger RNA (mRNA) is induced by activating transcription factor-6 (ATF6) and it is spliced by inositol-requiring enzyme 1 (IRE1), which is an ER-resident protein kinase and endonucleases. This splicing results in the production of the activated form of XBP1 (pXBP1[S]), and this is next translocated into the nucleus [14]. Spliced XBP1 (XBP1s) is induced following ERS, and the molecular weight is 56 kDa, while the unspliced XBP1's (XBP1u) molecular weight is 29 kDa. The XBP1s/XBP1u ratio correlates with the expression level of expressed proteins in order to adapt the folding capacity regarding the ER to the changed requirements. The authors used this method to select the highly productive clones in their experiments with Chinese hamster ovary cells [15]. Caspase 12 is an ER resident caspase which was recently identified to mediate ER stress-induced apoptosis (high calcium concentration or low oxygen) [16, 17]. Caspase 12 is an inflammatory caspase, and it is a negative regulator of the inflammatory response induced by infections, since it can activate the caspases 1 in inflammasome complexes, which will cause the production of the pro-inflammatory cytokines IL-1ß and IL-18 and the overall response to sepsis. Caspase 12 upregulation and processing has been observed following the ischemic episode, however its role in apoptosis is controversial. Observations suggest caspases 12 is cleaved and contributes to apoptosis, specifically in response to ERS inducing stimuli [18].

Pioglitazone (Pio) is a PPARγ agonist which is used in the treatment of type 2 diabetes. Furthermore, there are experiments proving its antioxidant and anti-inflammatory effects [19-34]. In addition to the insulin sensitizing effect regarding Pio, it can reduce inflammation and consequences of oxidative stress in the IRI model [35]. It can reduce the rate of apoptotic cells in a hypoxia/reperfusion experimental set [36]. Interestingly, there are experiments referencing the ERS reducing activity of Pio in pancreatic ß-cells from mouse insulinoma-6. Researchers found Pio can reduce the expression of inflammatory cytokines and ERS markers (GRP78 – glucose-regulated protein 78; ATF6 and CHOP – C/EBP homologous protein) [37]. Another experiment aimed to investigate the effects regarding Pio characteristic of cardiovascular complications of N-nitro-L-arginine methyl ester (L-NAME)-induced hypertension and to determine the role of oxidative and ERS involving its activity. The reduction of the ERS was PPAR-γ dependent [38].

In our novel experimental model, we applied a new setting to remodel the situation in human transplantation protocol and confirm the protective effect of Pio and insert the results in the international literature. We hypothesize that Pio can reduce the ERS and in such a way it protects cells from the consequences of ischemia and apoptosis. We administered Pio in different concentrations, and the aim was to investigate the effect of Pio in our novel in situ perfusion model through the histopathological and Western blot analyses regarding kidney and liver samples.

2. Materials and Methods

a) Animal model

Sixty male Wistar rats of the same age, weighing between 250-300g, were used for this study. The rats were housed in separate cages, under standard conditions (temperature was 25±2 ℃, in air-filtered room), with 12/12-hour light and dark cycle and were fed with standard rat chow and water ad libitum. The study protocol was approved by the National Scientific Ethical Committee on Animal Experimentation. (Number: BA02/2000-38/2019).

b) Experimental protocol

Animals were divided into six groups, ten rats in each group. The first group was the control (sham operated). In the other groups, we operated upon the rats and made the perfusion. The second group was the KH control (KH – Krebs-Henseleit buffer), the third group was the KH + Pio 10 mg/kg, the fourth group was the KH + Pio 20 mg/kg, the fifth group was the KH + Pio 30 mg/kg and the sixth group was the KH + Pio 40 mg/kg (Table 1). To standardize the study, all procedures were performed at similar time points in all groups. The drug was freshly dissolved into PBS + 10 % DMSO solution prior to the administration. The perfusion solution's temperature was maintained at 20℃ during the entire study.

c) Surgical procedure

The rats were preoperatively anesthetized using an intraperitoneal (i.p.) application of a mixture consisting of ketamine (2.7 ml/kg) and diazepam (2.7 ml/kg). The ratio was 1:1. The skin of the abdomen was depilated. During the operation, the animals were placed on a heated pad and ECG monitoring was also used. Following the middle laparotomy, the infrarenal abdominal aorta and inferior vena cava were dissected and heparin was administered into the mesenterial vein (400 IU/kg). Following two minutes, the inferior

vena cava was catheterized (22 gauge) and the in situ whole body perfusion was initiated. 250 ml perfusion solution was used in each experimental group. The perfusion equipment was set to 100-150 ml/h in the case of one sample, in which the perfusion lasted 80-100 minutes. At the same time while catheterizing the inferior vena cava, on the infrarenal abdominal aorta, we made a small incision, and it was the outflow of the perfusate which was removed from the abdominal cavity. The sham group was handled as a treated group without perfusion, in which the blood circulation was intact. The animals of the sham group were sacrificed due to bleed out following 80 minutes and treated groups' animals were sacrificed in an identical manner during the experiment (once the perfusion was initiated, the animals remained alive for 15±2 minutes, and was monitored using an ECG). At the end of the perfusion protocol, kidneys and liver were removed and were immediately stored at -80°C within individual containers (Fig. 1).

d) Histopathological analysis – Hematoxylin-eosin staining protocol

Tissues were fixed in a 10% neutral buffered formalin, embedded in paraffin, cut in three micrometers thick sections with a rotational microtome (Microm HM 325, Thermo Scientific, Ltd.) and mounted on coated glass microscope slides. Following deparaffinization and rehydration, samples were stained with hematoxylin, bluing was performed with tap water, and tissues were stained with eosin, dehydrated in alcohol, cleared in xylene, and mounted with permanent mounting medium. During analysis, the 11.3x magnification was used, since the representation of kidney and liver tissue damages are more detectable, and we focused on tissue not cell dimension.

e) Western blot protocol

Kidney and liver tissue samples were frozen in liquid nitrogen then manually pulverized in mortar and dissolved in ice-cold lysis buffer (containing 50 mM Tris, pH 7.4, 150 mM NaCl, 1 mm EGTA, 1 mM Na3VO4, 100 mM NaF, 5 μM ZnCl2, 10% glycerol, and 1% Triton X-100 plus 10 μg/ml of the protease inhibitor aprotinin). Lysates were subjected to centrifugation at 40,000 x g at 4°C for thirty minutes, and next the protein concentration of the supernatants was determined using Protein Assay Dye Reagent Concentration (Bio-Rad Laboratories, Inc., Hercules, California, USA) and light absorption measurement at 595 nm. The sample pools were prepared at the same time in a higher volume, which was enough to perform the indicated repeat number of Western blots. Samples containing 30 μg of denatured total protein were prepared and loaded onto 10% polyacrylamide gels. Proteins were separated based on size which were electro-blotted for thirty minutes onto

PVDF membranes using the Trans-Blot Turbo semi-dry system (Bio-Rad Laboratories, Inc., Hercules, California, USA), then blocked in 3% BSA dissolved in Tris-buffered saline containing 0.2% Tween 20. The probing of the membranes with the primary antibodies (pro-caspases 12 and XBP1 [Sigma-Aldrich, St. Louis, Missouri, USA]) were diluted 1:1000 in the blocking solution and stored overnight 4° C overnight. Binding of the antibodies to the membrane was detected by a secondary anti-rabbit IgG conjugated to horseradish peroxidase (Santa Cruz Biotechnology, Inc., Dallas, Texas, USA) and diluted 1:10,000. The enhanced chemiluminescent signal was visualized using a G:box gel documentation system (Syngene, India). All membranes were then stripped from the antibodies and detected again as described above for possible loading differences using a primary antibody against GAPDH (Cell Signaling Technology, Danvers, Massachusetts, USA) at a dilution rate of 1:3000. ImageJ software was used to analyze the blots. To demonstrate results, the most representative blot was chosen from each experiment.

f) Statistical analysis

Western blots were performed independently in triplicates. All samples from each experimental group were added into gels (6 experimental group, 10 animal samples in each group), and after three replications of Western blots under identical conditions was applies. Regarding statistical evaluation, one-way analysis of variance (ANOVA) was used, followed by post-hoc analysis of Bonferroni. All data are represented as the mean ± SD. The difference was considered statistically significant when the p-value was less than 0.05 and classified by asterisks as follows: $p<0.05$ (*); $p<0.001$ (**); $p<0.0001$ (***). The statistical analysis was calculated through GraphPad Prism software for Windows (version 5.03).

3. Results

a) Results of kidney samples

The representative pictures of histopathological examination in the renal tissue are depicted in Fig. 2. Our histopathological findings correlate with the Western blot results. In the control group, the basic tissue structures were mainly kept; edema, necrosis or inflammation cannot be detected. In the second experimental group, where KH (Krebs-Henseleit solution) perfusion was applied without Pio, tubular necrosis, tubular dilatation and dilatation of Bowman’s capsule can be seen. In the KH+40 Pio (Krebs-Henseleit

solution modified with 40 mg/kg Pio) group, the structure of the kidneys correlates to the control group's samples, and the basic tissue structure is mainly kept.

Western blot analysis was performed to examine the expressions regarding Caspase 12 and XBP1, both from liver and kidney samples, and explore the effect of the different doses regarding Pio. Expression of Caspase 12 was lower, dependent on the dosage of the drug regarding kidney samples. Pio was efficient in all of the four administered doses (control: 1.000 ± 0.1114 vs. KH: 3.3614 ± 0.4694 and KH + 10 Pio: 2.6794 ± 0.2788 p=0.0001 and p=0.05; KH: 3.3614 ± 0.4694 vs. KH + 20 Pio: 1.7900 ± 0.1420 and KH + 30 Pio: 1.5439 ± 0.3233 and KH + 40 Pio: 1.4373 ± 0.1519 p=0.0001; KH + 10 Pio: 2.6794 ± 0.2788 vs. KH + 20 Pio: 1.7900 ± 0.1420 and KH + 30 Pio: 1.5439 ± 0.3233 and KH + 40 Pio: 1.4373 ± 0.1519 p=0.0001) (Fig.3).

The Western blot analysis exhibited the significant differences in the case of XBP1 expression in kidney samples. The pattern of the pixel density appears similar in the case of XBP1s and XBP1u, however, the XBP1u had weaker bands and the expression of these proteins was lower. Nevertheless, the 40 mg/kg dose of Pio was significantly effective in reducing the expression of both of the XBP1s and XBP1u (XBP1s: control: 1.0000 ± 0.1405 vs. KH: 5.6946 ± 0.8711 p=0.001; KH: 5.6946 ± 0.8711 vs. KH + 30 Pio: 2.0773 ± 0.3394 and KH + 40 Pio: 1.5163 ± 0.2277 p=0.5 and p=0.0001) (XBP1u: KH: 2.9561 ± 0.6434 vs. KH + 40 Pio: 1.5087 ± 0.3540 p=0.05; KH + 10 Pio: 2.8705 ± 0.7607 vs. KH + 40 Pio: 1.5087 ± 0.3540 p=0.05) (Fig.4, 5).

b) Results of liver samples

Sections of rat livers from different treated groups were stained with hematoxylin and eosin and are presented in Fig. 6. The control group depicted a normal appearance. In the non-treated ischemic group (KH), we can detect pronounced nodular fibrosis of the parenchyma with hypertrophic hepatocytes and a swelling of the liver cells. In KH+20 Pio and KH+30 Pio groups, the basic tissue structure was mainly kept. We cannot detect any signs of oncosis or apoptosis among the treated groups. However, the changes are not significant, but viewing all the liver samples the tendency of the protective effect of the administered drug can be very well detected.

The expression of Caspase 12 regarding liver samples was significantly lower at 10 and 20 mg/kg Pio concentrations compared to the KH group (control: 1.0000 ± 0.0668 vs. KH:

3.0578 ± 0.4240 p=0.05; KH: 3.0578 ± 0.4240 vs. KH + 10 Pio: 2.0768 ± 0.2354 and KH + 20 Pio: 2.0591 ±0.4795 p=0.05) (Fig.7).

In regards to the liver samples, the pattern of the bands appeared similar, however, the significantly effective dosages of Pio were the 30 and the 40 mg/kg analyzing XBP1s and XBP1u (XBP1s: control: 1.0000 ± 0.3736 vs. KH: 5.1087 ± 0.9549 p=0.001; KH: 5.1087 ± 0.9549 vs. KH + 30 Pio: 1.6936 ± 0.6389 and KH + 40 Pio: 1.6460 ± 0.3627 p=0.05) (XBP1u: control: 1.0000 ± 0.3655 vs. KH: 5.5834 ± 0.4024 p=0.01; KH: 5.5834 ± 0.4024 vs. KH + 30 Pio: 2.1226 ± 0.5372 and KH + 40 Pio: 1.9820 ± 0.5670 p=0.05) (Fig.8, 9).

4. Discussion

The use of a proper drug to decrease the damage caused by IRI plays a crucial role in transplantation and surgery. Approximately 30% of DGF following kidney transplantation is linked to IRI [4]. In our experiment, we chose a drug, Pio, which is used as an insulin sensitizer agent in treatment of type 2 diabetes and according to published literature, it has anti-inflammatory and antioxidant effects, and can decrease the amount of cell damage and apoptosis. The initial ERS response is a defensive mechanism to detect unfolded and misfolded proteins and maintain ER homeostasis. Prolonged perturbation of ER triggers the activation of an adaptive signaling pathway referred to as UPR. Long-term UPR activation can lead to apoptotic programmed cell death [39, 40]. In the present study, we demonstrated the use of Pio as an antioxidant agent can suppress the expression of ERS markers. Activation of IRE1 induces altered communication between ER and mitochondria, leading to dysfunction in mitochondria, metabolic imbalance, and cell death. In the control group, we observed an enhanced expression of XBP1 and Caspase 12 and in a dose-dependent manner, Pio decreased the level of these ERS markers. These findings implicate Pio as a therapeutic target for the protection of ERS and ultimately cell death. The ratio pf the XBP1s/XBP1u presents the activity of IRE1 pathways, however, different gels and membranes were used to detect XBP1s and XBP1u. Therefore, the calculation of the ratio is not necessarily reliable.

In our experimental model, we used the in situ whole body perfusion system to perfuse the kidneys and liver with Krebs-Henseleit solution modified with different dosages of Pio. Dosages used were 10, 20, 30 and 40 mg/kg Pio. The literature stated these concentrations can be protective against cell damage and apoptosis, and a higher dose level is more

effective [20, 24, 25, 40]. This in situ perfusion model is suitable for mimicking the kidney or liver transplantation, when clinicians perfuse the organ with organ preservative solution, which helps to keep the organ functional and does not modify the cell structure. This process is inevitably necessary to decrease DGF and the consequently repeated transplantation. According to our results, we conclude Pio is suitable for reducing the cell damage and decreasing potential ERS and apoptosis. TUNEL staining was performed on all samples and it confirmed the results that Pio was not harmful in either administered concentrations. However, due to enzyme polymorphisms, our results have limited applicability in human transplantation protocol and cure, utilization of the results should be considered.

Concentrations used were based on published literature [20, 40]. Singh et al. used in their experiment, 20 and 40 mg/kg Pio orally 1 h prior to IRI induction. According to their results, the 40 mg/kg dosage decreased the serum urine acid, blood urea nitrogen, serum nitrogen and microproteinuria concentrations. Furthermore, Pio in higher concentrations lowers the myeloperoxidase activity regarding tissue. They highlight the renoprotective effect of Pio in diabetic and non-diabetic models in reference to a kidney injury [29, 31].

To set the perfusion time and perfusate volume, we used a perfusion fixation protocol and modified it since we used the vena cava as inflow and abdominal aorta section as outflow. The protocol recommended, passing through the abdominal aorta of the rat, we need 100 ml/h flow rate, thus, in our experiment, we initiated perfusion from 100 ml/h and then slowly increased the flow rate until the kidney and the liver became opalescent/white. According to the protocol, 250-300 ml of perfusate solution is optimal for one rat [41].

The group of thiazolidinediones (TZDs) is the most widely studied PPARγ ligands [42]. Activation of PPARγ results in insulin sensitization by opposing the effect of TNFα in adipocytes and enhances glucose metabolism. Recent studies show Pio protects kidneys, myocardium, and the brain against IRI [43-46]. The potential role of Pio and other PPARγ agonists are nephroprotective agents and is demonstrated in non-diabetic models of renal injury (such as IRI and induced renal toxicity by a drug or chemical) [29-31]. Renoprotective properties of Pio exhibits via facilitation of endothelium-dependent vasodilatation through amending abnormalities in NO production [32], developing the antioxidant profile [33] and control of the expression of inflammatory mediators [47, 48] and apoptotic factors [49]. Additionally, with regards to the insulin sensitizing effect of

Pio, it can reduce inflammation and consequences of oxidative stress in IRI model [34]. Experiments under hypoxic conditions on NRK-52 cells proved Pio increased the rate of cell survival and decreased the injury caused by hypoxia/reperfusion. According to TUNEL assay, they ascertain Pio can reduce the rate of apoptotised cells in treated groups compared with the untreated, hypoxia/reperfusion control group [35]. Furthermore, Pio has endothelial protective functionality which can be used beside methotrexate (MTX) therapy [18].

Previously, the effect of Pio was studied in IRI rat models, yet, in an in situ perfusion set, we cannot find any results. To the best of our knowledge, this is the first study in which Pio effects were thoroughly examined regarding an in situ perfusion model in reference to ERS and histological changes. We conclude Pio is most effective in acute use and in higher concentrations.

5. Conclusions

Pio is a clinically applicable and non-toxic agent, which can increase the ischemic tolerance of tissues in decreasing the endoplasmic reticulum stress and consequent apoptosis. The results support the finding in which Pio has an ERS decreasing effect in higher dosage levels, both in the case of kidney and liver perfusion. Furthermore, we could not detect any necrotic effect regarding Pio, which may indicate for a short period of time, an acute administered higher dosage of this PPARγ agonist Pioglitazone can help in maintaining the basic organ structure in the case of both the kidney and liver. Further experiments are needed to examine other PPARγ agonists referenced this methodological set and prove their potential role in ischemia and organ preservation by in situ perfusion. In our preliminary study, we aimed to confirm the protective effect of Pio in our novel in situ perfused rat model. Other ERS pathways should be examined in this experimental set to get a broader knowledge of ERS reducing activity of Pio. Furthermore, we plan to examine the effects of reperfusion on kidney tissue using renal damage and apoptosis markers.

6. References

[1] Philipponnet C, Aniort J, Garrouste C, Kemeny J, Heng A. Ischemia reperfusion injury in kidney transplantation. Medicine (Baltimore). 2018; 97(52): e13650. DOI: 10.1097/MD.0000000000013650

[2] Nagy T, Hardi P, Takács I, Tóth M, Petrovics L, Jancsó G, Sínay L, Fazekas G, Pintér Ö, Arató E. Pentoxifylline attenuates the local and systemic inflammatory response after infrarenal abdominal aortic ischemia-reperfusion. Clin Hemorheol Microcirc. 2017; 65(3):229-240. DOI: 10.3233/CH-16169

[3] Petrovics L, Nagy T, Hardi P, Bognar L, Pavlovics G, Tizedes Gy, Takacs I, Jancso G. The effect of trimetazidine in reducing the ischemia-reperfusion injury in rat epigastric skin flaps. Clin Hemorheol Mircocirc. 2018;69(3):405-415. DOI: 10.3233/CH-170335

[4] Womer K, Vela J, Sajegh M. Chronic allograft dysfunction: mechanisms and new approaches to therapy. Semin Nephrol. 2000; 20: 126-147

[5] Klarik Z, Tamas R, Toth E, Kiss F, Kovacs E, Jäckel M, et al. Intra and postoperative evaluations of microcirculation and micro-rheological parameters in a rat model of musculocutaneous flap ischemia-reperfusion. Acta Cir Bras. 2015; 30: 551-60. DOI: 10.1590/D0102-865020150080000006

[6] Grau M, Kollikowski A, Bloch W. Remote ischemia preconditioning increases red blood cell deformability through red blood cell-nitrite oxide synthase activation. Clin Hemorheol Microcirc. 2016; 63(3): 185-97. DOI: 10.3233/CH-152039

[7] Matschkee K, Jung F. Regulation of the myocardial microcirculation. Clin Hemorheol Microcirc. 2008; 39: 265-279. DOI: 10.3233/CH-2008-1093

[8] Varga G, Ghanem S, Szabo B, Nagy K, Pal N, Tanczos B, Somogyi V, Barath B, Deak A, Matolay O, Bidiga L, Peto K, Nemeth N. Which remote ischemic preconditioning protocol is favorable in renal ischemia-reperfusion injury in the rat? Clin Hemorheol Microcirc. 2020; 76(3): 439-451. DOI: 10.3233/CH-200916

[9] Boyse M, Yuan J. Cellular response to endoplasmic reticulum stress: a matter of life or death. Cell Death Differ. 2006; 13: 363-73. DOI: 10.1038/sj.cdd.440187

[10] Verkhratsky A. Physiology and pathophysiology of the calcium store in the endoplasmic reticulum of neurons. Physiol Rev. 2005; 85: 201-79. DOI: 10.1152/physrev.00004.2004

[11] Mori K. Tripartite management of unfolded proteins in the endoplasmic reticulum. Cell. 2000; 101: 451-4. DOI: 10.1016/s0092-8674(00)80855-7

[12] Patil C, Walter P. Intracellular signaling from the endoplasmic reticulum to the nucleus: the unfolded protein response in yeast and mammals. Curr Opin Cell Biol. 2001; 13: 349-55. DOI: 10.1016/s0955-0674(00)00219-2

[13] Sasaki K, Joshida H. Organelle autoregulation-stress responses in the ER, Golgi, mitochondria and lysosome. J. Biochem. 2015; 157(4): 185-195. DOI: 10.1093/jb/mvv010

[14] Yoshida H, Matsui T, Yamamoto A, Okada T, Mori K. XBP1 mRNA is induced by ATF6 and spliced by IRE1 in response to ER stress to produce a highly active transcription factor. Cell. 2001; 107: 881-91. DOI: 10.1016/s0092-8674(01)00611-0

[15] Kober L, Zehe C, Bode J. Development of a novel ER stress based selection system for the isolation of highly productive clones. Biotechnology and Bioengineering. 2012; 109(10): 2599-611. DOI: 10.1002/bit.24527

[16] Nakagawa T, Yuan J. Cross-talk between two cysteine protease families. Activation of caspase-12 by calpain in apoptosis. J Cell Biol. 2000; 150: 887-894. DOI: 10.1083/jcb.150.4.887

[17] Nakagawa T, Zhu H, Morishima N, Li E, Xu J, Yankner B, et al. Caspase-12 mediates endoplasmic-reticulum-specific apoptosis and cytotoxicity by amyloid-beta. Nature. 2000; 403: 98-103. DOI: 10.1038/47513

[18] El-Gowilly S, Helmy M, El-Gowelli H. Pioglitazone ameliorates methotrexate-induced renal endothelial dysfunction via amending detrimental changes is some antioxidant parameters, systemic cytokines and Fas production. Vascular Pharmacology. 2015; 74: 139-150. DOI: 10.1016/j.vph.2015.07.002

[19] Chen W, Xi X, Zhang S, Zou C, Kuang R, Ye Z, et al. Pioglitazone protects against renal ischemia/reperfusion injury via the AMP-activated protein kinase-regulated autophagy pathway. Front. Pharmacol. 2018; 9(851): 1-12. DOI: 10.3389/fphar.2018.00851

[20] Singh A, Singh N, Bedi P. Pioglitazone ameliorates renal ischemia reperfusion injury through NMDA receptor antagonism in rats. Mol Cell Biochem. 2016; 417: 111-118. DOI: 10.1007/s11010-016-2718-x

[21] Reel B, Bagriyanik A, Atmaca S, Aykut K, Albaxrak G, Hazan E. The effect of PPAR-gamma agonist pioglitazone on renal ischemia/reperfusion injury in rats. 2013; 182: 176-184. DOI: 10.1016/j.jss.2012.08.020

[22] Zanchi A, Perregaux C, Maillard M, Cefai D, Nussberger J, Burnier M. The PPARgamma agonist pioglitazone modifies the vascular sodium-angiotensin II relationship in insulin-resistant rats. Am J Physiol Endocrinol Metab. 2006; 291: E1228-E1234. DOI: 10.1152/ajpendo.00171.2006

[23] Paciello F, Fetoni A, Roesi R, Wright M, Grassi C, Troiani D, et al. Pioglitazone represents an effective therapeutic target in preventing oxidative/inflammatory cochlear damage induced by noise exposure. Front Pharmacol. 2018; 9(1103): 1-15. DOI: 10.3389/fphar.2018.01103

[24] Medic B, Stojanovic M, Rovcanin B, Kekic D, Skodric S, Jovanovic G, et al. Pioglitazone attenuates kidney injury in an experimental model of gentamicin-induced nephrotoxicity in rats. Nature Scientific Reports. 2019; 9: 13689. DOI: 10.1038/s41598-019-49835-1

[25] Oliveira A, Bertollo C, Rocha L, Nascimento Jr. E, Costa K, Coelho M. Antinociceptive and antiedematogenic activities of fenofibrate, an agonist of PPAR alpha, and pioglitazone, an agonist of PPAR gamma. European Journal of Pharmacology. 2007; 561: 194-201. DOI: 10.1016/j.ejphar.2006.12.026

[26] Kaplan J, Nowell M, Chima R, Zingarelli B. Pioglitazone reduces inflammation through inhibition of nuclear factor kappa-B in polymicrobial sepsis. Innate Immun. 2014; 20(5): 519-528. DOI: 10.1177/1753425913501565

[27] Khooder D, Zaitone S, Farag N, Moustafa Y. Cardioprotective effect of pioglitazone in diabetic and non-diabetic rats subjected to acute myocardial infarction involves suppression of AGE-RAGE axis and inhibition apoptosis. Can. J. Physiol. Pharmacol. 2016; 94(5): 463-76. DOI: 10.1139/cjpp-2015-0135

[28] Elshazly S, Soliman E. PPAR gamma agonist, pioglitazone, rescues liver damage induced by renal ischemia/reperfusion injury. Toxicology and Applied Pharmacology. 2019; 362: 86-94. DOI: 10.16/j.taap.2018.10.022

[29] Sivarajah A, Chatterjee P, Patel N, Todorovic Z, Hattori Y, Brown P, et al. Agonists of peroxisome proliferator activated receptor-gamma reduce renal ischemia/referfusion injury. Am J Nephrol. 2003; 23: 267-276. DOI: 10.1159/000072088

[30] Chung B. Protective effect of peroxisome proliferator activated receptor gamma agonists on diabetic and non-diabetic renal diseases. Nephrology. 2005; 10: 40-43. DOI: 10.1111/j.1440-1797.2005.00456.x

[31] Pereira M, Camara N, Campaholle G, Cenedeze M, Teixeira V, Antonia dos Reis M, Pacheco-Silva A. Pioglitazone limits cyclosporine nephrotoxicity in rats. Int Immunopharmacol. 2006; 6: 1943-1951. DOI: 10.1016/j.intimp.2006.07.024

[32] Abd-Elrahman K, El-Gowelli H, Saad E, Abdel-Galil A, El-Mas M. Role of PPAR gamma/nitric oxide synthase signaling in the cyclosporine-induced attenuation of endothelium-dependent renovascular vasodilatation. J Cardiovasc Pharmacol. 2010; 56: 195-202. DOI: 10.1097/FJC.0b013e3181e74d83

[33] El-Mas M, El-Gowelli H, Adb-Elrahman K, Saad E, Abdel-Galil A, Abdel-Rahman A. Pioglitazone abrogates cyclosporine-evoked hypertension via rectifying abnormalities in vascular endothelial function. Biovhem Pharmacol. 2011; 81: 526-533. DOI: 10.1016/j.bcp.2010.11.013

[34] Cao Z, Ye P, Long C, Chen K, Li X, Wang H. Effect of pioglitazone a peroxisome proliferator-activated receptor gamma agonist, on ischemia reperfusion injury in rats. Pharmacology. 2007; 79: 184. DOI: 10.1159/000100870

[35] Xi X, Zou C, Ye Z, Huang Y, Chen T, Hu H. Pioglitazone protects tubular cells against hypoxia/reoxygenation injury through enhancing autophagy via AMPK-mTOR signaling pathway. European Journal of Pharmacology. 2019; 863: 172695. DOI: 10.1016/j.ejphar.2019.172695

[36] Hong S, Lee J, Cho J, Kwon H, Park S, Rhee E, et al. Pioglitazone attenuates palmitate-induced inflammation and endoplasmic reticulum stress in pancreatic ß-cells. Endocrinol Metam (Seoul). 2018; 33(1): 105-113. DOI: 10.3803/EnM.2018.33.1.105

[37] Soliman E, Behairy S, El-Maraghy N, Elshazly S. PPAR-γ agonist, pioglitazone, reduced oxidative and endoplasmic reticulum stress associated with L-NAME-induced hypertension in rats. Life Siences. 2019; 239: 117047. DOI: 10.1016/j.lfs.2019.117047

[38] Schroder M, Kaufman R. The mammalian unfolded protein response. Annu. Rev. Biochem. 2005; 74: 739-789. DOI: 10.1146/annurev.biochem.73.011303.074134

[39] Ron D, Walter P. Signal integration in the endoplasmic reticulum unfolded protein response. Nat. Rev. Mol. Cell Biol. 2007; 8: 519-529. DOI: 10.1038/nrm2199

[40] Birnbaum Y, Long B, Qian J, Perez-Polo J, Ye Y. Pioglitazone limits myocardial infarct size, activates Akt, and upregulates cPLA2 and COX-2 in a PPAR-gamma-independent manner. Basic Res Cardiol. 2011; 106: 431-46. DOI: 10.1007/s00395-011-0162-3

[41] Gage G, Kipke D, Shain W. Whole animal perfusion fixation for rodents. J Vis Exp. 2012;(30): 3564. DOI: 10.3791/3564

[42] Michalik L, Wahli W. Involvement of PPAR nuclear receptors in tissue injury and wound repair. J Clin Invest. 2006; 116(3): 598-606. DOI: 10.1172/JCI27958

[43] Ahmed L, Salem H, Attia A, Agha A. Pharmacological preconditioning with nicorandil and pioglitazone attenuates myocardial ischemia/reperfusion injury in rats. Eur. J. Pharmacol. 2011; 663: 51-58. DOI: 10.1016/j.ejphar.2011.04.038

[44] Zhang H, Xu M, Qin A, Liu C, Hong L, Zhao X, et al. Neuroprotective effects of pioglitazone in a rat model of permament focal cerebral ischemia are associated with peroxisome proliferator-activated receptor gamma-mediated suppression of nuclear factor-kB signaling pathway. Neuroscience. 2011; 176: 381-395. DOI: 10.16/j.neuroscience.2010.12.029

[45] Zhang X, Xiao Y, Zhang Y, Ye W. Protective effect of pioglitazone on retinal ischemia/reperfusion injury in rats. Ophtalmol. Vis. Sci. 2013; 54: 3912-3921. DOI: 10.1167/iovs.13-11614

[46] Zou X, Hu H, Xi X, Shi Z, Wang G, Huang X. Pioglitazone protects against renal ischemia-reperfusion injury by enhancing antioxidant capacity. J. Surg. Res. 2013; 184: 1092-1095. DOI: 10.1016/j.jss.2013.03.027

[47] Ibrahim M, El-Sheikh A, Khalaf H, Abdelrahman A. Protective effect of peroxisome proliferator activator receptor (PPAR)-alpha and gamma ligands against methotrexate-induced nephrotoxicity. Immunopharmacol. Immunotoxicol. 2014;(36): 130-137. DOI: 10.3109/08923973.2014.884135

[48] Vijay S, Mishra M, Kumar H, Tripathi K. Effect of pioglitazone and rosiglitazone on mediators of endothelial dysfunction, markers of angiogenesis and inflammatory cytokines in type-2 diabetes. Acta Diabetol. 2009; 46: 27-33. DOI: 10.1007/s00592-008-0054-7

[49] Chen J, Li D, Zhang X, Mehta J. Tumor necrosis factor-alpha-induced apoptosis of human coronary artery endothelial cells: modulation by the peroxisome proliferator-activated receptor-gamma ligand pioglitazone. J. Cardiovasc. Pharmacol. 2004;(9): 35-41. DOI: 10.1177/107424840400900i106

Table 1. Regarding matters of clarification, the experimental groups and the treatments are listed below (KH – Krebs-Henseleit solution; Pio – Pioglitazone).

Groups (n=10 in each groups)	Treatments
1. group	control (sham operated)
2. group	perfused with KH
3. group	perfused with KH + 10 mg/kg Pio
4. group	perfused with KH + 20 mg/kg Pio
5. group	perfused with KH + 30 mg/kg Pio
6. group	perfused with KH + 40 mg/kg Pio

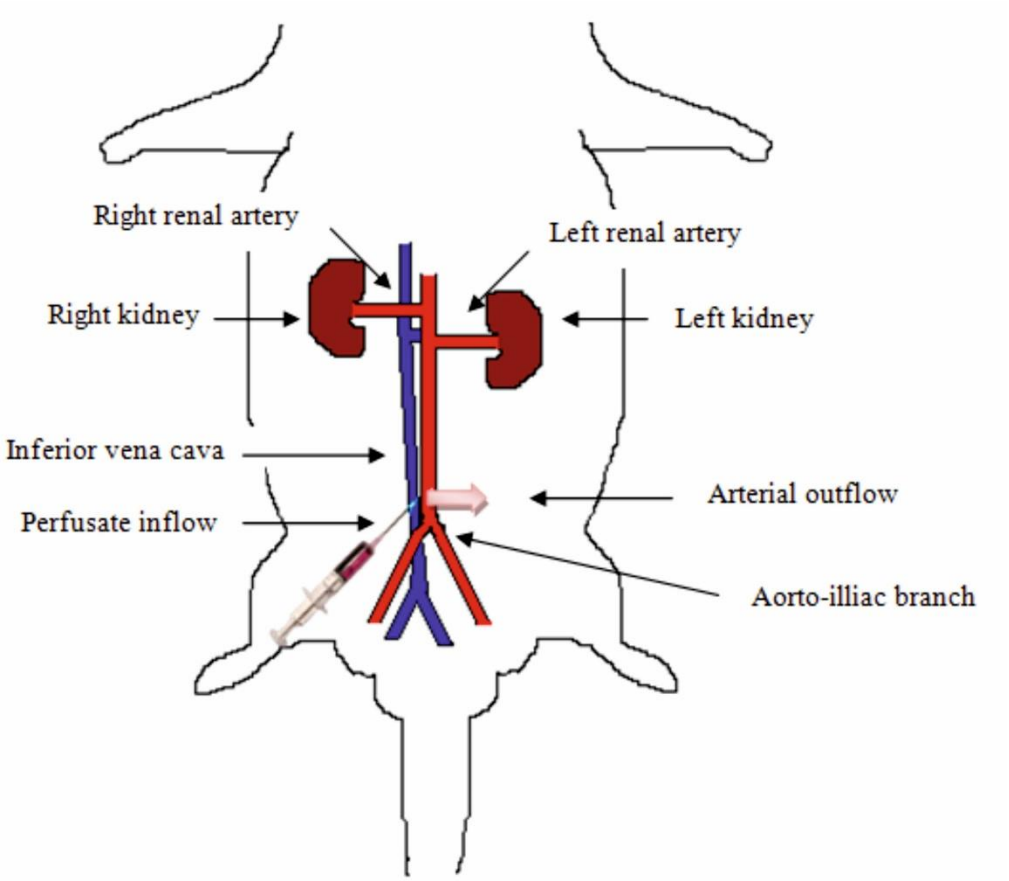

Figure 1. Schematic representation of an animal regarding in situ perfusion model.

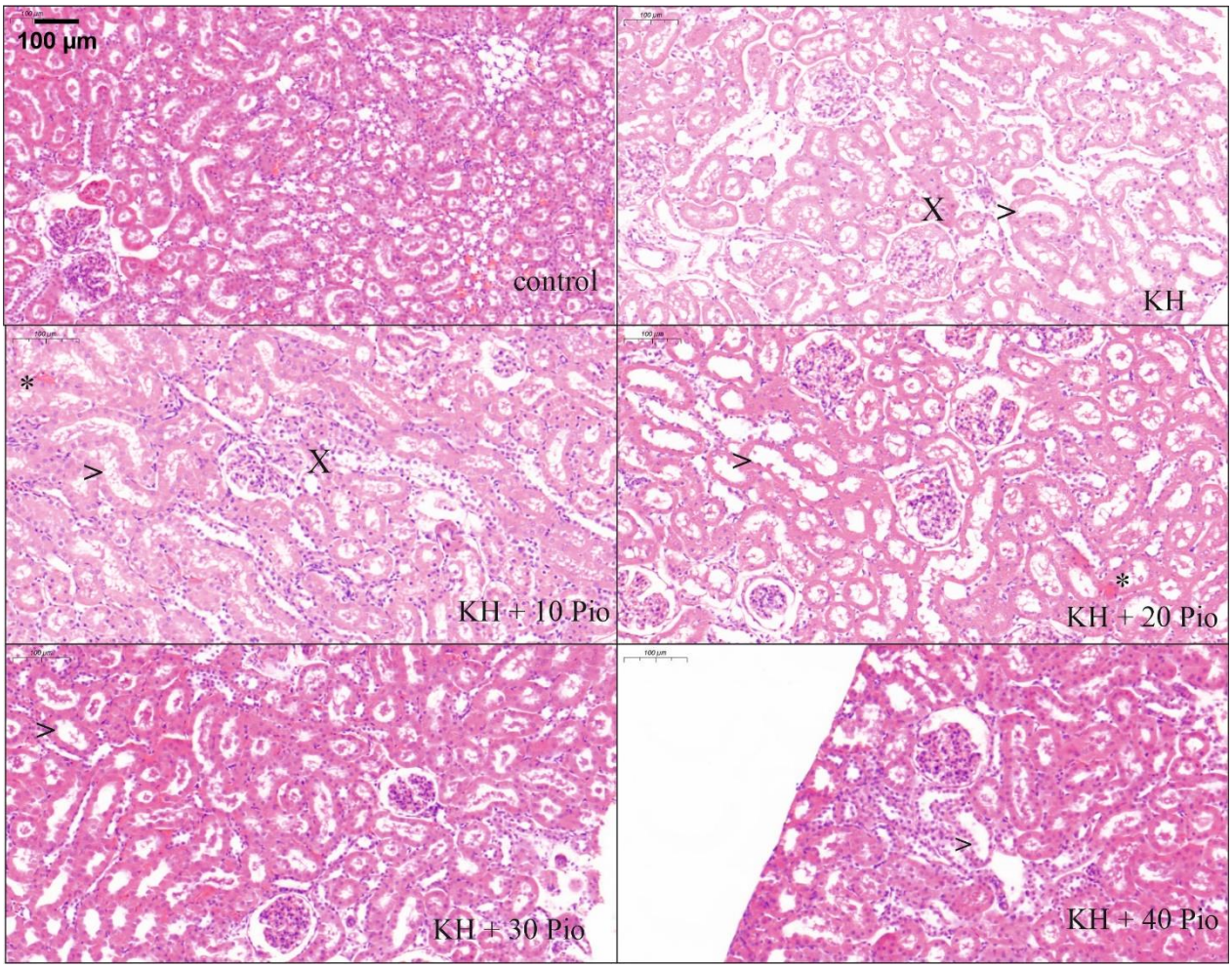

Figure 2. Staining: HE, magnification: 11.3x. In the control group of kidney samples, the basic tissue structures were kept; edema, necrosis or inflammation cannot be detected. In the treated groups, we detected eosinophil particles, disorders in Bowman's capsule. The asterisk (*) represents eosinophilia and the arrowhead (>) points at the swelling of endothelial tubules, and the X's serve as to show the swelling of Bowman's capsules. [KH – Krebs-Henseleit solution; KH + 10 Pio – Krebs-Henseleit solution modified with 10 mg/kg Pio; KH + 20 Pio – KH modified with 20 mg/kg Pio; KH + 30 Pio – KH modified with 30 mg/kg Pio; KH + 40 Pio – KH modified with 40 mg/kg Pio).

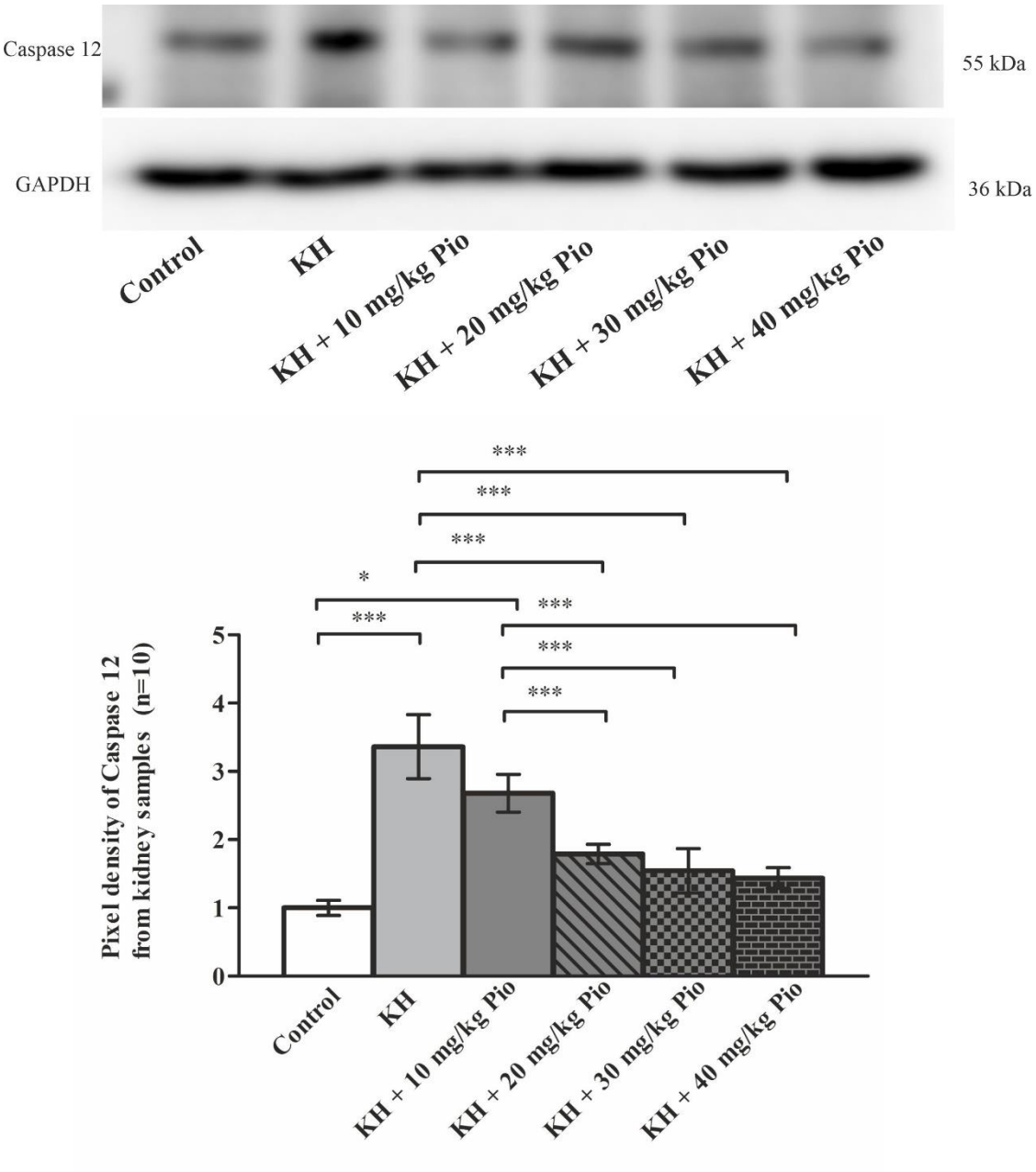

Figure 3. Western blot results for expression of Caspase 12 from kidney samples. GAPDH served as a normalization control. Blots and relative quantities of Caspase 12 are presented.

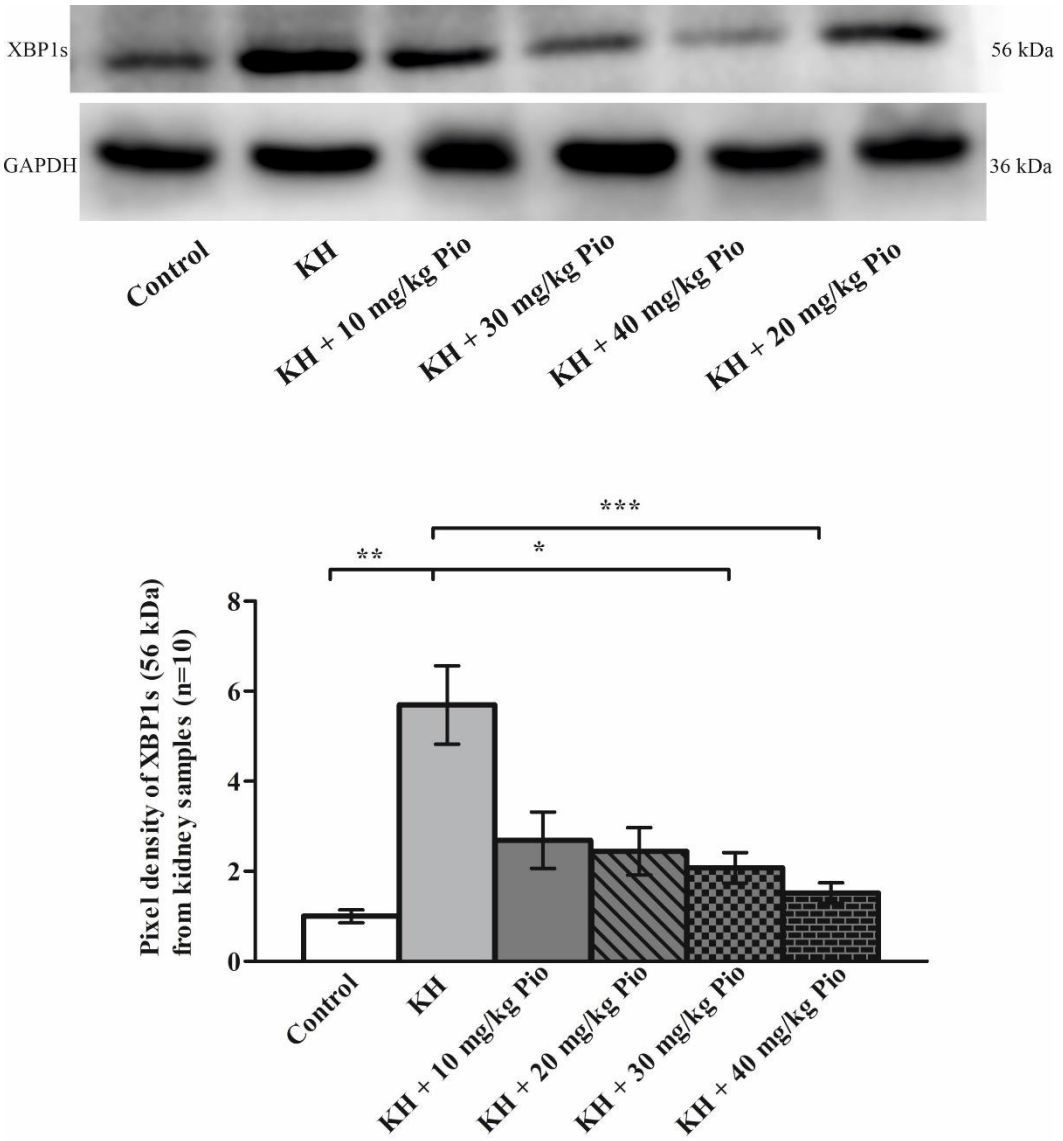

Figure 4. Protein expression of XBP1s (56 kDa) in pixel density. GAPDH served as a normalization control.

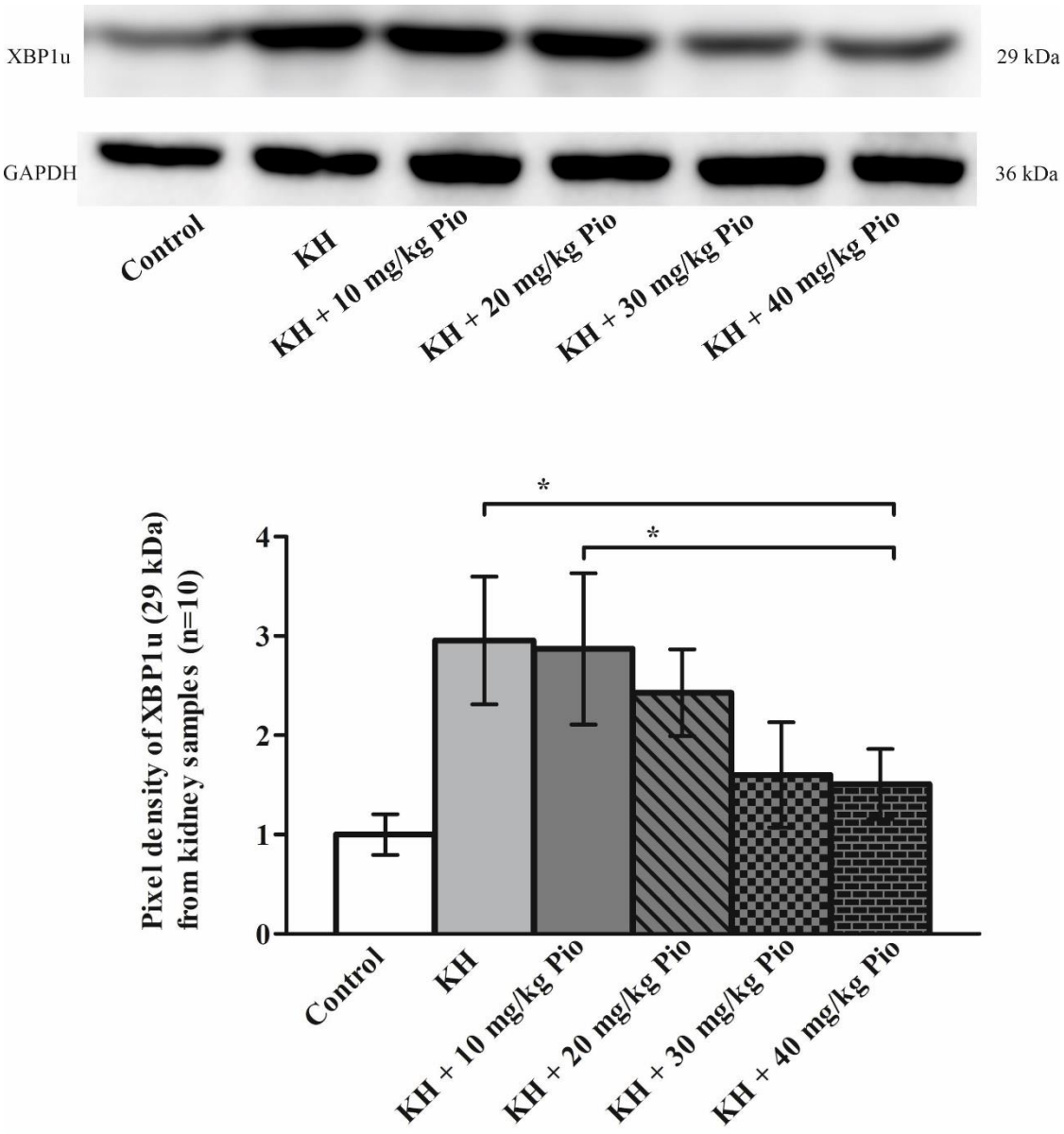

Figure 5. Protein expression of XBP1u (29 kDa) in pixel density from densitometry analyses. GAPDH served as a normalization control.

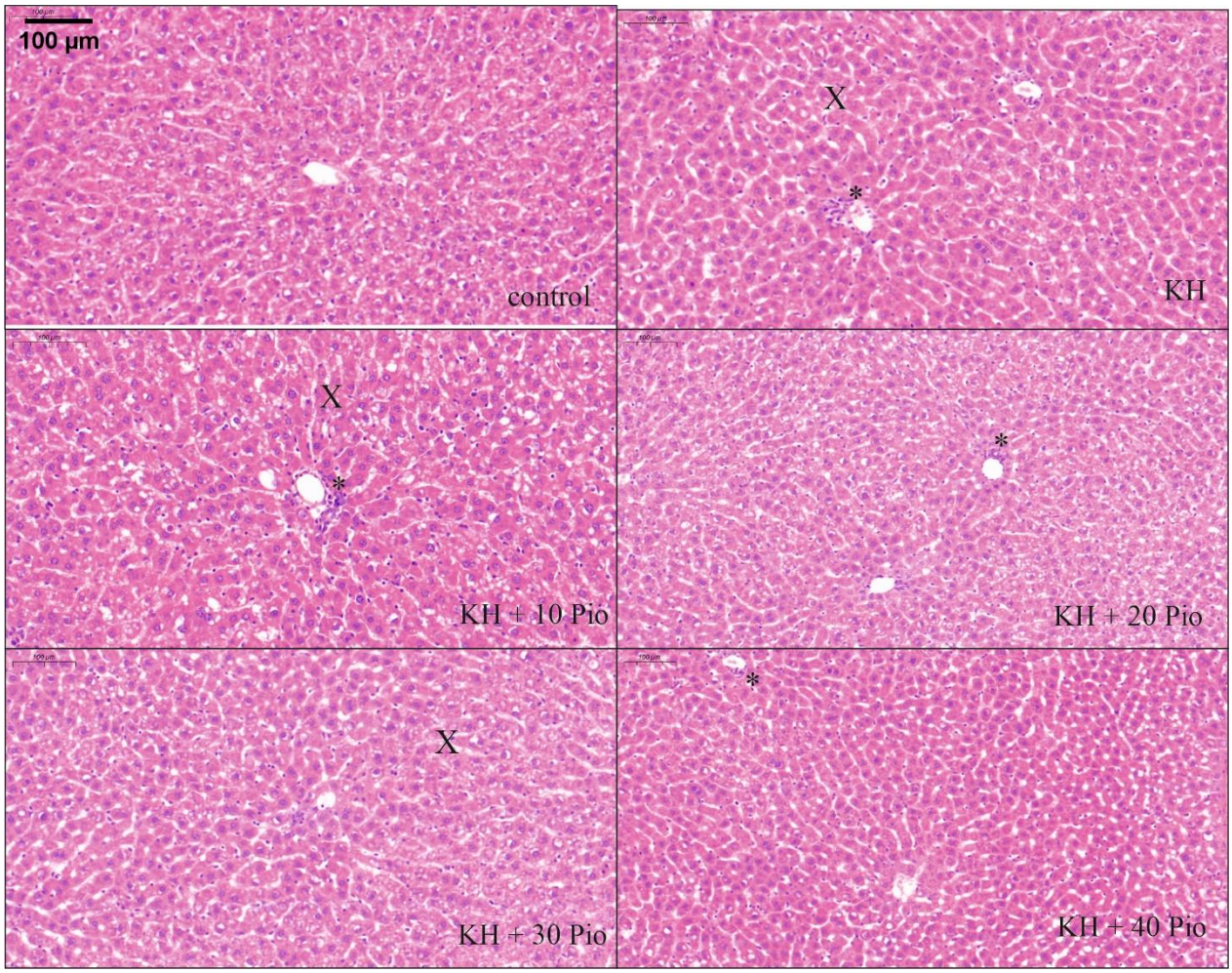

Figure 6. Staining: HE, magnification: 11.3x. The control group depicted a normal appearance. In the non-treated ischemic group, we detect pronounced nodular fibrosis of the parenchyma with hypertrophic hepatocytes. In the KH+20 Pio and KH+30 Pio groups, the basic tissue structure was mainly kept, and it is correlated to the control group. The X's point represents the swollen liver cells. The asterisk (*) shows nodular fibrosis of the parenchyma. We cannot detect any signs of oncosis nor apoptosis.

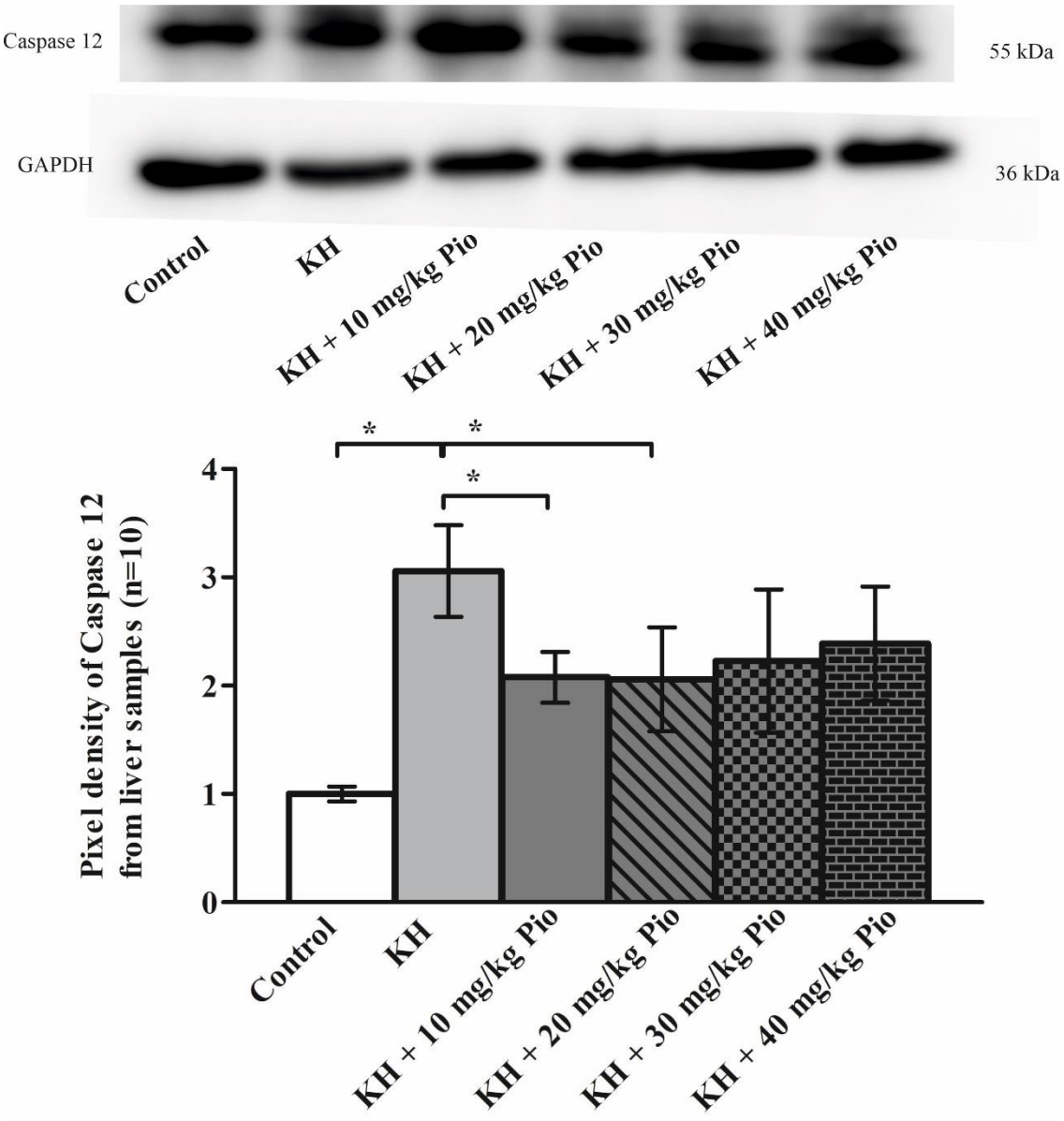

Figure 7. Drug treatment effect on expression of Caspase 12 from liver samples. GAPDH served as a normalization control.

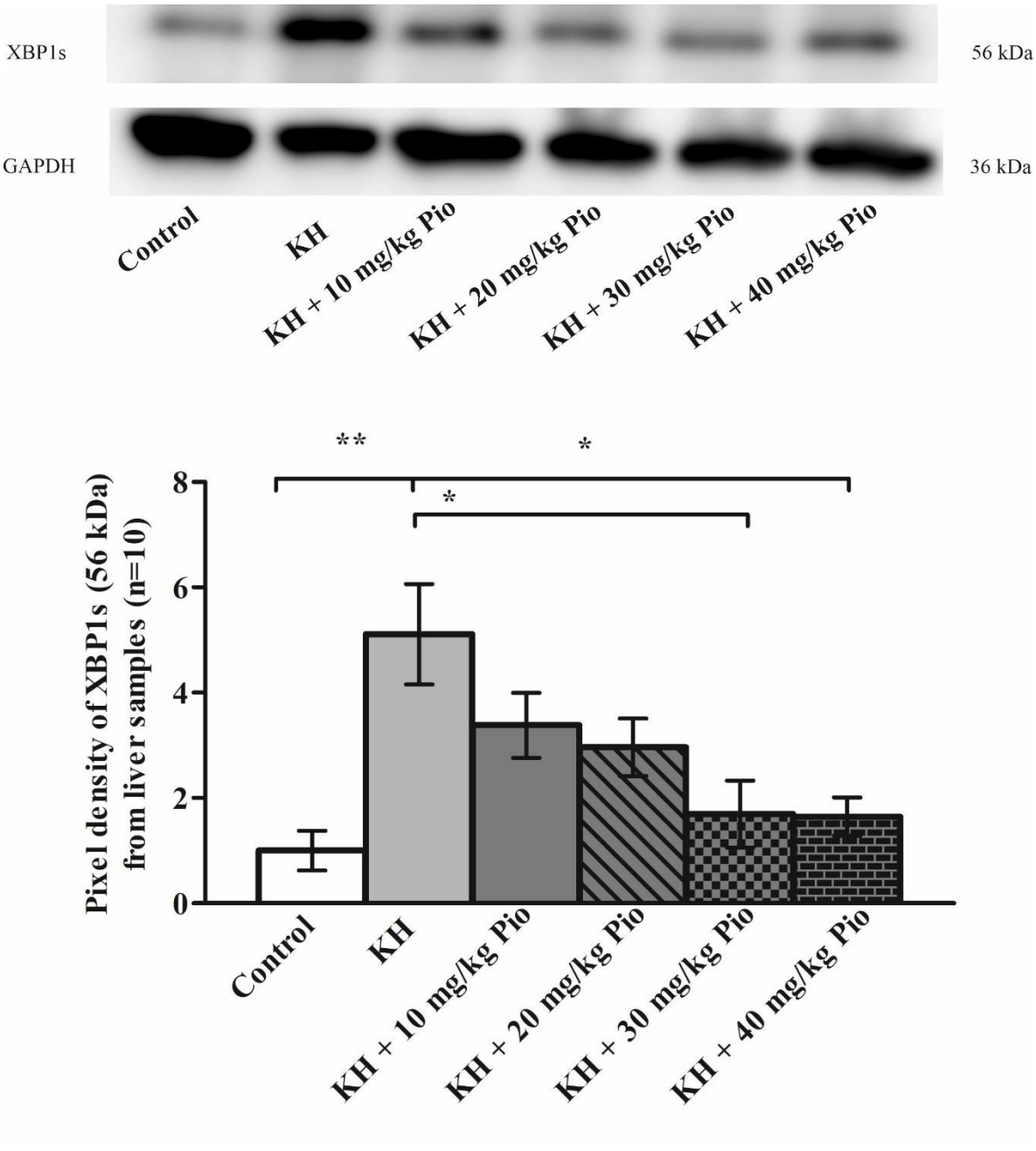

Figure 8. Validation of proteomic results using Western blot analysis of protein extracts from liver samples with antibodies against XBP1s (56 kDa). GAPDH was used as a normalization control.

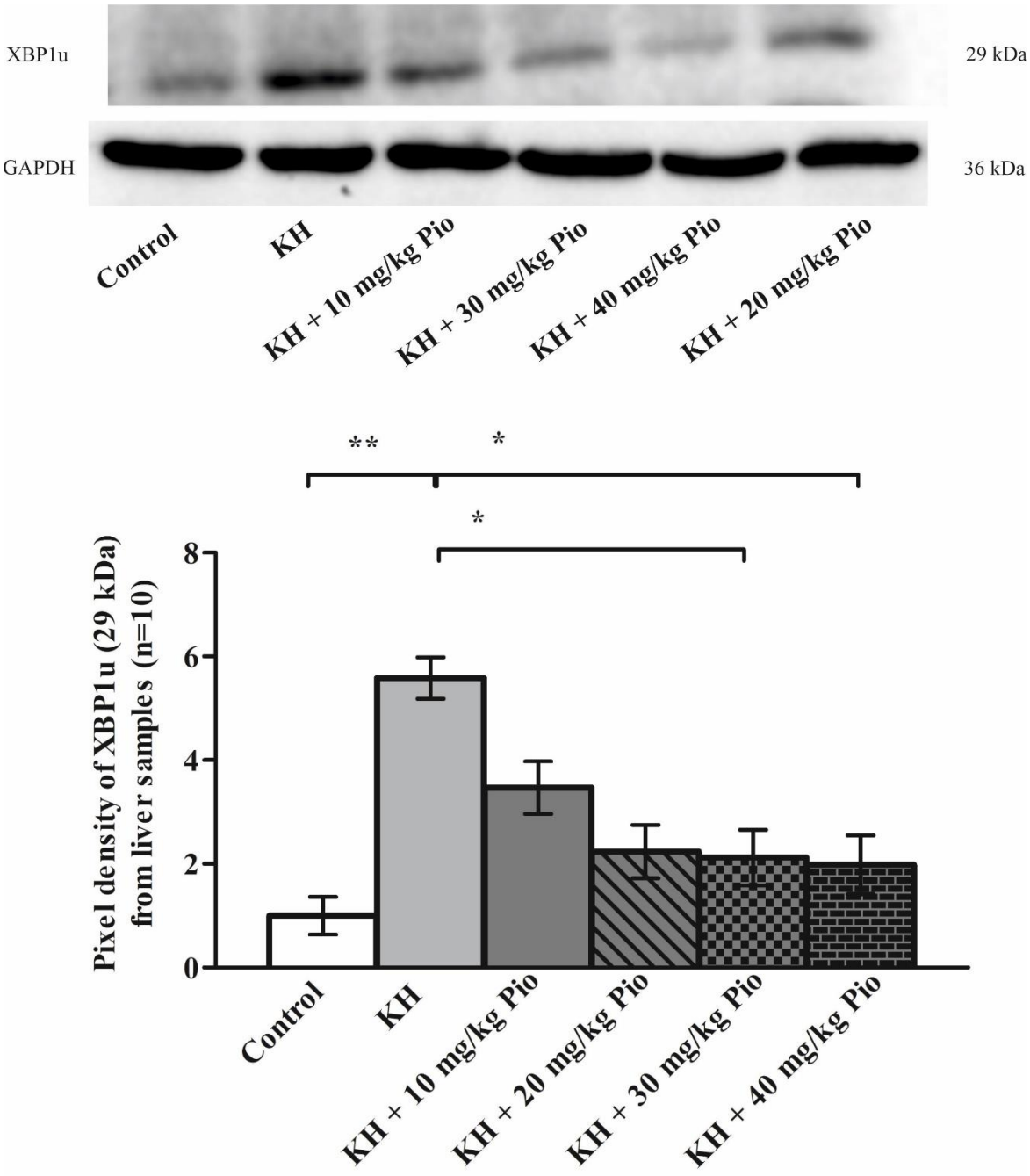

Figure 9. Protein expression of XBP1u (29 kDa). GAPDH was used as a normalization control.

Figure 1. Schematic representation of an animal regarding in situ perfusion model.

Figure 2. Staining: HE, magnification: 11.3x. In the control group of kidney samples, the basic tissue structures were kept; edema, necrosis or inflammation cannot be detected. In the treated groups, we detected eosinophil particles, disorders in Bowman's capsule. The asterisk (*) represents eosinophilia and the arrowhead (>) points at the swelling of endothelial tubules, and the X's serve as to show the swelling of Bowman's capsules. [KH – Krebs-Henseleit solution; KH + 10 Pio – Krebs-Henseleit solution modified with 10 mg/kg Pio; KH + 20 Pio – KH modified with 20 mg/kg Pio; KH + 30 Pio – KH modified with 30 mg/kg Pio; KH + 40 Pio – KH modified with 40 mg/kg Pio).

Figure 3. Western blot results for expression of Caspase 12 from kidney samples. GAPDH served as a normalization control. Blots and relative quantities of Caspase 12 are presented.

Figure 4. Protein expression of XBP1s (56 kDa) in pixel density. GAPDH served as a normalization control.

Figure 5. Protein expression of XBP1u (29 kDa) in pixel density from densitometry analyses. GAPDH served as a normalization control.

Figure 6. Staining: HE, magnification: 11.3x. The control group depicted a normal appearance. In the non-treated ischemic group, we detect pronounced nodular fibrosis of the parenchyma with hypertrophic hepatocytes. In the KH+20 Pio and KH+30 Pio groups, the basic tissue structure was mainly kept, and it is correlated to the control group. The X's point represents the swollen liver cells. The asterisk (*) shows nodular fibrosis of the parenchyma. We cannot detect any signs of oncosis nor apoptosis.

Figure 7. Drug treatment effect on expression of Caspase 12 from liver samples. GAPDH served as a normalization control.

Figure 8. Validation of proteomic results using Western blot analysis of protein extracts from liver samples with antibodies against XBP1s (56 kDa). GAPDH was used as a normalization control.

Figure 9. Protein expression of XBP1u (29 kDa). GAPDH was used as a normalization control.

Editorial letter:

Dear Dr. Telek:

Your manuscript (21-1163-R) has been accepted in Clinical Hemorheology and Microcirculation. A proof of your manuscript will arrive within the next weeks.

Please complete the required Author Publication Fee Payment form:
http://www.iospress.nl/journal-fee-form/?id=15&journal=29265.

If you experience any problems with the payment, please contact Authorfees@iospress.nl.

More information is available at our website:
http://www.iospress.nl/journal/clinical-hemorheology-and-microcirculation.

Thank you for your excellent contribution, and we look forward to receiving further submissions from you in the future.

Sincerely,

F. Jung
Clinical Hemorheology and Microcirculation

To obtain reviews and confirm receipt of this message, please visit:
https://mstracker.com/reviews.php?id=164688&aid=352706